951970

N.T.

MISSILE AND SPACE DIVISION

GPO PRICE $ ________

CFSTI PRICE(S) $ ________

Hard copy (HC) 3.50

Microfiche (MF) .65

ff 653 July 65

FACILITY FORM 602

N68-21879 (ACCESSION NUMBER)

(THRU)

138 (PAGES)

1 (CODE)

CR # 94243 (NASA CR OR TMX OR AD NUMBER)

03 (CATEGORY)

GENERAL ELECTRIC

REPORT NO. 68SD4246
15 APRIL 1968

FEASIBILITY STUDY OF A 30 WATTS PER POUND ROLL-UP SOLAR ARRAY

QUARTERLY TECHNICAL REPORT NO. 3

1 JANUARY 1968 TO 31 MARCH 1968

PREPARED FOR

JET PROPULSION LABORATORY
CALIFORNIA INSTITUTE OF TECHNOLOGY
4800 OAK GROVE DRIVE
PASADENA, CALIFORNIA

PREPARED UNDER
CONTRACT NO. 951970
CONTRACTING OFFICER C.E. PRICE
PROJECT MANAGER W.A. HASBACH

PREPARED BY:

N.F. SHEPARD
K.F. MERTEN
F.A. BLAKE

APPROVED BY:

K.L. Hanson

K.L. HANSON,
PROGRAM MANAGER

This work was performed for the Jet Propulsion Laboratory, California Institute of Technology, as sponsored by the National Aeronautics and Space Administration under Contract NAS 7-100.

GENERAL ELECTRIC
MISSILE AND SPACE DIVISION
Valley Forge Space Technology Center
P. O. Box 8555 • Philadelphia, Penna. 19101

"This report contains information prepared by the General Electric Co., Space Systems Organizations under a JPL Subcontract. Its content is not necessarily endorsed by the Jet Propulsion Laboratory, California Institute of Technology, or the National Aeronautics and Space Administration."

ABSTRACT

Results of the activities performed during the third quarter of this program for establishing the feasibility of a 30 Watts Per Pound Roll-up Solar Array are reported. Included are the complete definition of a model to demonstrate the deployability of the selected flight array configuration, the thermal cycling tests of a 5-cell by 5-cell module, and the investigation of factors affecting the array blanket edge curling phenomenon.

TABLE OF CONTENTS

LIST OF ILLUSTRATIONS

LIST OF TABLES

SECTION 1
INTRODUCTION AND SUMMARY

This report covers the third quarter of the Feasibility Study of a 30 Watts per Pound Roll-up Solar Array Program being performed by the Space Systems Organization of the General Electric Company under Contract No. 951970 for the Jet Propulsion Laboratory of the California Institute of Technology. The objective of the program is to perform a preliminary design and design analysis of a 250-square foot deployable (roll-up) solar panel which shall have a specific power capability of 30 watts per pound or greater and which shall be capable of meeting the environmental requirements of JPL Specification No. SS 501407, Revision A.

The power capability of the array is to be based on cells having an efficiency such that an electrical output of 10 watts per square foot will be achieved at air mass zero, 55°C, and 1.00 AU. Cells to be considered in the design are 0.008-inch thick and N/P protected by a 0.003-inch thick filtered microsheet shield.

The initial section of the program consisted of studies of candidate arrangements and deployment concepts to sufficient depth that a basis for the selection of the system configuration was established. These system tasks were supported by two additional detailed studies: one involving deployment boom and deployment mechanism preliminary design, and the other involving conversion of empirical solar cell data into forms required by general array design computer program. Dynamic and static structural analyses were conducted. These tasks were essentially completed during the first quarter and are reported in Quarterly Technical Report No. 1 (Reference 1).

The second major segment of the program involved the preliminary detailed design of the components making up the 30 watts per pound roll-up solar array panel. During the second quarter, the preliminary design of all major components was completed. Design tradeoff studies were completed which led to the selection of the baseline configuration. A component specification for the solar panel actuator (deployable boom) was prepared and issued.

Based on this specification, the SPAR Aerospace Products* BI-STEM was selected as the solar panel actuator. The preliminary design details of the selected flight configuration are documented in Quarterly Technical Report No. 2 (Reference 2).

A technical review of the first six months of this feasibility study was presented at JPL on 30 January 1968. Appendix A includes the visual aids used during this technical presentation.

During this third quarter, the detailed design was completed for an Engineering Demonstration Model (EDM) which exhibits the deployability of the selected flight configuration. The fabrication of this EDM was started, and thermal cycling tests are currently being conducted on a 5-cell by 5-cell module with the proposed interconnections.

---

*Formerly SPAR Division of deHavilland Aircraft of Canada

SECTION 2

TECHNICAL DISCUSSION

The technical effort during this third quarter has been concentrated on the detailed design of the component parts for the Engineering Demonstration Model. Engineering support during the model fabrication cycle is continuing. An investigation of the array blanket edge curling phenomenon was undertaken and the results are reported in this section. The I-V characteristics for 2-ohm cm, 8-mil solar cells were reduced to the form required by the digital computer program which calculates the array I-V characteristics.

2.1 ARRAY BLANKET EDGE CURLING CONSIDERATIONS

Observable array blanket edge curling should not occur on the flight configuration roll-up solar array design.

Figure 1 illustrates the edge curling phenomenon observed on the full-size demonstration model which was displayed at the mid-term contract review presentation. This type of edge curling can readily be observed on an ordinary household roll-type window shade. Some possible explanations for the edge curl phenomenon considered here are as follows:

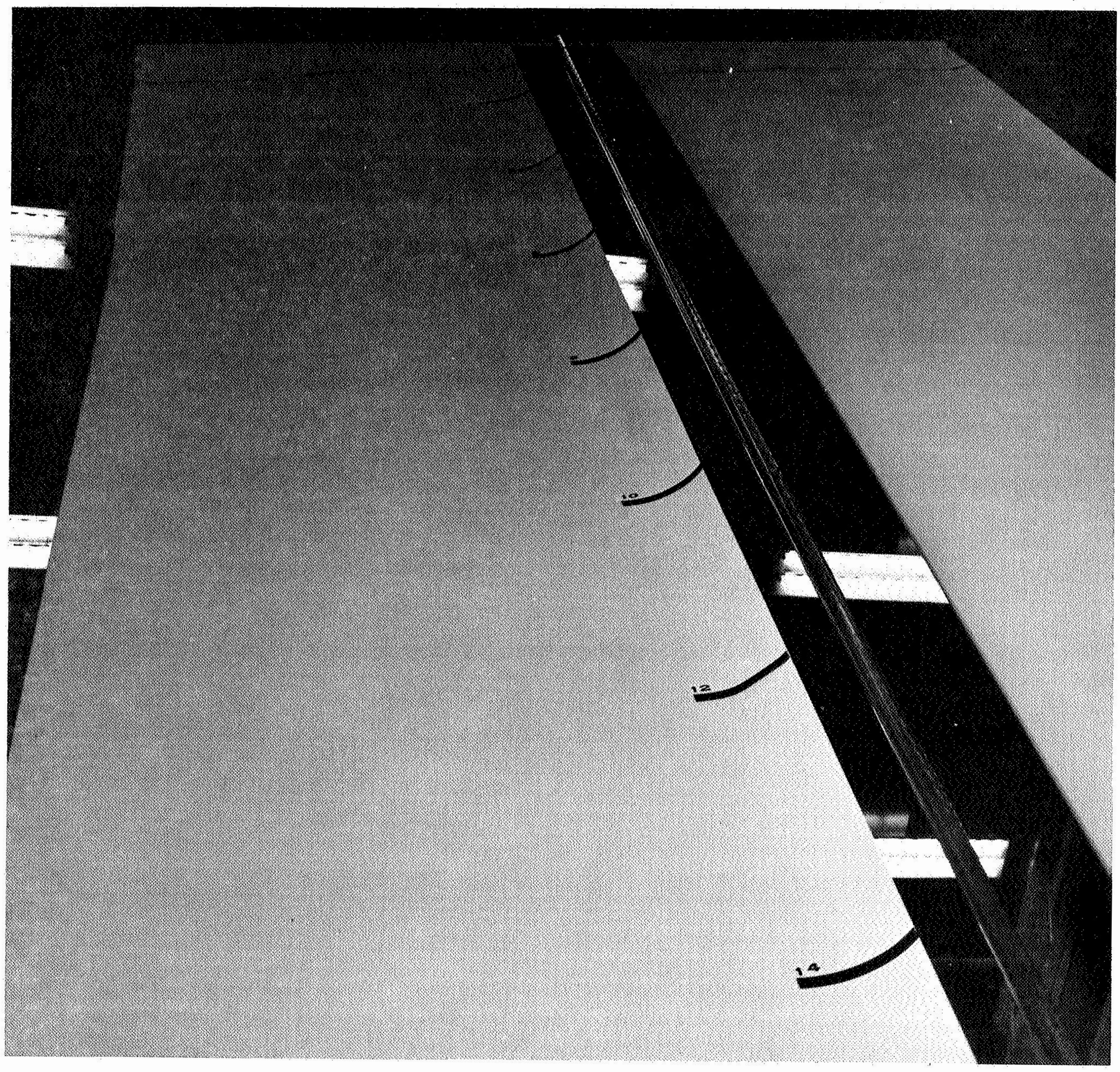

Figure 1. Blanket Edge Curl on a Solar Array Demonstration Model Using a Paper Blanket

a. It is induced by the stresses produced in the blanket by the effects of the end loads applied to the blanket.

b. It is induced by the stresses resulting from the unrolling of the blanket from the drum. Stresses are created because of the normal residual curvature formed in a sheet when it is wrapped around a drum.

c. It is induced by the edges being of greater length than the center section, due to previous high edge loadings or environmental effects.

It was concluded from consideration of these explanations that the stress patterns in the blanket due to the normal deployed loading conditions do not produce edge curl (explanation a) and that, although the phenomena of explanations b and c can explain observed edge curls for some materials and conditions, they do not apply to the material and loading conditions for the array blanket. Therefore, the overall conclusion is that the edges will not curl on the proposed array blanket.

2.1.1 EFFECTS OF END LOADS

2.1.1.1 Unrestrained Sheet

First, the possibility that edge curl can result from the tension loads developed in the blanket by the deployment rod was explored using simple analytical models. A thin flat sheet of material (not subjected to end restraints) with tensile forces p uniformly distributed along the ends, was considered as shown in the following sketch:

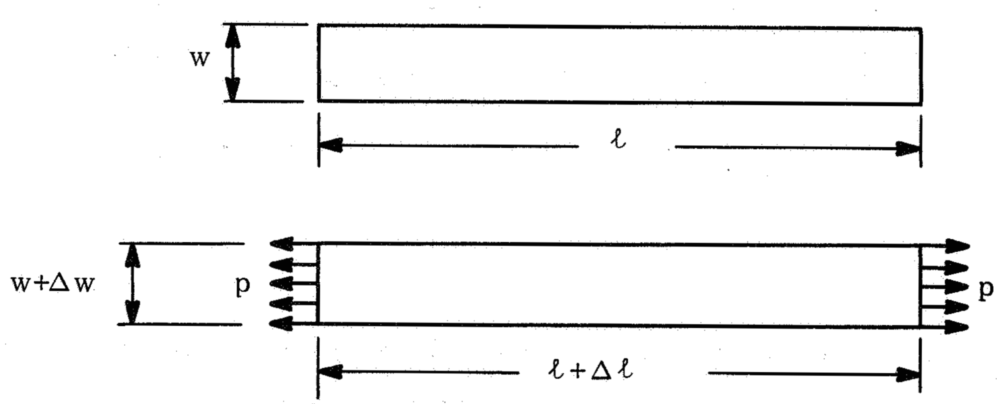

Under these conditions, the length, ℓ, will change due to a uniform unit strain resulting from the direct tensile stresses. The unit strain, $\Delta\ell/\ell$, is given by $\frac{\Delta\ell}{\ell} = \frac{S}{E}$, where S is the stress and E is the modulus of elasticity. In addition, the tensile stresses will produce a uniform lateral contraction of the sheet proportional to Poisson's ratio (μ), $\frac{\Delta w}{w} = -\mu \frac{S}{E}$.

The conclusion drawn is that these uniformly distributed stresses and strains could not produce out-of-plane deflections; and therefore no explantion of the edge curl phenomenon is provided.

2.1.1.2 Sheet With End Restraints

The next approach was to consider the effects of the ends of the sheet being laterally restrained as they are on the drum and leading edge member of roll-up array. The lateral strain and associated edge displacement, Δw, are then fully suppressed at the ends; while lateral contraction midway between the ends and away from the end effects will be practically unsuppressed, as in the sheet without end restraints. A nonuniform stress and strain distribution, therefore, results between the restrained edges of the sheet and the unaffected midsection, with the possibility of the sheet assuming the shape shown in the following sketch (exaggerated for explanatory reasons):

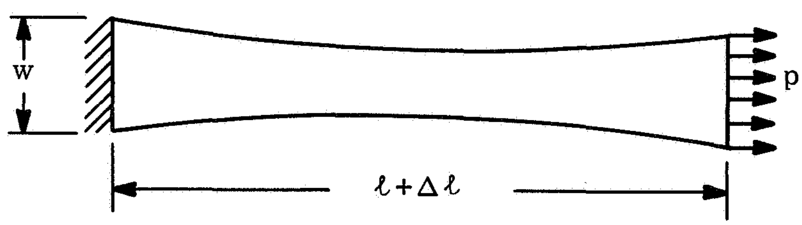

To establish bounds on the differences in length between end and center fibers, a uniform stress distribution along the length, ℓ, is assumed, though variations across the sheet will be allowed.* The lengthwise strain of the center fibers near the ends of the sheet will be slightly less than before. This is due to the suppression of lateral strain and is given by the relationship, $\epsilon_{\ell} = (1 - \mu^2) \frac{S}{E}$, where ϵ_{ℓ} is the unit strain in the direction of ℓ. However, the strain at the edge of the sheet, where the lateral restraint is zero, is still given by the previously developed relationship, $\epsilon_{\ell} = \frac{S}{E}$.

These equations (for two locations in the sheet near an end) illustrate the varying effects of the end restraint on the equations governing the fiber stresses. A complete analysis of the stress and strain distribution throughout the sheet is complex and not readily amenable to hand calculations. However, General Electric's Missile and Space Division has a computer program (SAFE) which allows a detailed solution of this problem and will be used if deemed necessary. This program is described in Section 2.1.4. However, before this program can be used, consideration must be given to the fact that analyses of nonuniform local end-load problems show that the effects of stress and strain become negligible at a distance from the end of the sheet that is approximately equal to the width.

The fact that the length/width ratio of the proposed array blankets is approximately 9:1 led to the conclusion that nonuniform stresses due to end effects would not explain the edge curl observed at the midsection of the blanket away from the ends. There is also no obvious stress or strain pattern that causes out-of-plane displacements. Therefore, a computer program stress analysis was not carried out, and other explanations of the edge phenomenon were sought.

To verify this conclusion, a simple test was conducted to confirm that end loads will not produce the stresses required to produce the edge curl. This test is described in the next section.

* This stress distribution cannot be the actual stress distribution in the blanket, but it provides results which give greater insight to the problem.

2.1.1.3 Test Sheet

An initially flat sheet of 1-mil Kapton-H film of approximately the same length/width ratio as the proposed array blanket was looped around a pencil at each end (the loop was closed with mylar tape) and pulled by hand to provide end tension loads. In this simple experiment, no tendency for edge curling was observed under either low or high end loads. This confirms the above analytical conclusion that blanket end tensile loads do not induce edge curling.

2.1.2 EFFECTS OF WRAPPING BLANKET ON DRUM

Consideration of the effects of wrapping the blanket on the drum led to the following explanation of the edge curling phenomenom observed in the demonstration model and in household window shades. However, experience with the Kapton-H film indicates that an occurrence would not exist in an array blanket using this material.

If it is hypothesized that wrapping the blanket material onto the drum will stress the material so highly as to produce a permanently curved deformation, then when the sheet is pulled flat by the end loads, the tension load distribution through the thickness of the sheet would become unequal by an amount equal to the magnitude of the additional tension loads in the top fibers required to bend the sheet flat. At a distance from the ends of the sheet, where end effects may be ignored, the otherwise uniform tensile stress distribution through the thickness would be modified by the addition of tension and compression (stresses probably nonlinear in distribution) such as the following:

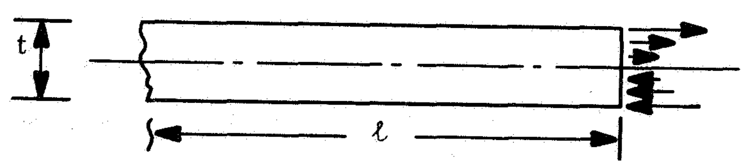

As noted in Section 2.1.1, the tensile stresses in the top fibers will tend to produce lateral contraction of the top fibers across the width of the plate, and correspondingly, the compression stresses in the bottom fibers will tend to produce lateral expansion across the width of the plate. It is apparent that these combined contraction and expansion tendencies through the thickness of the sheet will tend to produce a curvature across the width of the sheet. With the sheet restrained flat at the ends, the net result would be an edge curl. Thus, it may be concluded that if the blanket material properties are such that it takes on the curved shape of the drum after wrapping, the above analysis could explain its edge curvature. Experience with paper and window shades, which do tend to take a curved shape after wrapping, would indicate the analysis is applicable to these materials. However, experience with Kapton-H film, which does not assume any residual curvature even after being wrapped on a lead pencil, would indicate the analysis does not apply to the proposed array blanket material.

2.1.3 EFFECTS OF BLANKET EDGE STRETCHING

The following analysis shows that the flatness of a sheet is highly dependent upon all elements being of equal length. Therefore, if the edges of the sheet should become permanently stretched relative to the center section, this could explain the out-of-plane edge curvature. Again, experience with paper material, where stresses and/or mositure absorption due to edge exposure or handling could cause edge lengthening, indicates the applicability of this explanation to the paper blanket of the demonstration model. Similarly, recognizing that window shades are often pulled down at the edges might explain a stretched edge condition there. However, with controlled handling of a material like Kapton-H film, this edge stretching would not be expected. The following example illustrates the sensitivity of the out-of-plane deflections to a difference in element lengths.

Assume a blanket length of 409 inches. If the outer edges were 0.0019 inches longer than the midsection, then, maintaining compatibility at parallel ends and assuming the edges take a circular arc shape, the corresponding out-of-plane displacement, h, is 0.53 inches, as illustrated below. The angle formed by the normals at the ends of the arc is less than 0.10 degrees.

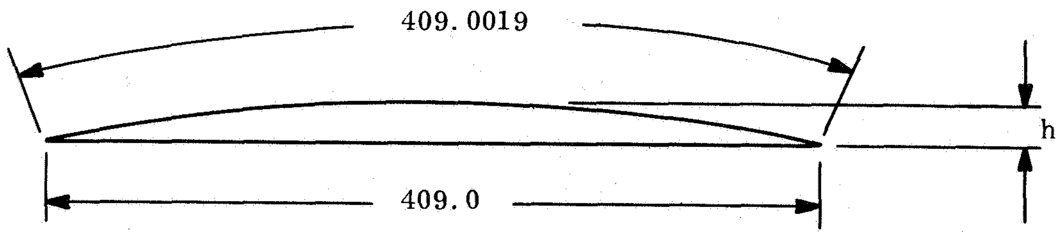

2.1.4 STRESS ANALYSIS FINITE ELEMENT PROGRAM (SAFE)

SAFE is a general computer program developed by General Electric for the structural analysis of isotropic and/or orthotropic bodies using finite element techniques. In general, SAFE has the capability of computing stresses, strains, and displacements throughout the cross section of an axisymmetric or in the plane of a planar body. The loading must be axisymmetric (or in-plane) but otherwise may vary arbitrarily. In addition to arbitrary thermal gradients, loading functions may include pressures, shears, arbitrary loads, or displacements, and body forces or accelerations which may be specified within any point of the model. The model may have as many as six distinct materials, all of which may be temperature dependent.

It is possible to have individual properties in every element. This allows great flexibility in solving complex thermostructural problems, evaluating edge stress problems, and computing the effects of geometric and material discontinuities on the stress distribution. The program also provides optional graphic output, on the SC-4020 printer-plotter, of all computer data from the main computational link. The plot program can be run separately with saved tapes at any time in order to obtain additional output not requested at the time of the initial run. Graphic output options include a deformed grid and plots of any of the stress or strain components, either as contour plots or as distribution plots at any given station.

2.1.5 ANALYTICAL TECHNIQUES

The analytical techniques described in References 3 and 4 are also applicable to this problem. However, they have not been programmed for a digital computer and therefore would be less convenient than the SAFE Computer Program.

2.2 ARRAY I-V CURVE USING 2-OHM CM, 8-MIL CELLS

The use of 2-ohm cm, 8-mil solar cells results in a calculated array power output of 2523 watts at 55°C, 1.000 A.U. or 10.09 watts/ft^2 of gross module area

A set of coefficients for use in the GE-MSD Solar Array I-V Curve Computer Program was generated for 8-mil thick solar cells with a 2-ohm cm base resistivity. This computer program calculates the current/voltage characteristics of the whole array, taking into a account the following performance parameters:

a. Solar intensity

b. Temperature

c. Solar incidence angle

d. Series cells in a string

e. Parallel cells in a string

f. Number of strings

g. Basic cell characteristics (temperature-dependent, I-V characteristics based on measured cell data)

h. Losses and uncertainties

The output of the program is a listing, for each different operating condition, of voltage versus total current and power.

It calculates the array output based on the I-V characteristics of a single cell, adjusting the voltage and current scale factors to account for the numbers of cells in series and parallel. The single-cell, I-V curve is obtained from

$$I = I_{sc} - \frac{V}{R_p} - I_o \left[e^{K(V+R_s I)} - 1 \right]$$

where

I = cell current output

V = voltage on cell.

The coefficients are:

I_{sc} = Illumination current (virtually equal to the short circuit current)

R_p = Shunt resistance of the cell

I_o = Reverse saturation current of the ideal diode characteristic

K = Coefficient of the exponent, $(V + R_s I)$

R_s = Series resistance of the cell.

The coefficients are treated as functions of temperature, using sixth-degree polynomial approximations to more accurately reflect changes in cell characteristics with temperature.

The correction for angle of incidence includes the cosine and an allowance for increased reflection from the cell and filter at large incidence angles, and is applied to I_{sc} as a multiplier. Other loss factors are also applied to I_{sc}, and the voltage component of radiation damage is applied as a downward voltage shift to the basic I-V curve.

I-V calculations were made using this program with 8-mil, 2-ohm cm cell characteristics. These results were checked against the empirical data contained in Reference 5 for various temperatures ranging from +120°C to -120°C. Figure 2 shows some of these data plotted in Figure 4 of Reference 5. There is very good agreement between these curves and the calculated points obtained from the I-V Curve Computer Program.

This program with the coefficients for 8-mil, 2-ohm cm cells, was used to obtain the I-V curve shown in Figure 3 for the proposed array configuration described in Reference 2.

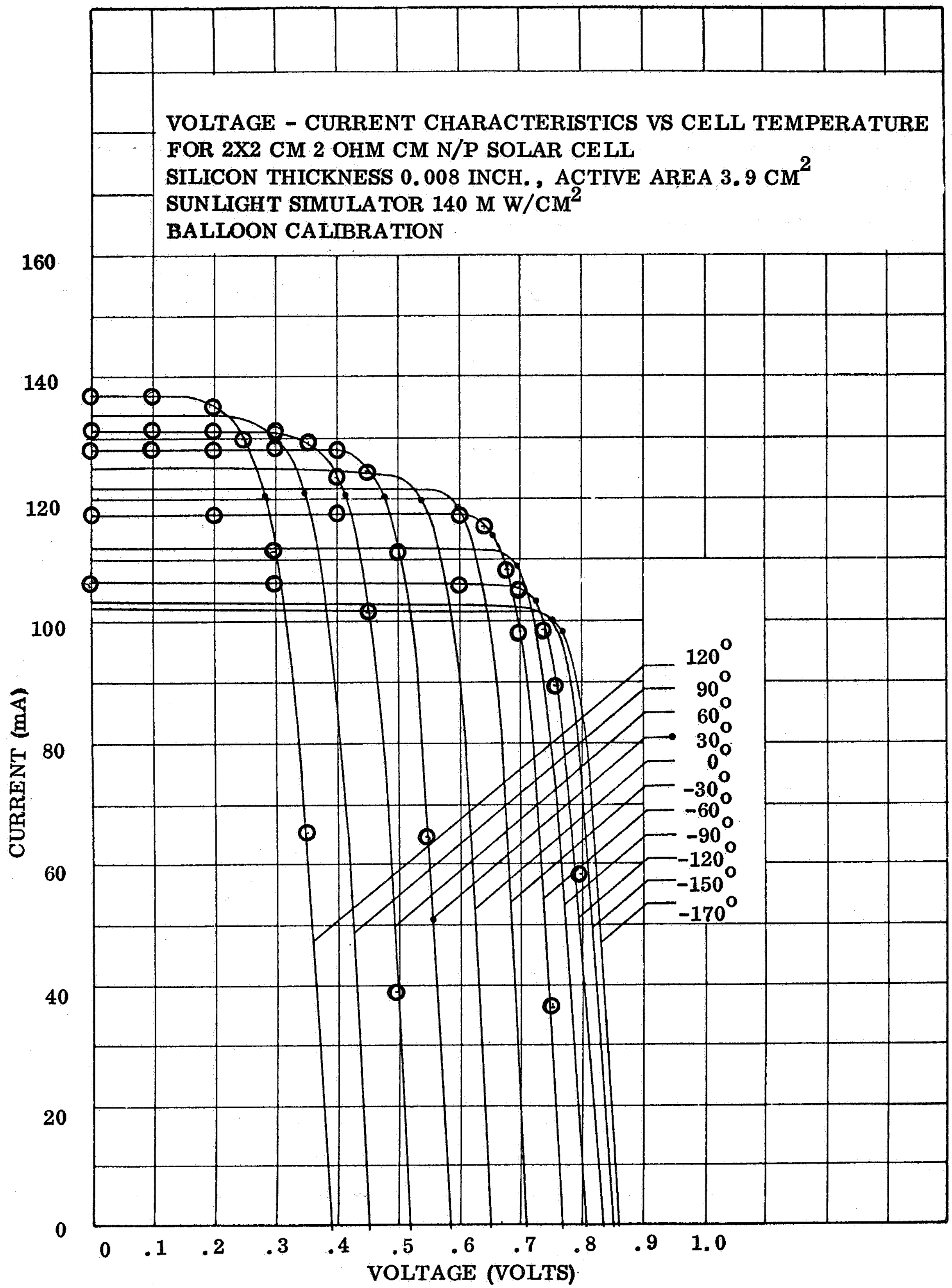

Figure 2. Solar Cell Characteristics, 2-Ohm Cm, 8-Mil

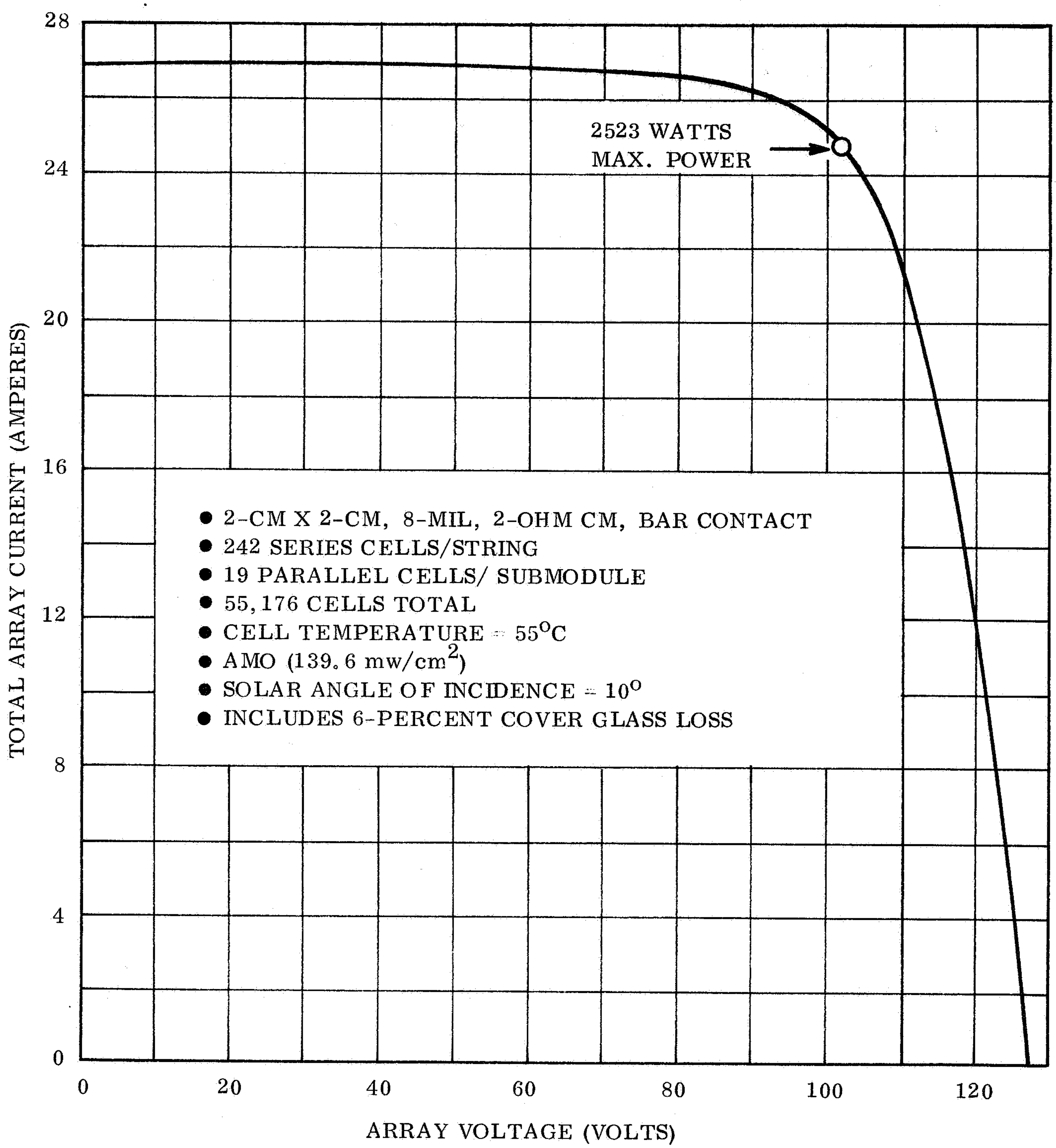

Figure 3. Array I-V Curve, 2-Ohm Cm, 8-Mil

Note that the utilization of these cells results in calculated maximum power (at 55^{o}C) of 2523 watts at 102 volts. This is based on 3.8 cm^2 of active area per cell (bar contact) and includes an estimated cover glass loss of six percent and the loss associated with a 10-degree solar angle of incidence.

A similar I-V curve based on coefficients for 8-mil, 10-ohm cm cells (References 1 and 5) is shown in Figure 4. Under the same assumptions and operating conditions, these cells result in a calculated maximum power at 55^{o}C of 2294 watts at 90 volts.

Thus, cells with a 2-ohm cm base resistivity meet the requirement of 10 watts/ft^2 of module area.

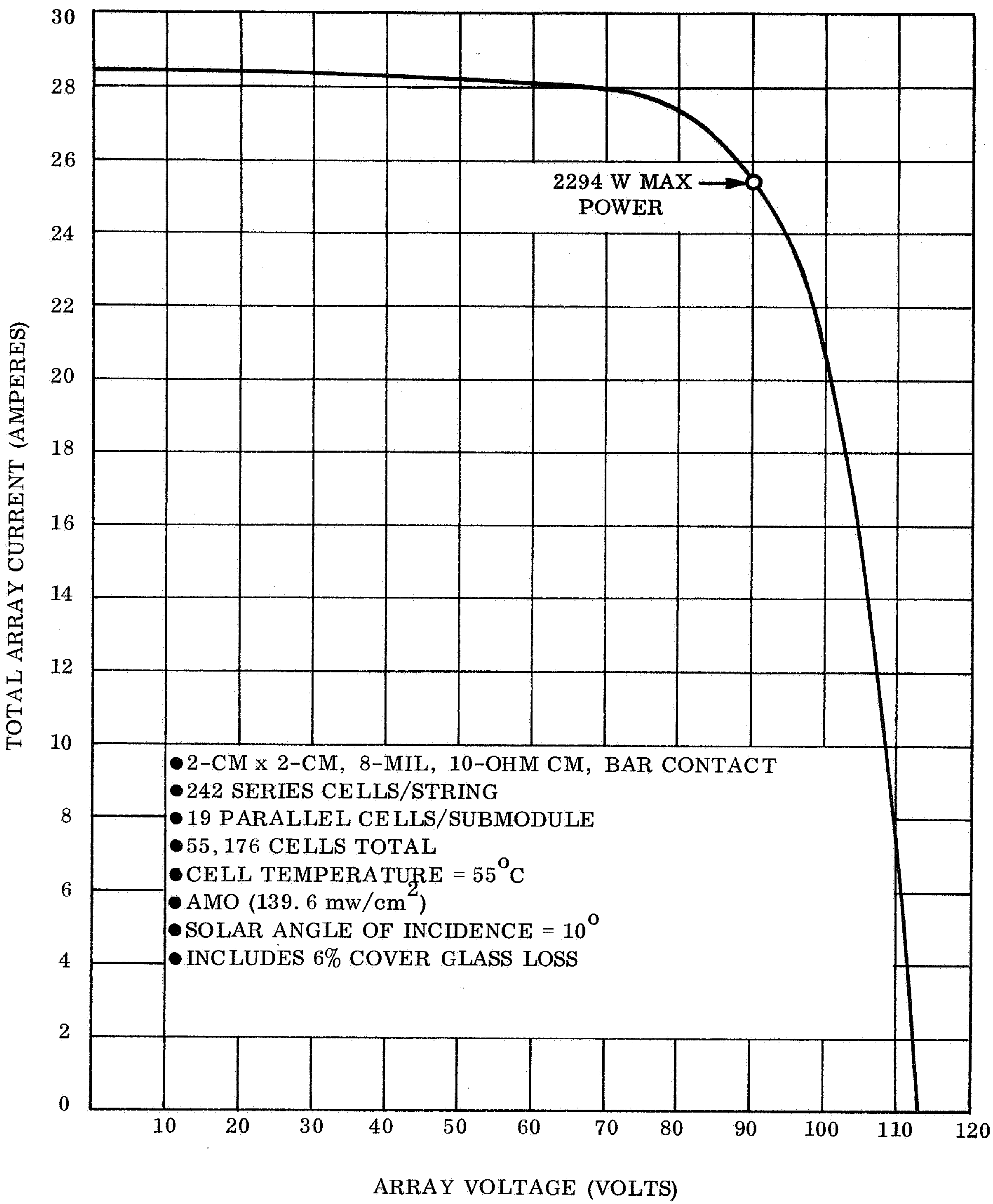

Figure 4. Array I-V Curve, 10-Ohm Cm, 8-Mil

2.3 THERMAL CYCLING TEST RESULTS

To date, no conclusive results have been obtained. Testing will continue into the fourth quarter.

The 5-cell by 5-cell module shown in Figure 5 was fabricated for the purpose of obtaining experimental verification of the ability of the interconnections to perform satisfactorily in a thermal cycling environment. The thermal cycling test fixture is shown in Figure 6. The 5-cell by 5-cell module is shown mounted to the heat sink. The open-cell foam and glass disc are used to apply light pressure to hold the module in contact with the heat sink. The open-cell nature of this foamed sheet allows the cells to be illuminated through a window in the chamber.

An initial I-V curve on the 5-cell by 5-cell module was obtained under a tungsten stimulator to establish a baseline for detecting electrical degradation which resulted from the thermal cycling test. The module was placed in the chamber on the heat sink and cycled 114 times between $-200^{o}F$ and $+200^{o}F$. The short-circut current was continuously monitored during this test. During removal from the heat sink, the module was damaged while being released from the grease which was used to maintain good thermal conductivity between the heat sink and the module substrate. This handling damage was extensive and made it impossible to detect any possible thermal cycling damage. An examination of the short-circuit current record made during the test revealed no recognizable degradation.

A second module was fabricated which was identical to the damaged module. Thermal cycling tests were started on 28 March 1968, and their results will be reported during the fourth quarter.

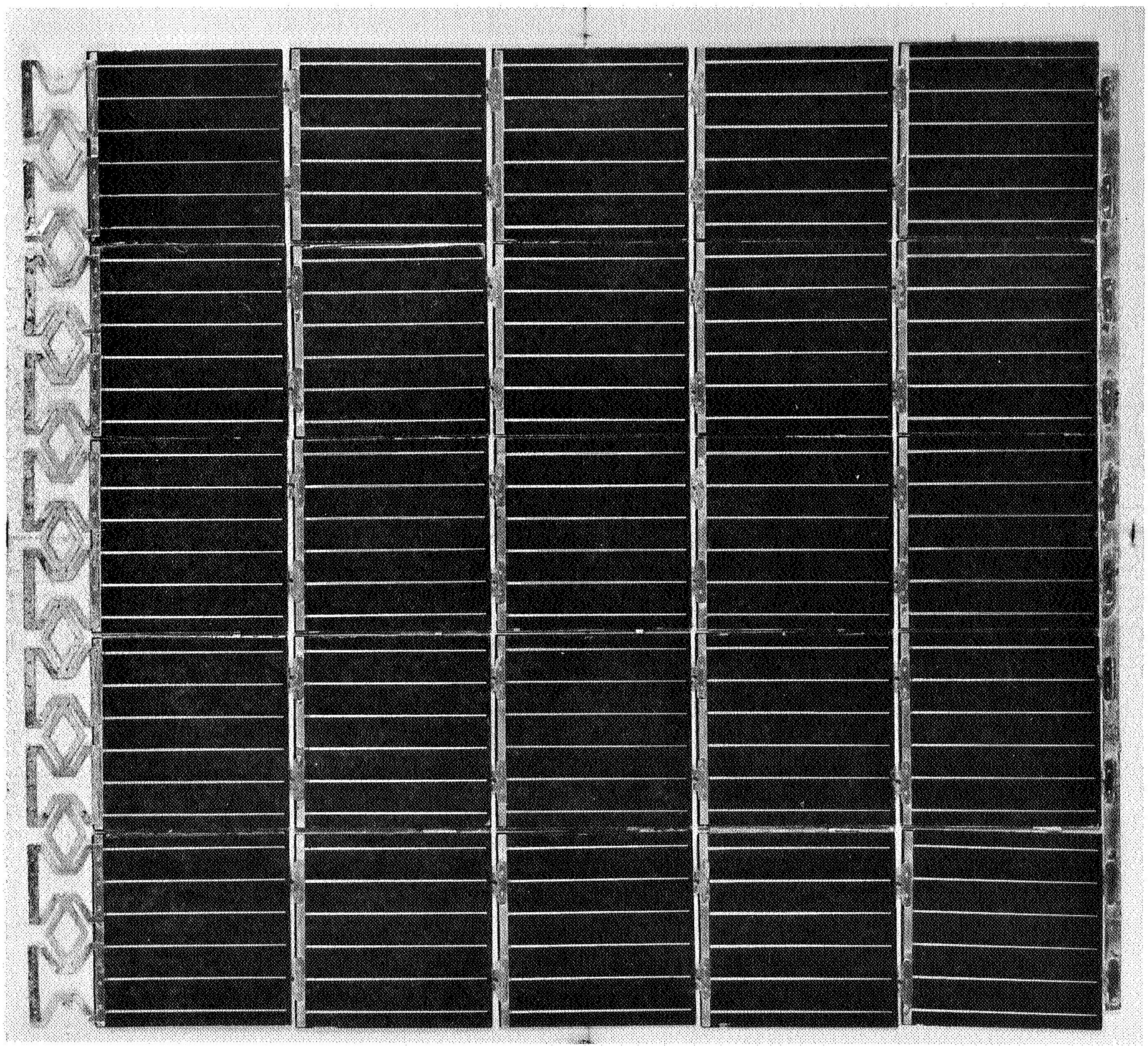

Figure 5. 5-Cell x 5-Cell Module, Front Side

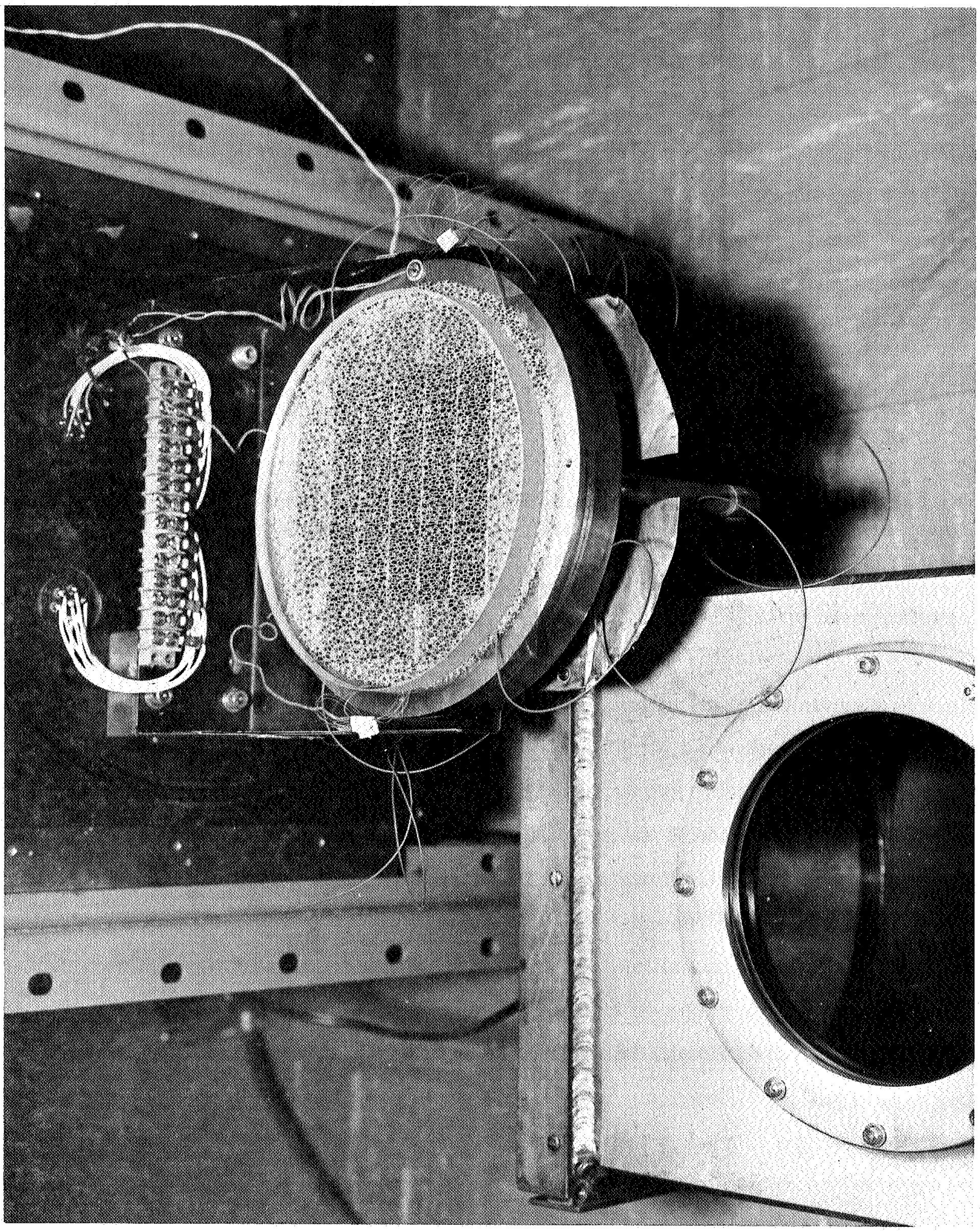

Figure 6. Thermal Cycling Test Fixture

2.4 MATERIAL CONSIDERATIONS

All polymeric materials which are utilized in the proposed design have been reviewed in regards to suitability for use in a space environment.

The polymeric materials which are proposed for the 30 Watts per Pound Roll-Up Solar Array have been reviewed with respect to the experimental data contained in Reference 6. This report presents data on the behavior of polymeric materials in a thermal-vacuum environment. Loss of weight and the amount of released material which may condense on cool surfaces adjacent to the warmed polymer are important criteria in the determination of a material's suitability for use in a space environment. The criteria proposed in Reference 6 is stated as follows:

> "Thus, a polymeric material should not be considered suitable for use in spacecrafts or be subjected to further evaluation, unless it exhibits a 1-percent or less weight loss and a 0.1-percent or less maximum volatile condensable materials (VCM) content on exposure to the thermal-vacuum environment of 125°C and 10^{-6} torr."

Table 1 is a summary of the organic materials proposed for use in the roll-up solar array, along with the corresponding values for percent weight loss and percent by weight of VCM. An examination of this table shows that the foamed RTV 580, which is used for the cushioning buttons on the rear side of the array substrate, does not meet the established criteria for an acceptable material. However, it is still desirable to consider the use of foamed RTV 580 for the following reasons: (1) it has experimentally demonstrated the ability to protect the cell/glass combination, (2) it provides high frictional damping which limits the axial motions of the wraps on the storage drum and (3) processes for aerospace applications are already developed. In order to reduce the weight loss and VCM values, it is proposed to "post-cure" the array substrate with the foamed buttons under the vacuum and at an elevated temperature for a minimum of 48 hours. Note that the buttons are a nominal 0.040-inch thick, and the total weight of the foamed material on the 250-ft^2 array is 1.20 pounds.

Table 1. Roll-up Array Polymeric Materials VCM Data
(24 Hours at 125°C and 10^{-6} Torr, VCM Collectors at 25°C)

Material	How Used	Treatment	Total Weight Loss (%)	VCM Wt. (%)	Reference
Epon 934	Bonding beryllium	1 hour @ 82°C	0.10	0.08	6
Kapton-H Film	Array substrate	As received	0.14	0.09	6
Delrin	Neg'ator take-up spool	As received	0.58	0.06	6
Sylgard - 182	Cell-to-cover glass bond	As received	1.5 @ 100°C 0.5 @ 50°C	*	7
RTV - 580	Cushioning buttons	24 hrs @ 25°C + 24 hrs @ 150°C	1.81	0.81	6
SMRD 745	Cell-to-substrate bond	*	*	*	*
Epiall 1914	Drum power feed-thru slip ring dielectric	24 hrs @ 150°C	0.55	0.03	6
GT-100	Bus strip-to-substrate bond	*	*	*	*

*No data available at the time of this writing.

2.5 ENGINEERING DEMONSTRATION MODEL STATUS

The design of the Engineering Demonstration Model (EDM) is complete and fabrication is proceeding. All purchased parts have been ordered.

The general description and purpose of the EDM remain essentially unchanged from that contained in Reference 2. Figure 7 shows an isometric sketch of the proposed model. The only basic change in design which has occurred since the second quarterly report is the incorporation of a pneumatic system for the actuation of the separation nuts.

2.5.1 MECHANICAL DESIGN

The mechanical design of all components for the EDM has been completed. The fabrication of all subassemblies has been started and, in some cases, completed. Figure 8 is a photograph showing the storage drum, leading edge member, center support, and outboard end support (movable part). For cost effectiveness, the storage drum shell and end caps, and the leading edge member have been fabricated from aluminum instead of beryllium.

The separation nuts (Hi-Shear Part No. SN7311-2) are designed for actuation with pyrotechnic cartridges. This is a one-shot operation since the nuts are not reusable due to contamination from the explosive. In order to reuse the separation nuts on the model, they are actuated pneumatically, an approach that has been verified experimentally. A schematic diagram of the proposed self-contained, high-pressure pneumatics system is shown in Figure 9. A high pressure reservoir (2100 psig, 57 in.^{3}) will be strapped to the test stand of the model. This pressure will be applied to the separation nuts through a flexible hose connected to a 2-way, 2-position solenoid actuated value. A push button switch on the control panel will apply power to the solenoid to initiate release of the outboard end supports. A relief valve, pressure gage, cylinder valve, and charge/vent valve are also provided in the system as shown in the schematic. The cylinder on the model should provide enough capacity for approximately 10 actuations before requiring recharge. It then can be recharged with nitrogen or air through the charge/vent valve, as required, or the system may be supplied from an external reservoir through this same valve.

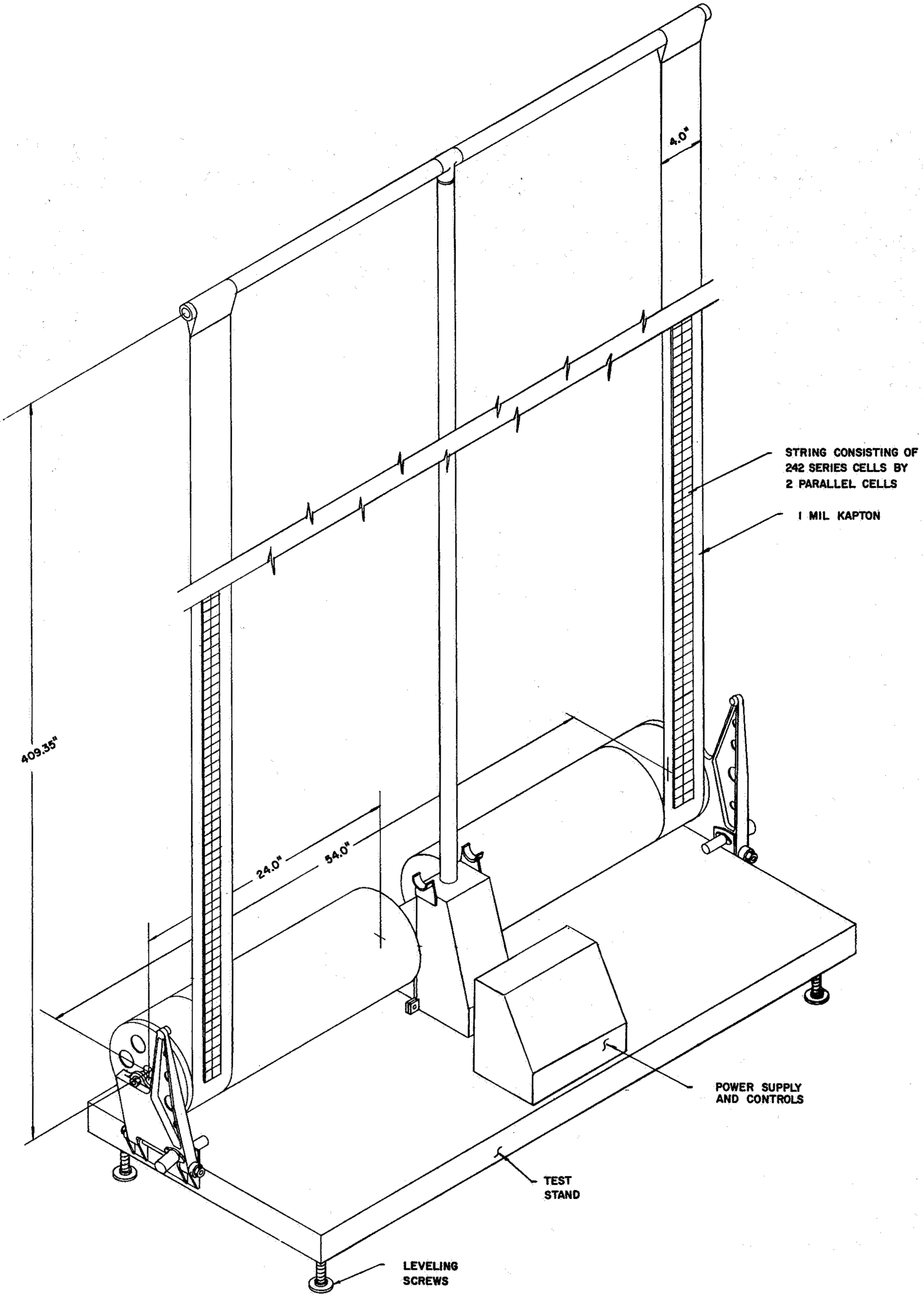

Figure 7. Isometric View of Engineering Demonstration Model

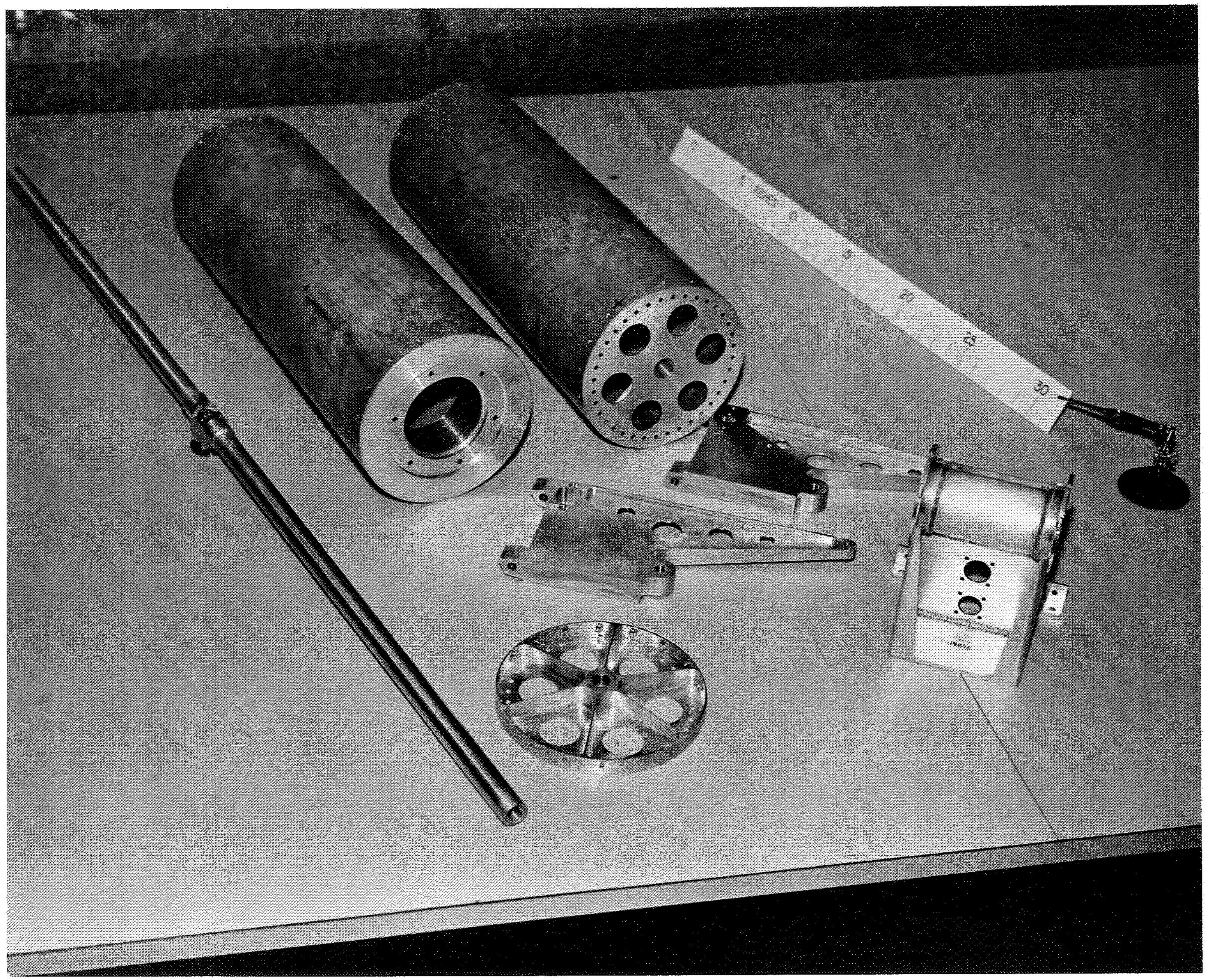

Figure 8. Completed Assemblies for the Engineering Demonstration Model

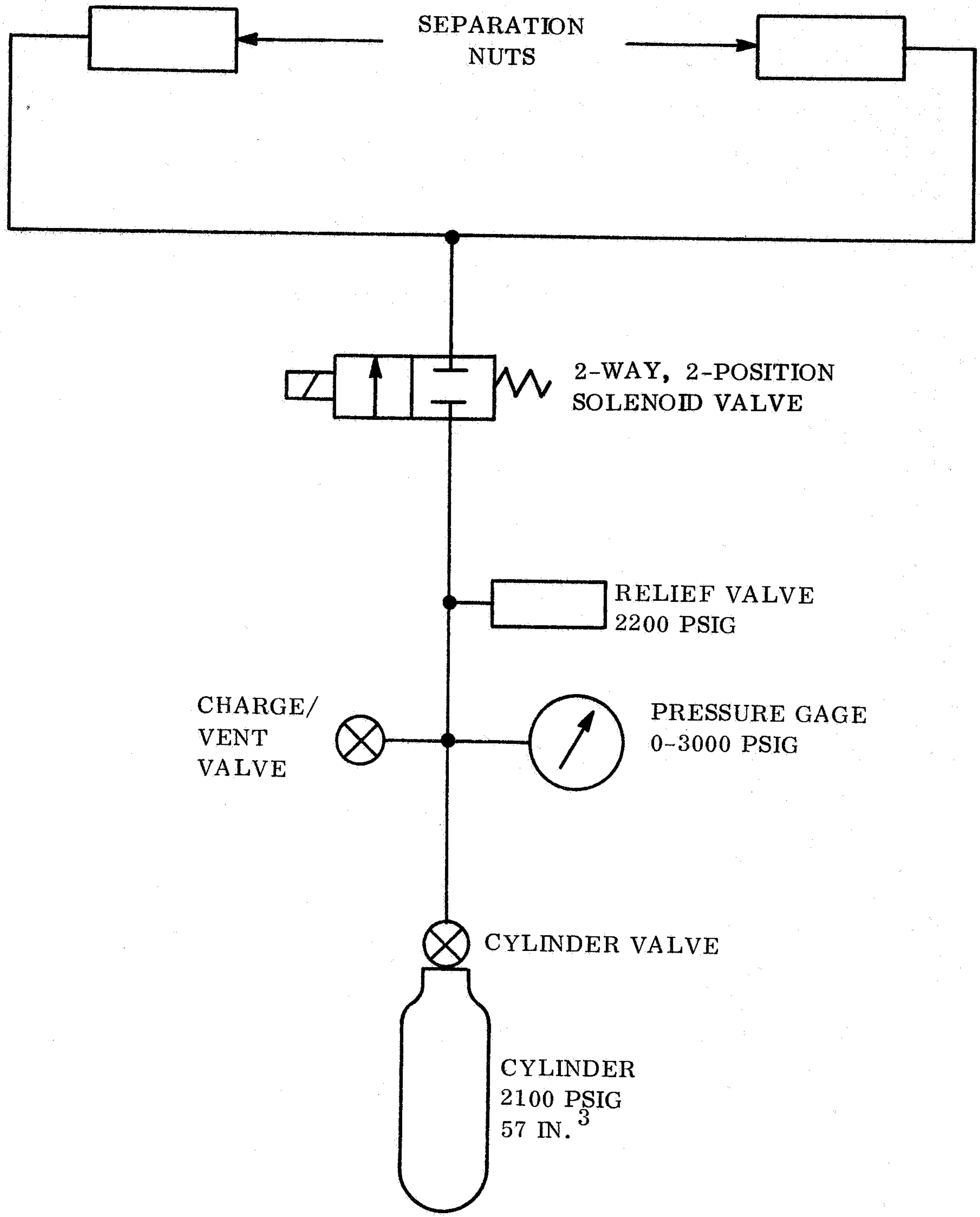

Figure 9. Schematic Diagram of the Separation Nut Actuation System

2.5.2 ELECTRICAL DESIGN

Electrical power (18 to 30 vdc) is required for the BI-STEM motor and the solenoid valve. Figure 10 is a schematic of the proposed electrical system that will control the power for these functions. This electrical system is self-contained in that it includes a 4-ampere hour, rechargeable alkaline battery. A DPST toggle switch (SW6) which turns the battery power on or off. External power jacks (Figure 11) are located on the control panel in order for a laboratory dc power supply to furnish the power for motor operation or for recharging the battery. A DPDT toggle switch (SW5) controls the power to the BI-STEM motor. This switch has three positions: EXTEND, NEUTRAL, and RETRACT. In the EXTEND position, power is applied to the BI-STEM motor in the extend direction through switches SW1, SW3, and SW4. SW1 is the BI-STEM extension limit switch which changes position when the full extension of 33.5 feet is reached. Microswitches SW3 and SW4 are located on the outboard end supports. These switches (one on each support) are held open, as shown, when the outboard end supports are in the closed, or stowed, position. Thus, power can not be applied to extend the rod until the end supports have been released.

With SW5 in the RETRACT position, power is applied to the BI-STEM motor in the retract direction through the retraction limit switch, SW2. This switch changes position as soon as the rod is extended beyond its fully retracted position. A push button switch (SW7) applies power to the solenoid valve in order to actuate the separation nuts.

2.5.3 1-G VERTICAL DEPLOYMENT

It is the intent to deploy the EDM vertically upward to its fully extended length of 402 inches. The detailed structural analysis of this condition is described in Reference 2. The loading on the deployable rod is shown in Figure 12. Equation 2-14 from Reference 2 can be used to establish the allowable combined loading on the tip of the rod ($\tan k\ell = -\frac{W}{T} k\ell$).

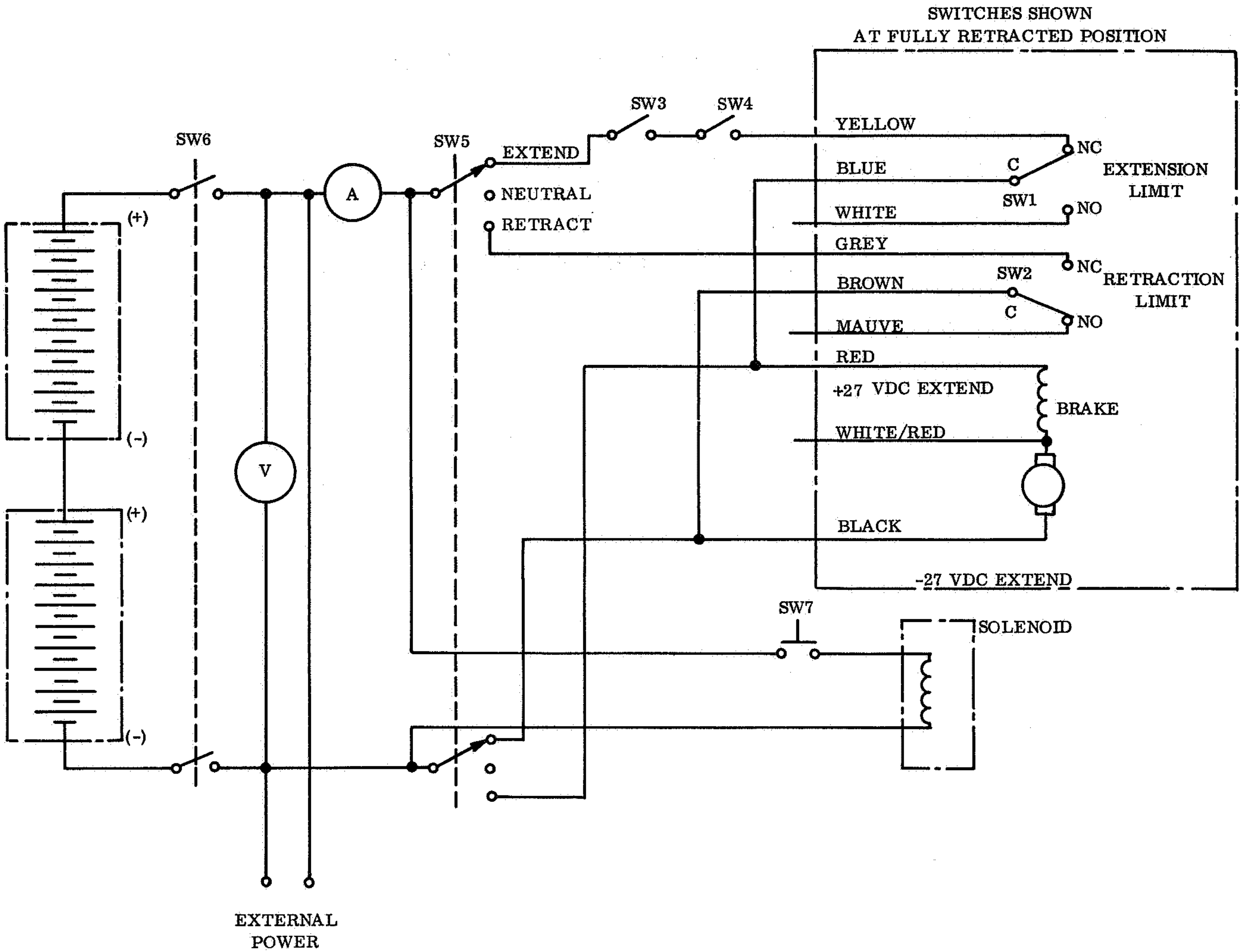

Figure 10. Electrical Schematic Diagram of the Engineering Demonstration Model

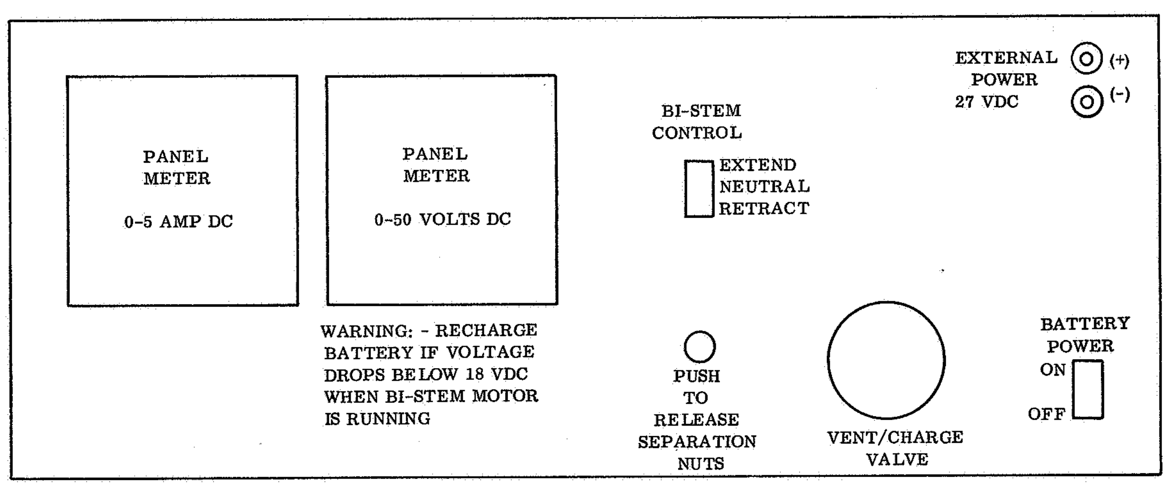

Figure 11. Control Panel Layout

The solution of this equation is shown graphically in Figure 13.

For the present loading on the model:

$T = 4.25$ pounds (9 in.-lb Neg'ator B motors are used in the EDM)

$W = w_1 + w_2 + 0.30\ w_3$*

where

w_1 = weight of leading edge member
= 1.13 lbs.

w_2 = weight of array strips
= 0.90 lbs.

w_3 = weight of deployable rod
= 6.37 lbs

$\therefore W = 3.94$ lbs

For $\frac{W}{T} = 0.927$, $m = 2.06$ (from Figure 13).

$$(T + W)_{CR} = \frac{m^2 EI}{\ell^2} = \frac{(2.06)^2 (29 \times 10^6)(0.01185)}{(402)^2}$$

$$(T + W)_{CR} = 9.02 \text{ lbs}$$

$$T + W = 4.25 + 3.94 = 8.19 \text{ lbs (limit)}$$

$$MS = \frac{9.02}{1.25\ (8.19)} - 1 = -0.12$$

Thus, this analysis shows a slight negative margin of safety based on design loads for vertical, full length deployment in 1G. This indicates that a deployment aid may be required

*These weights have been revised from those contained in Reference 2 to reflect the current status of the EDM.

if the rod is to be deployed to its fully extended length of 33.5 feet. This deployment aid may be as simple as a ring around the rod at 1/3 the distance from the root to limit lateral displacement at this point and effectively reduce the length of the column.

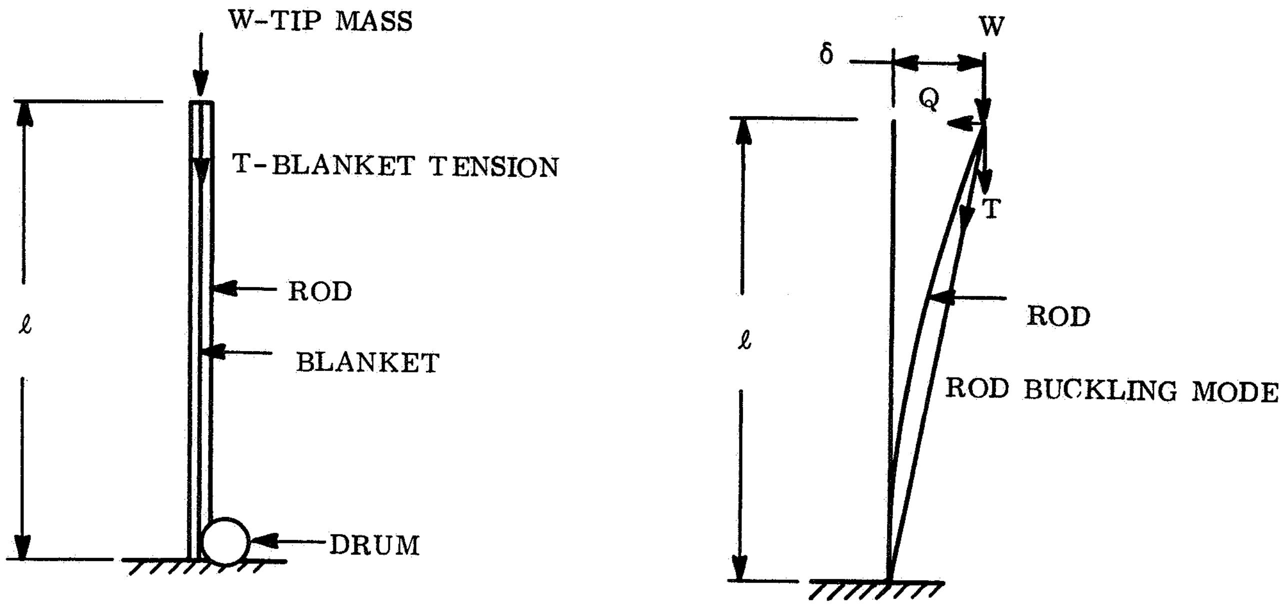

Figure 12. Rod Loading, 1-G, Demonstration Model

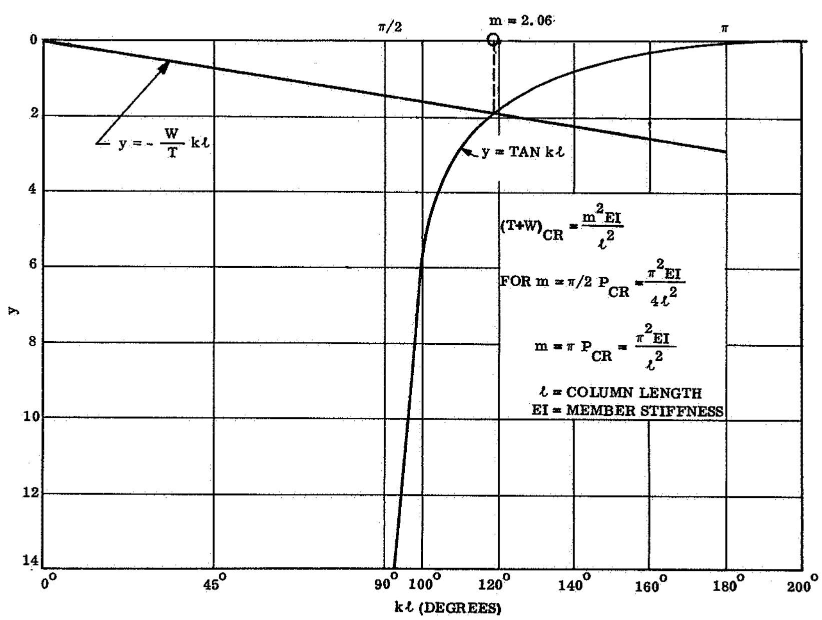

Figure 13. Critical Buckling Load for 1-G Model Rod

SECTION 3

CONCLUSIONS

Based on the discussion presented in Section 2.1, it is concluded that array blanket edge curling will not be observable on the flight configuration roll-up solar array.

The use of 2-ohm cm base resistivity cells is required to obtain the specified power-to-area ratio of 10 watts/ft^2.

SECTION 4
RECOMMENDATIONS

It is recommended that the fabrication of the Engineering Demonstration Model, as described in Section 2.5, be completed. The thermal cycling tests, which were started during this quarter, should continue into the final quarter in order for conclusive results to be obtained.

SECTION 5
NEW TECHNOLOGY

No reportable items of new technology have been identified.

SECTION 6

REFERENCES

1 "Quarterly Technical Report No. 1, Feasibility Study - 30 Watt per Pound Roll-up Solar Array," GE Document No. 67SD4403, October 15, 1967.

2 "Quarterly Technical Report No. 2, Feasibility Study - 30 Watt per Pound Roll-up Solar Array," GE Document No. 68SD4208, January 24, 1968.

3 Horvay, G. "The End Problem of Rectangular Strips," Journal of Applied Mechanics, March, 1953.

4 Horvay, G., and Born, J. S., "Tables of Self-Equilibrating Functions," Journal of Mathematics and Physics, Vol. XXXIII, No. 4, January, 1955.

5 Ralph, E. L., "Performance of Very Thin Silicon Solar Cells," Sixth Photovoltaic Specialists Conference, March 28-31, 1967.

6 Muraca, R. F. and Whittick, J. S., "Polymers for Spacecraft Applications, Final Report," JPL Contract No. 950745, September 15, 1967.

7 Whipple, C. L., "Progress Report - Thermal-Vacuum Performance of Silicones," Aerospace Applications Laboratories, Dow Corning Corporation, Midland, Mich., September 20, 1963.

APPENDIX A

TECHNICAL PRESENTATION

TECHNICAL PRESENTATION

30 WATT PER POUND ROLL-UP SOLAR
ARRAY FEASIBILITY STUDY

JPL CONTRACT 951970

GENERAL ELECTRIC CO.
SPACECRAFT DEPARTMENT
VALLEY FORGE SPACE TECHNOLOGY CENTER

JANUARY 30, 1968

(VISUAL AIDS USED DURING THE MID-TERM
CONTRACT REVIEW PRESENTATION)

AGENDA

INTRODUCTION	K. L. HANSON
DESCRIPTION OF SELECTED FLIGHT SYSTEM	K. L. HANSON
TRADEOFF STUDIES	K. L. HANSON
PERFORMANCE ANALYSIS	N. F. SHEPARD
COMPONENT DESIGNS	N. F. SHEPARD
DESIGN REVIEW	F. A. BLAKE
ENGINEERING DEMONSTRATION MODEL	F. A. BLAKE
SUMMARY	K. L. HANSON
QUESTION PERIOD	STAFF

INTRODUCTION

REQUIREMENTS

- 250 FT^2 PANEL (TOTAL OF 1000 FT^2 FOR VEHICLE)
- WEIGHT GOAL : 30 WATT / POUND
- GROUND RULES
  - 10 WATTS PER SQUARE FOOT
  - 8 MIL SOLAR CELLS
  - 3 MIL COVER GLASS
- FIRST MODE RESONANT FREQUENCY ABOVE 0.04 Hz
- DESIGN TO USE MATERIALS AND TECHNOLOGIES THAT CAN BE DEVELOPED TO PRODUCTION WITHIN ONE YEAR
- STOW WITHIN ENVELOPE OF SATURN SHROUD
- DEPLOYED SURFACE SOLAR ANGLE OF INCIDENCE $< 10°$
- FABRICATE ENGINEERING MODEL

ENVIRONMENTAL REQUIREMENTS

- VIBRATION

  SINE 0-200 Hz, 4 g(O-P), 2 OCT/MIN

  RANDOM $0.1g^2/Hz$, 200-600 Hz,
  ROLLOFF 6db/OCT, 3 MINUTES

- ACOUSTIC NOISE

  SPL = 146db OVERALL

- ACCELERATION

  +13g OR -4g LONGITUDINAL AXIS
  6 g LATERAL AXIS

- THERMAL SHOCK

  -100 TO +75°C, 30°C/MIN

- MATERIALS SELECTION CRITERIA

  95% RH AT 30°C FOR 50 HRS

  -20° TO +60°C, 150 THERMAL CYCLES

  -195° TO +140°C, 10^{-7} TORR, 10 THERMAL CYCLES

- SOLAR INTENSITY

  140 TO 260 mw/cm^2

- RADIATION DOSE

  10^7 RADS

- DEPLOYED STEP ACCELERATION

  2×10^{-5} RAD/SEC^2 PITCH ANGLE ACCELERATION,

  13 SEC TO 5 MINUTE DURATION

TYPICAL NOSE FAIRING AND SPACECRAFT ENVELOPE

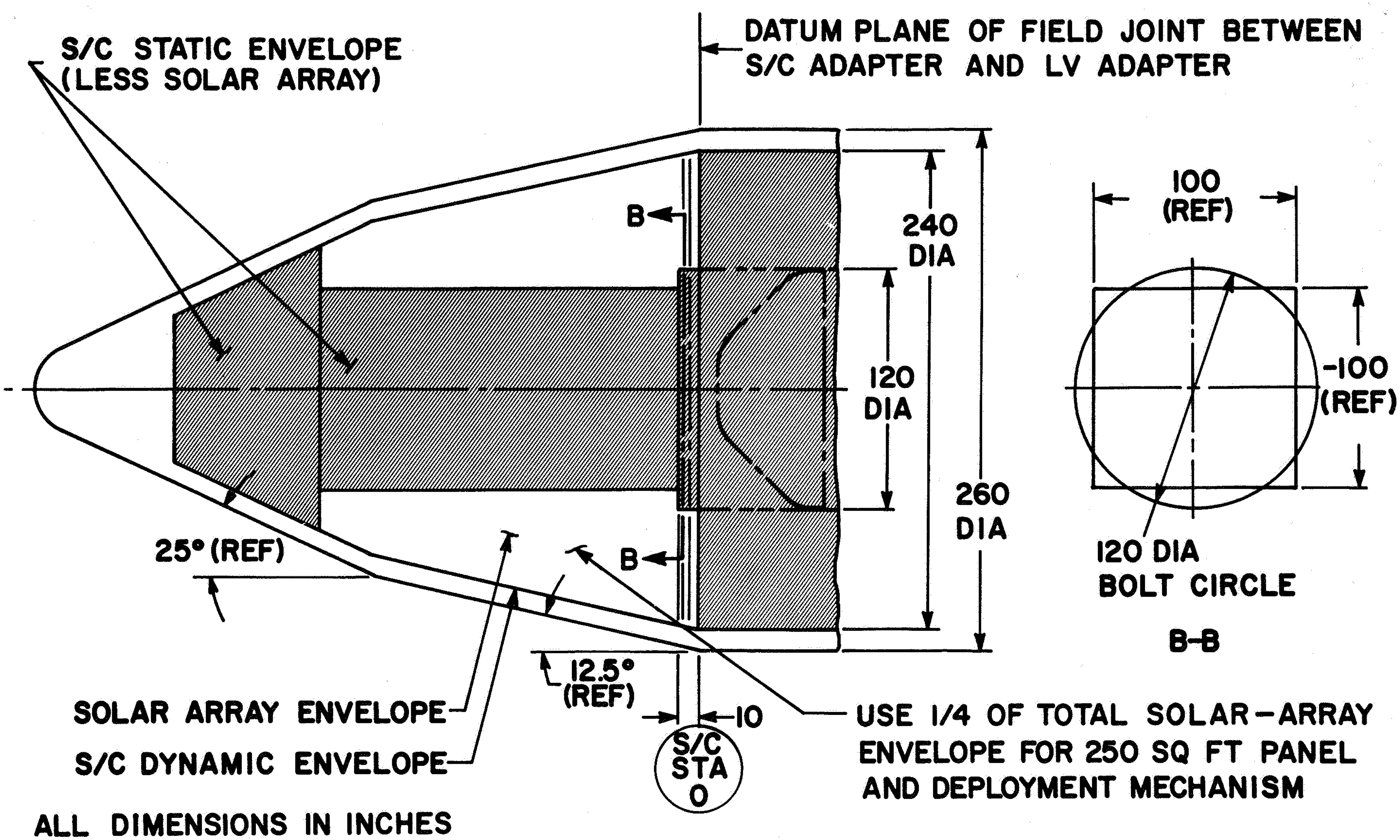

FUNDAMENTALS

250 FT^2 10 WATTS/FT^2 30 WATTS/POUNDS	=	2500 WATTS 83.3 POUNDS TOTAL 0.33 POUND/FT^2
8 MIL SOLAR CELLS 3 MIL COVERS SUBSTRATE INTERCONNECTIONS	≈	43 POUNDS 0.172 POUND/FT^2

- STRUCTURE, MOUNTING, AND DEPLOYMENT HARDWARE MUST WEIGH LESS THAN 40 POUNDS

GOALS

- EXCEED PERFORMANCE REQUIREMENTS

- ADAPTABLE DESIGN

GOALS

- NO TECHNOLOGICAL BREAKTHROUGHS REQUIRED
- USE OFF-THE-SHELF HARDWARE

GOALS

- TEST DESIGN AGAINST SUCCESSFUL FLIGHT SYSTEMS
- ROLL-UP ARRAYS FOR NEXT SPACECRAFT

PROGRAM STRUCTURE

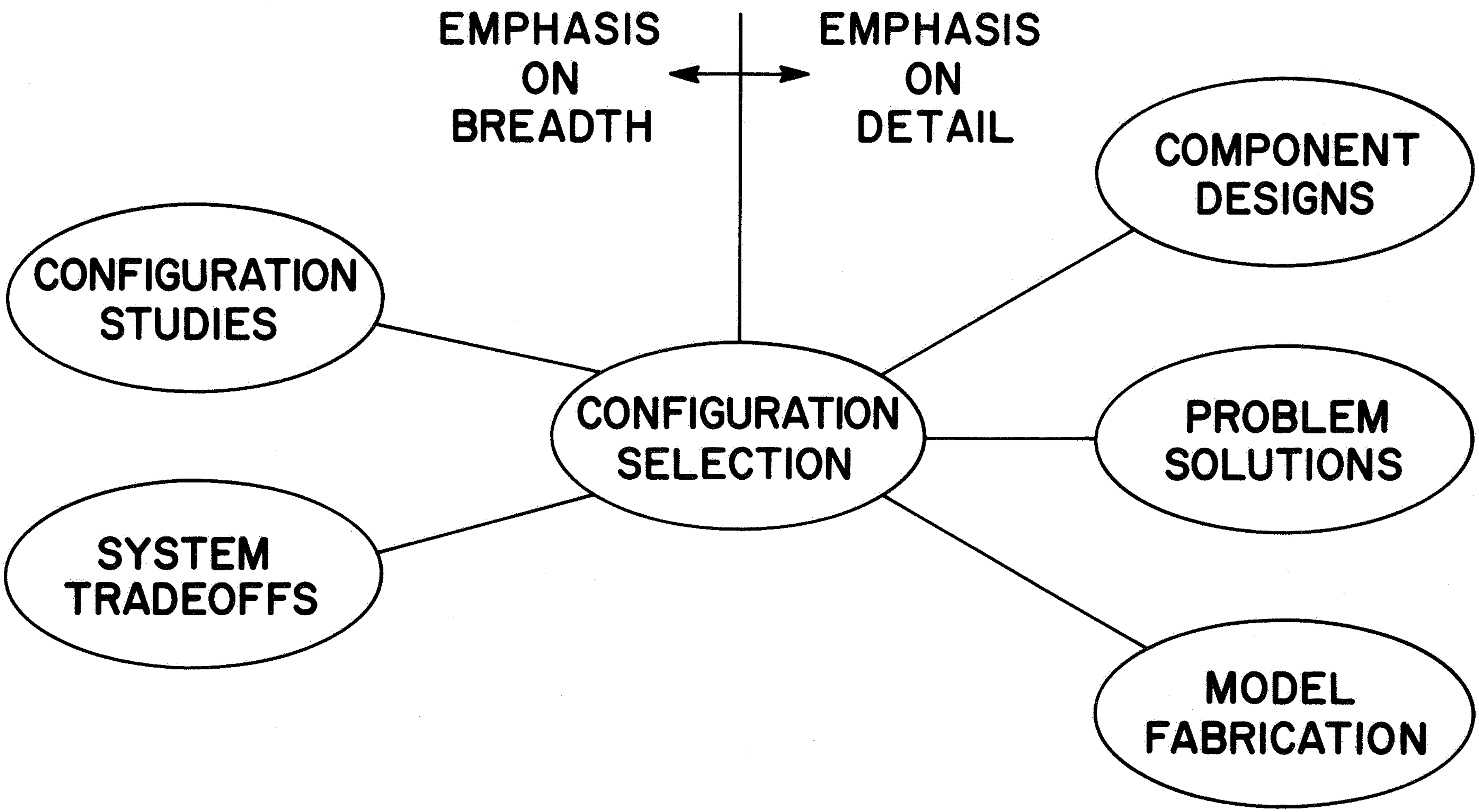

SUMMARY OF ARRAY PERFORMANCE

REQUIRED	DESIGN
1. 30 WATTS/LB (MIN)	33.1
2. 10 WATTS/FT^2 NOMINAL	10.0
A. 2X2 CM CELL 0.008 INCH THICK	2X2 CM CELL 0.008 INCH THICK
B. 225 CELL/FT^2 (MAX)	220.62
C. 49.5 MW/CELL (MAX) AT 140 MW/CM^2 AND 55 °C	45.31
3. 250 FT^2 NOMINAL PANEL AREA	250.09 FT^2 GROSS MODULE AREA
4. 2.5 KW OF ELECTRICAL POWER PER PANEL	2.5 KW AT 1,000 AU AND 55° C

DESCRIPTION OF SELECTED FLIGHT SYSTEM

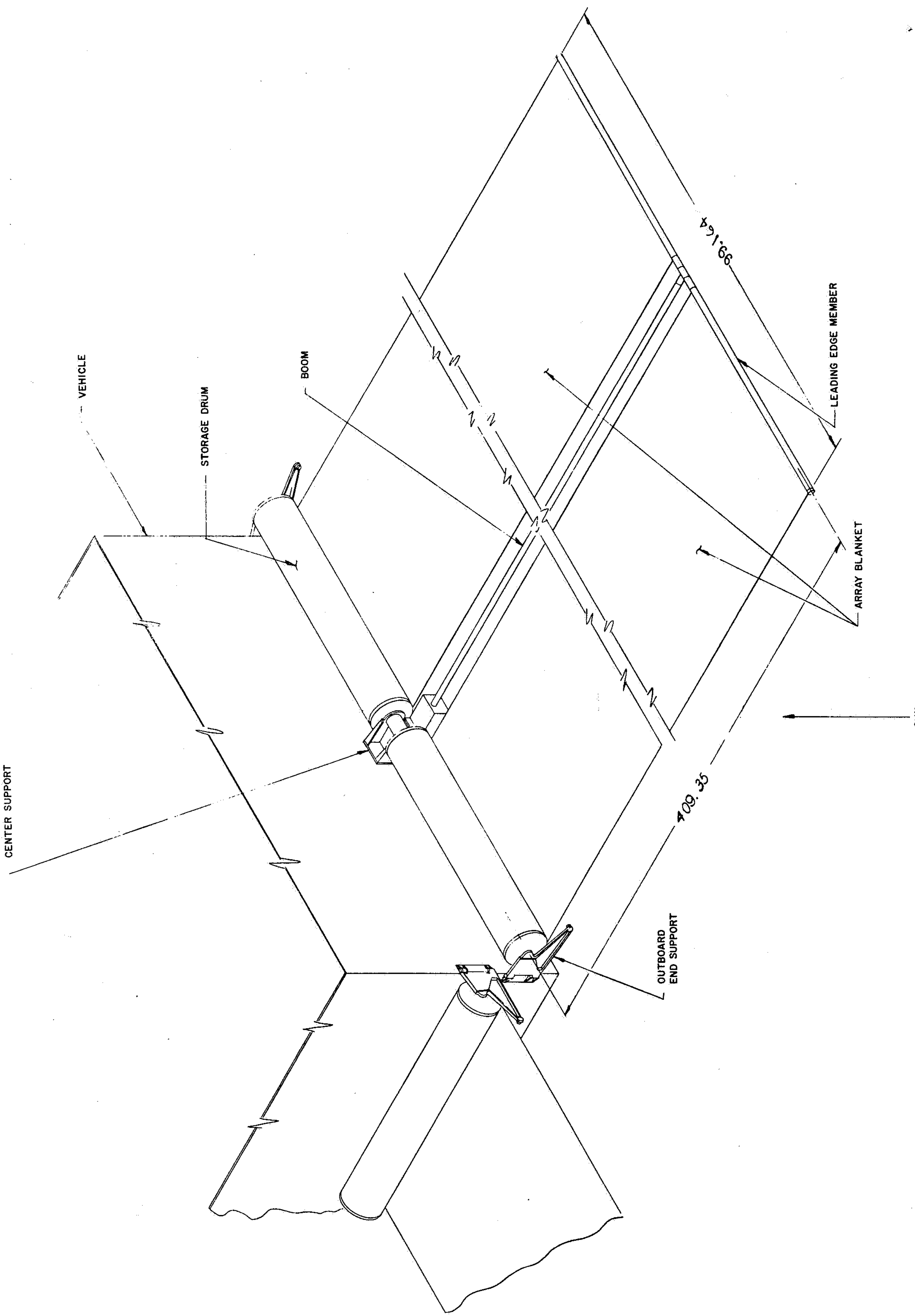
VEHICLE
STORAGE DRUM
BOOM
LEADING EDGE MEMBER
99.164
ARRAY BLANKET
SUN
409.35
CENTER SUPPORT
OUTBOARD
END SUPPORT

ROLL-UP SOLAR ARRAY ASSEMBLY

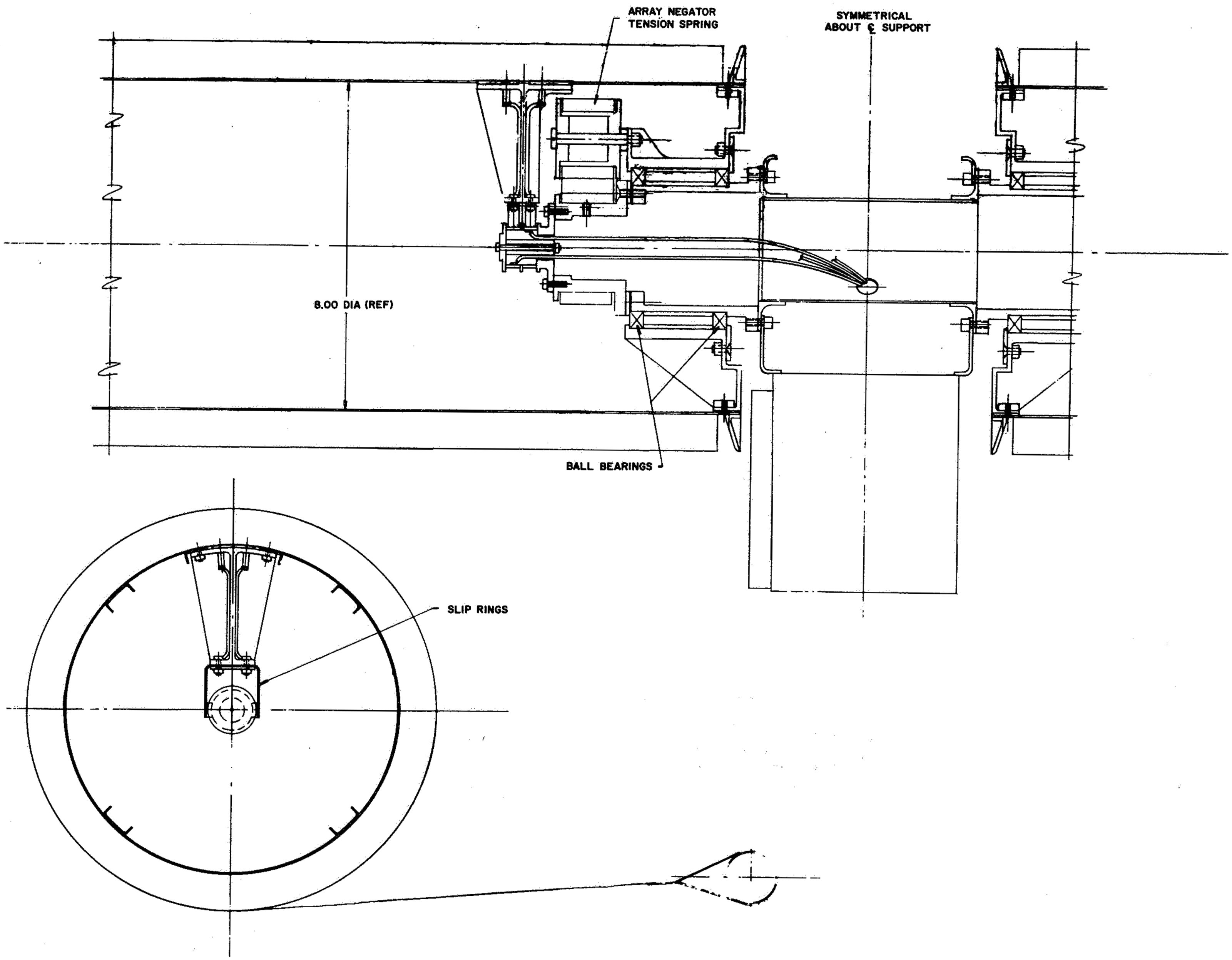

TRADEOFF STUDIES

- ARRANGEMENT ON VEHICLE
- SINGLE VERSUS DOUBLE BOOM
- ROD AND DEPLOYER CONSIDERATIONS
- DRUM SUPPORT ARRANGEMENT
- ARRAY BUS STRIP CONSIDERATIONS
- POWER TAKEOFF CONSIDERATIONS

ARRANGEMENT ON VEHICLE

ARRANGEMENT OF ARRAYS ON VEHICLE

- **REQUIREMENTS**

  1000 FT^2 OF DEPLOYABLE ARRAY
  (250 FT^2 PER ARRAY ELEMENT)

  ARRAY, DRUM, AND DEPLOYMENT DEVICE MUST FIT WITHIN THE MOUNTING ENVELOPE

  ARRAY SURFACES ARE NORMAL TO THE LONGITUDINAL AXIS OF THE VEHICLE

SELECTED CONFIGURATION

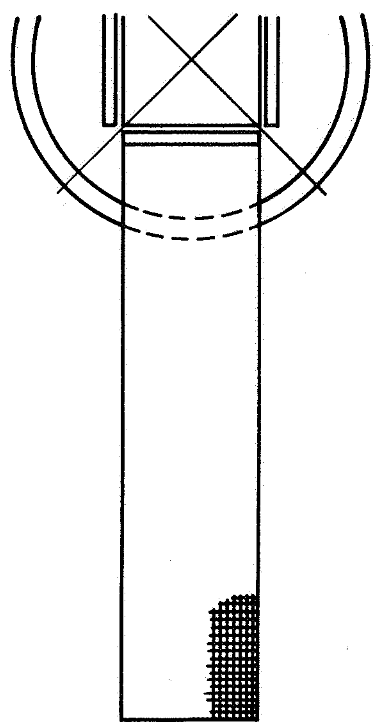

- 4 FIXED STORAGE DRUMS
- DRUM LENGTH $\leq$ 100 INCHES
- ONE ARRAY BLANKET PER DRUM

LOWER ASPECT RATIO CONFIGURATIONS

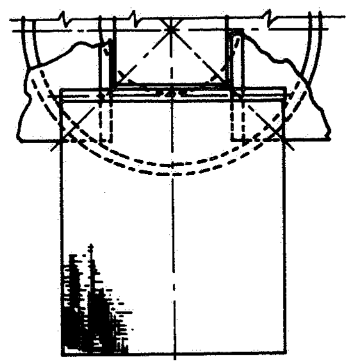

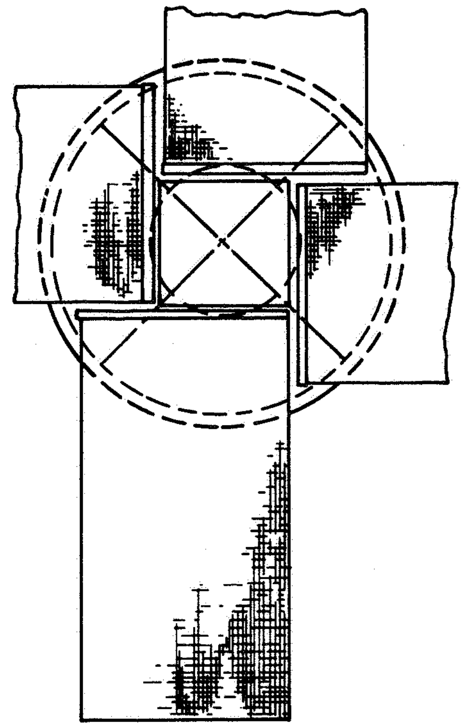

- 4 FIXED DRUMS
- ONE ARRAY BLANKET PER DRUM

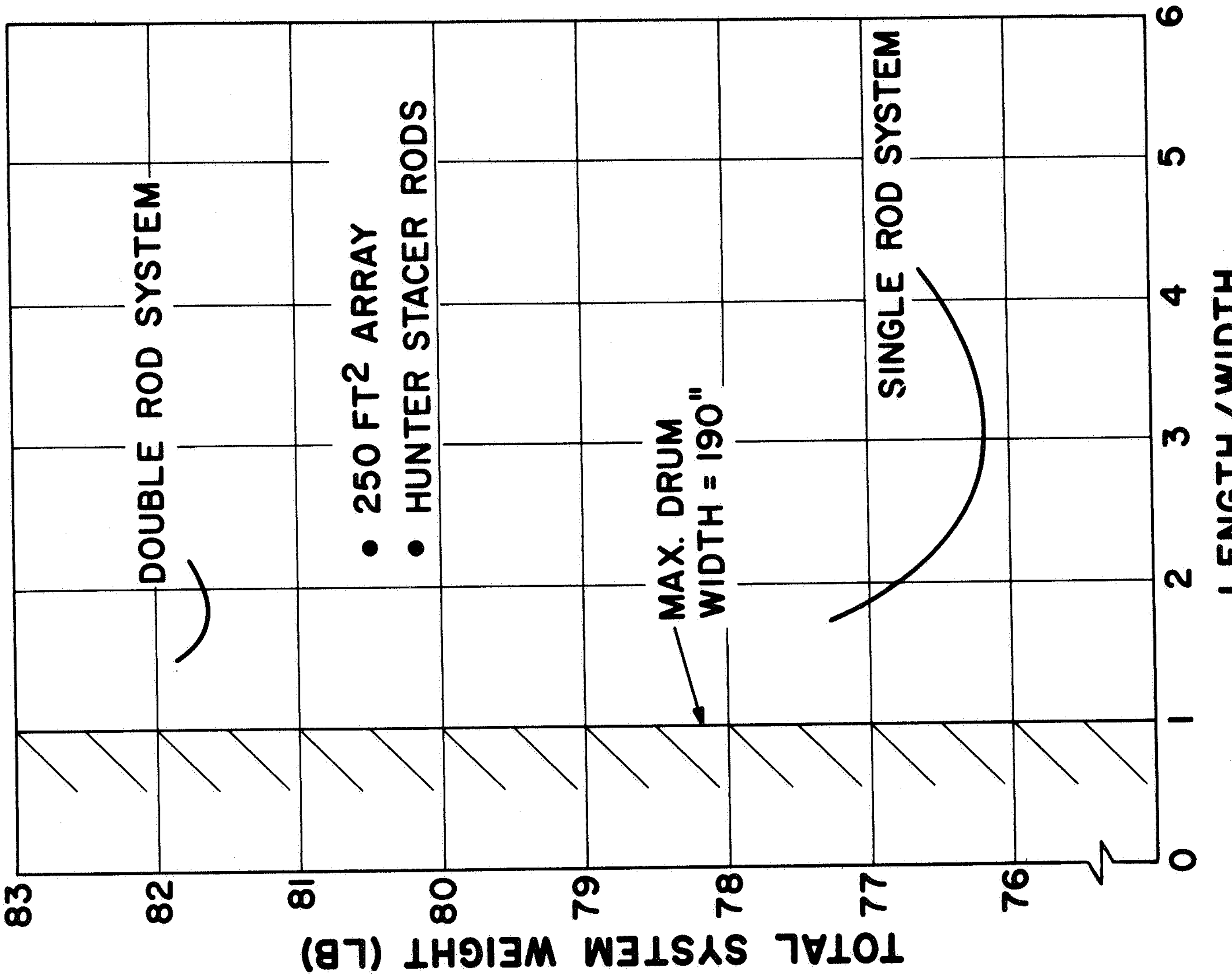
DOUBLE ROD SYSTEM
• 250 FT2 ARRAY
• HUNTER STACER RODS
MAX. DRUM
WIDTH = 190"
SINGLE ROD SYSTEM
TOTAL SYSTEM WEIGHT (LB)
83
82
81
80
79
78
77
76
LENGTH / WIDTH
0
1
2
3
4
5
6

A SINGLE VERSUS DOUBLE BOOM

TYPICAL SINGLE AND DOUBLE BOOM CONFIGURATIONS

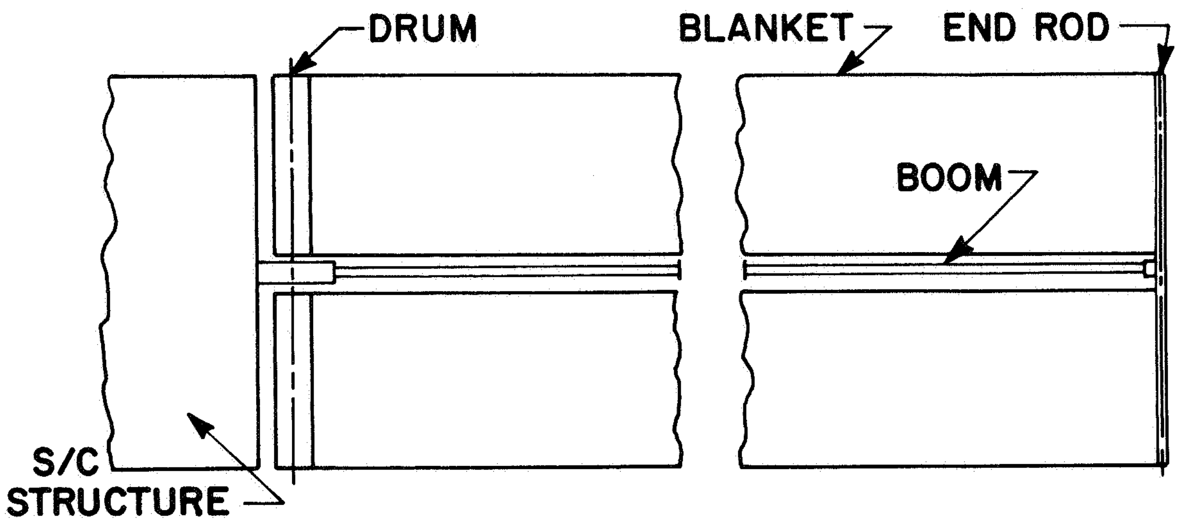

(A) SINGLE BOOM SYSTEM

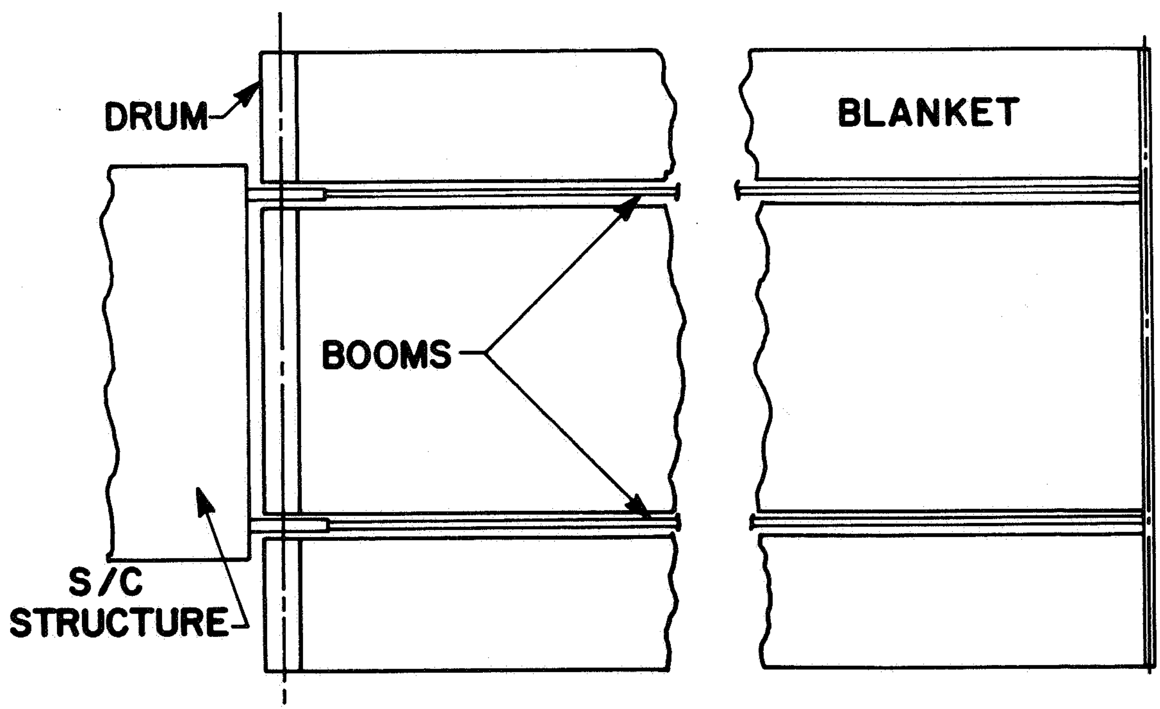

(B) DOUBLE BOOM SYSTEM

COMPARISON OF SINGLE AND DOUBLE ROD SYSTEMS

SINGLE ROD

- LIGHTEST SYSTEM FOR ALL RODS STUDIED
- NO DEPLOYMENT SYNCHRONIZATION
- MORE DRUM SUPPORT OPTIONS
- SINGLE POINT VEHICLE MOUNTING

DOUBLE ROD

- TORSIONAL STIFFNESS PROVIDED BY ROD BENDING

ROD AND DEPLOYER CONSIDERATIONS

TYPES OF DEPLOYABLE BOOMS

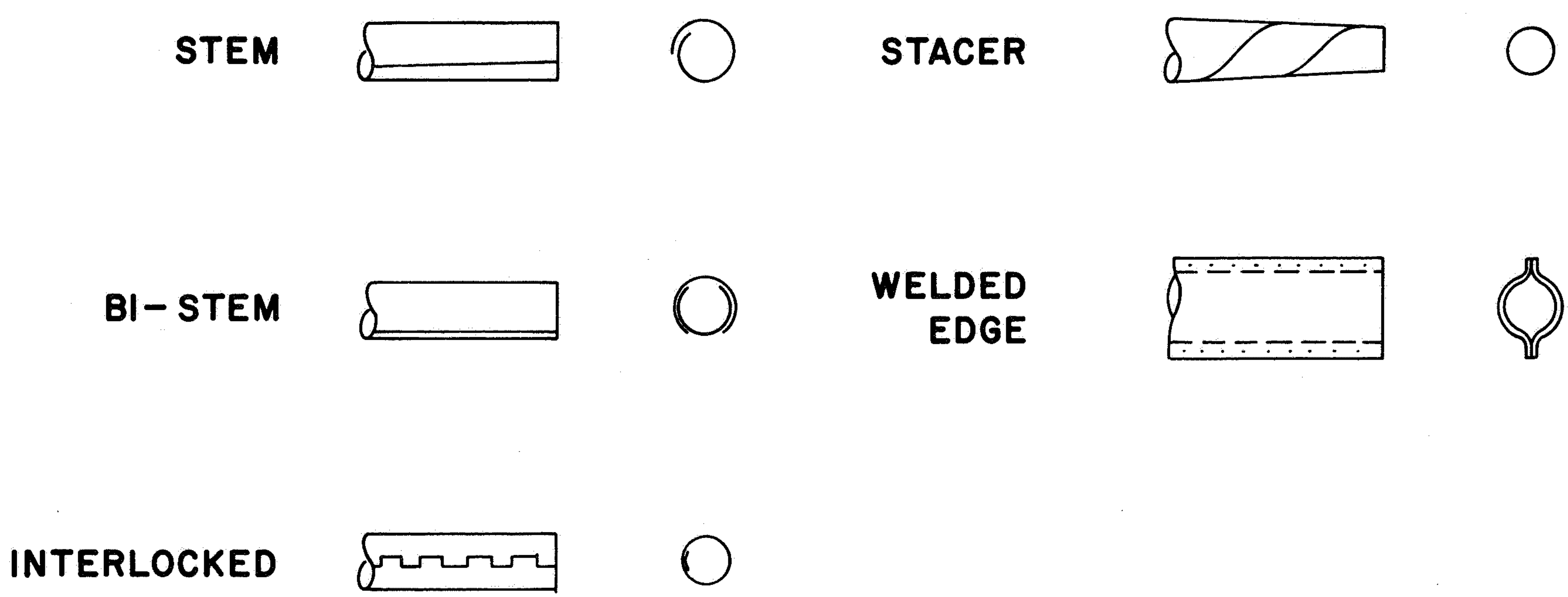

A BI-STEM ACTUATOR

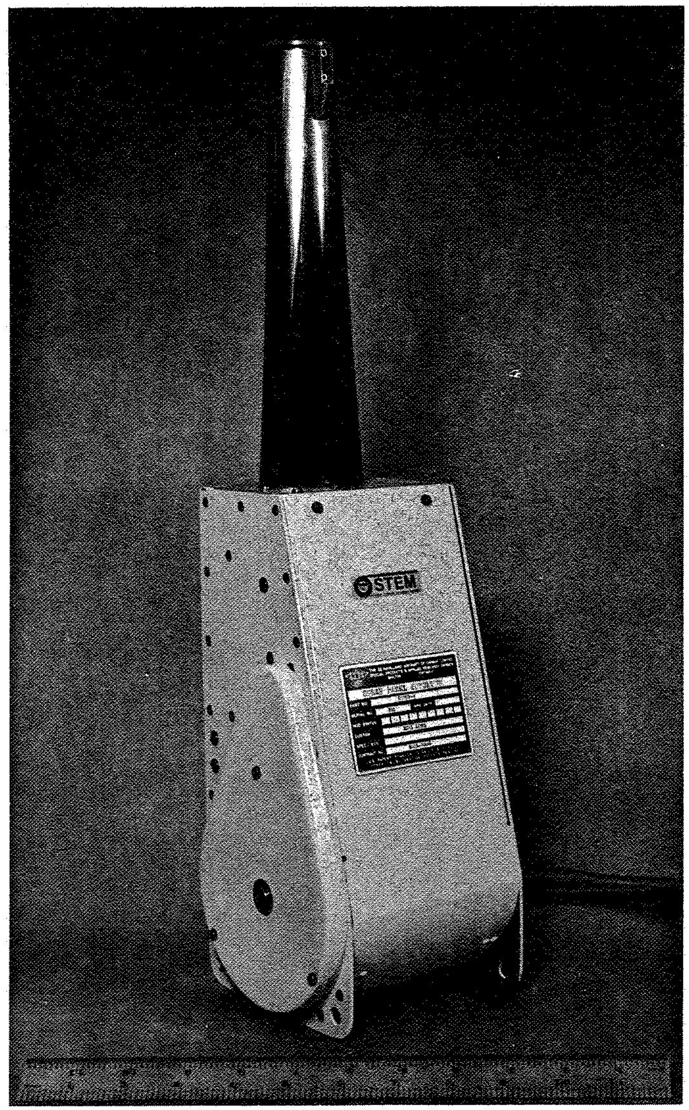

33.5 FT BOOM

BOOM TYPE	CONFIG-URATION	DEPLOYER WEIGHT (LB.)	BOOM WEIGHT (LB.)	TOTAL WEIGHT (LB.)	COMPONENT LENGTH (IN.)
STEM	1.5 x .006 Be Cu OR S/S	8.1	5.13	13.23	18
INTERLOCKED	1.5 x .006 Be Cu OR S/S	9.4	3.78	13.18	30
BI-STEM	1.34 x .007 Be Cu OR S/S	4.6	6.37	10.97	11
WELDED EDGE	NO DATA RECEIVED				
STACER	NO DATA RECEIVED				

REASONS FOR SELECTING BI-STEM

- DEMONSTRATED CAPABILITY
- VERY COMPACT SIZE
- LIGHTWEIGHT
- OFF-THE-SHELF AVAILABILITY
- BASIC SIMPLICITY OF CONCEPT

DRUM SUPPORT ARRANGEMENT

DRUM SUPPORT ARRANGEMENT

METHOD OF MOUNTING OR ATTACHING THE DRUM TO THE VEHICLE

- FOUR BASIC METHODS WERE EVALUATED
- MAJOR TRADEOFFS CONSIDERED

  (1) THE DEPENDENCE OF DRUM BEARING ALIGNMENT AND PRELOAD ON STRUCTURAL INTERACTIONS WITH THE VEHICLE

  (2) WEIGHT OF DRUM AND SUPPORTS

DRUM SUPPORT ARRANGEMENT

DRUM CONFIGURATIONS

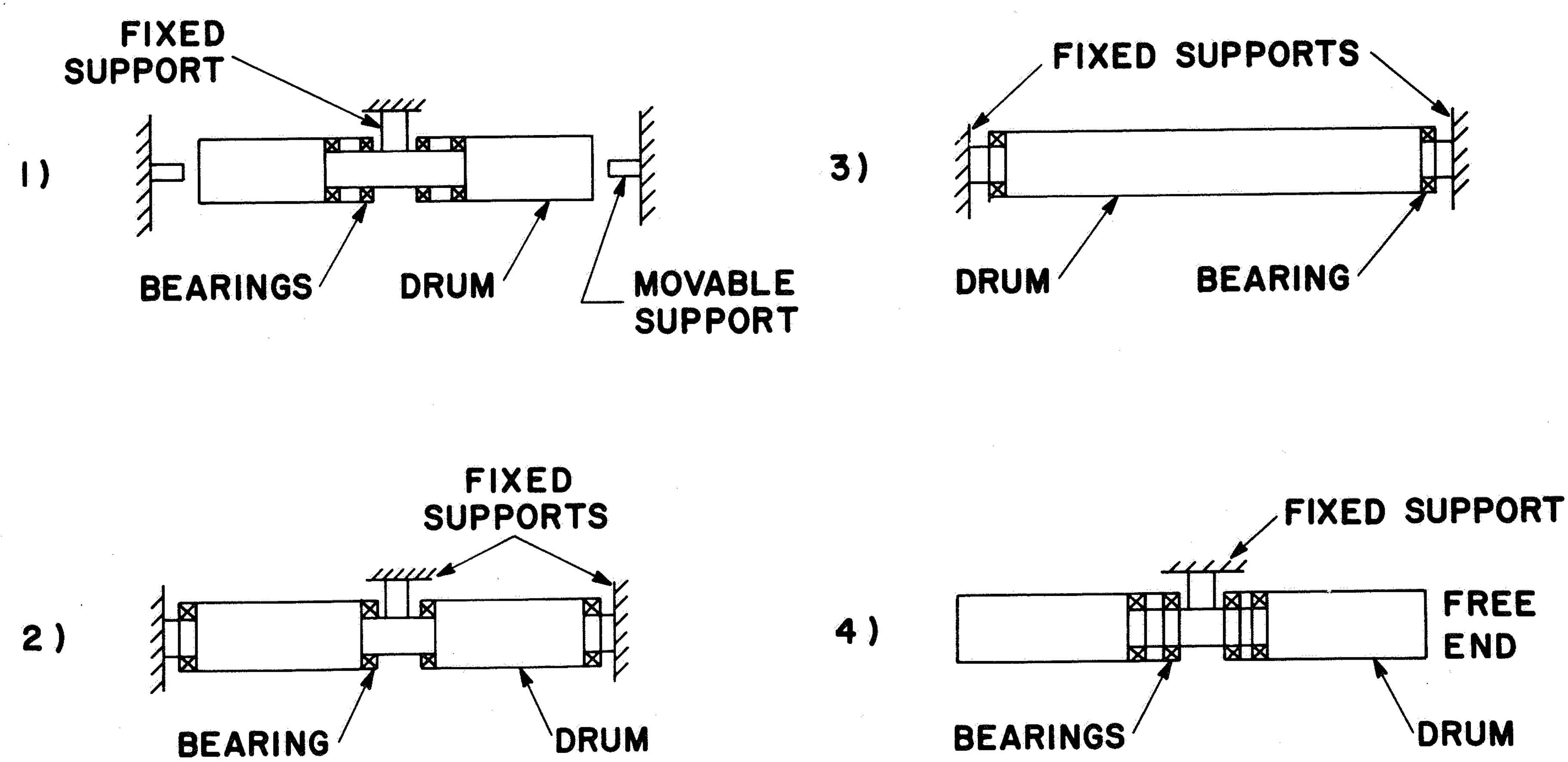

POWER TAKEOFF CONSIDERATIONS

POWER TAKEOFF

- **FUNCTION**

  TRANSFER POWER FROM ARRAY BLANKET TO ARRAY SUPPORT STRUCTURE

- **FOUR APPROACHES CONSIDERED**

  1. COPPER SPIRALS, SEPARATE (+) AND (−), NEG'ATORS PROVIDE BLANKET FORCE
  2. Be Cu SPIRALS, SEPARATE (+) AND (−), NO NEG'ATORS
  3. Be Cu SPIRALS, COMBINE (+) AND (−) ON ONE SPIRAL, NO NEG'ATORS
  4. SLIP RINGS, NEG'ATORS PROVIDE BLANKET FORCE

- **MEASURE OF PERFORMANCE**

  EFFECTIVE WEIGHT = TOTAL SPIRAL (OR SLIP RING) WEIGHT

  $+$ NEG'ATOR WEIGHT (IF ANY)

  $$+ \frac{\text{POWER DISSIPATION}}{30}$$

SUMMARY OF POWER TAKEOFF PARAMETERS

CONFIGURATION	POWER TAKEOFF WEIGHT (LB)	NEGATOR WEIGHT (LB)	POWER DISSIPATION AT 20°C (WATTS)	EFFECTIVE WEIGHT (LB)
1 (NEG'ATOR/ Cu SPIRAL)	1.48	1.30	5.3	2.96
2 (Be Cu SPIRAL)	3.43	—	3.7	3.55
3 (Be Cu SPIRAL)	2.46	—	4.0	2.59
4 (NEG'ATOR/ SLIP RINGS)	0.80	1.30	3.5	2.20

ARRAY BUS STRIP CONSIDERATIONS

BUS STRIP MATERIAL
SCHJELCLAD L5550
(1/2 OZ COPPER ON 1/2 MIL MYLAR)

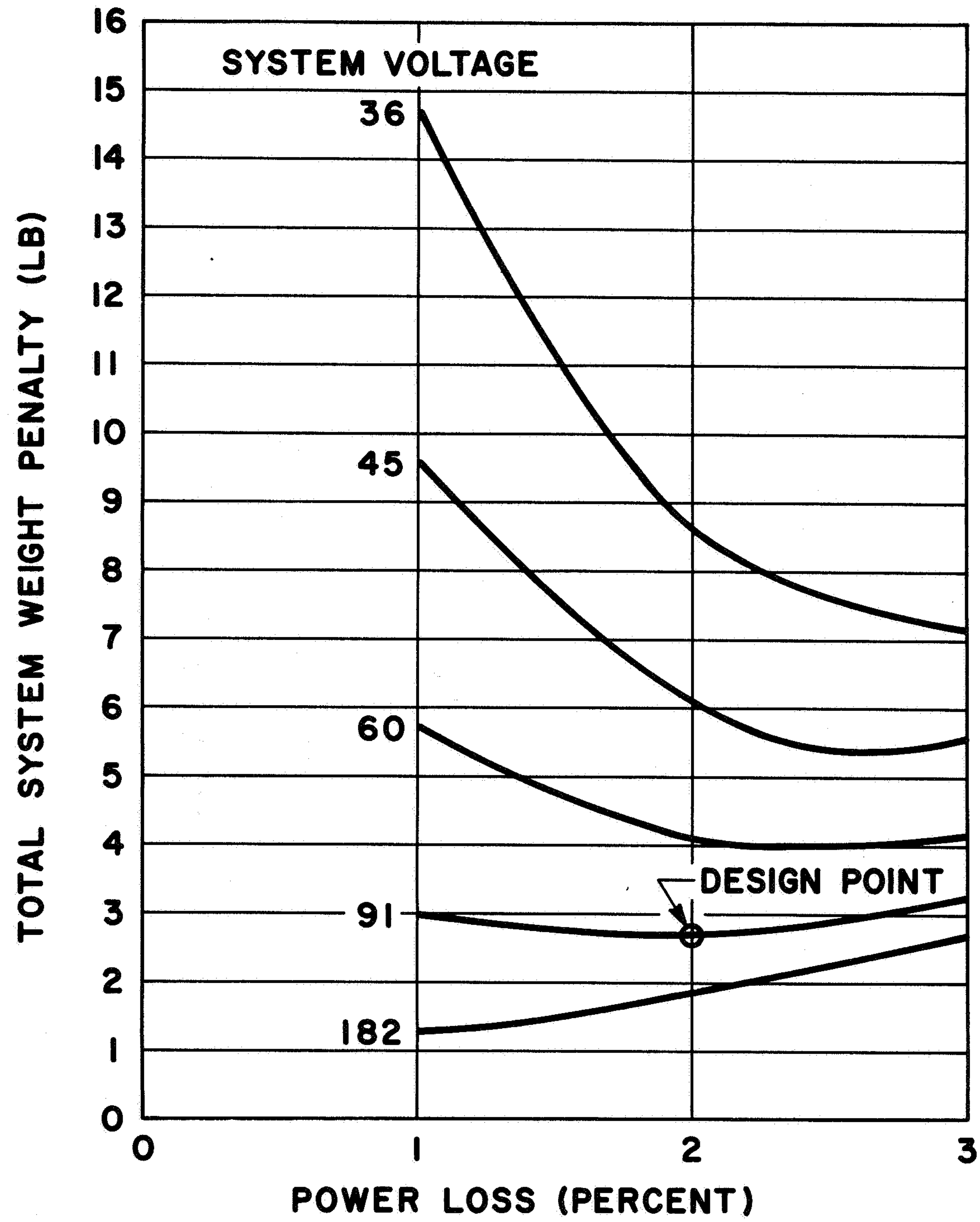

PERFORMANCE ANALYSIS

- DYNAMIC ANALYSIS
- BEAM-COLUMN ANALYSIS
- WEIGHT SUMMARY
- POWER LOSSES

STRING ANALYSIS

$$f_n = \frac{(2n-1)}{4L} \left(\frac{T}{\delta}\right)^{1/2}$$

WHERE

- n = MODE NUMBER
- L = LENGTH OF STRING
- T = TENSION IN STRING [LB]
- δ = LINEAR DENSITY [SLUG/FT]

BOUNDARY CONDITIONS: FIXED, FREE

$$\delta = \frac{\gamma W}{g}$$

WHERE γ = AREA DENSITY [LB/FT^2]

W = WIDTH [FT]

FOR THIS CASE

- L = 34.1 FT
- W = 7.68 FT
- γ = 0.170 LB/FT^2

$$f_1 = 0.213 \left(\frac{T}{L}\right)^{1/2}$$

SINGLE ROD CONFIGURATION

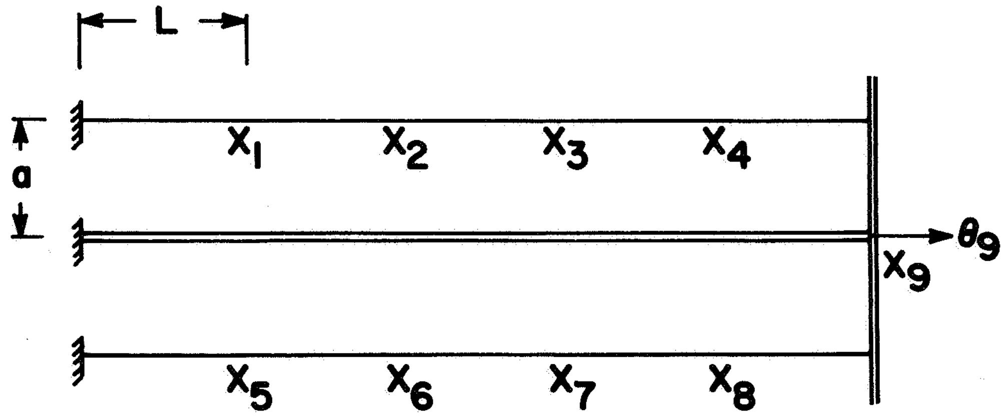

MATHEMATICAL MODEL

- 10 DEGREES-OF-FREEDOM
- 9 MASS POINTS
- ARRAY BLANKETS ACT AS EQUIVALENT STRINGS ATTACHED TO THE LEADING EDGE MEMBER AT 2/3 THE BLANKET WIDTH FROM THE ROD CENTERLINE

FIRST MODE NATURAL FREQUENCIES

SINGLE ROD

LENGTH (FT)	PRELOAD (LB)	FREQUENCY (Hz)	TYPE
33.5	4.0	0.099	BENDING
33.5	9.0	0.130	BENDING
33.5	4.0	0.075	TORSION
33.5	9.0	0.112	TORSION

EFFECTS OF TENSION ON MEMBRANE FREQUENCY

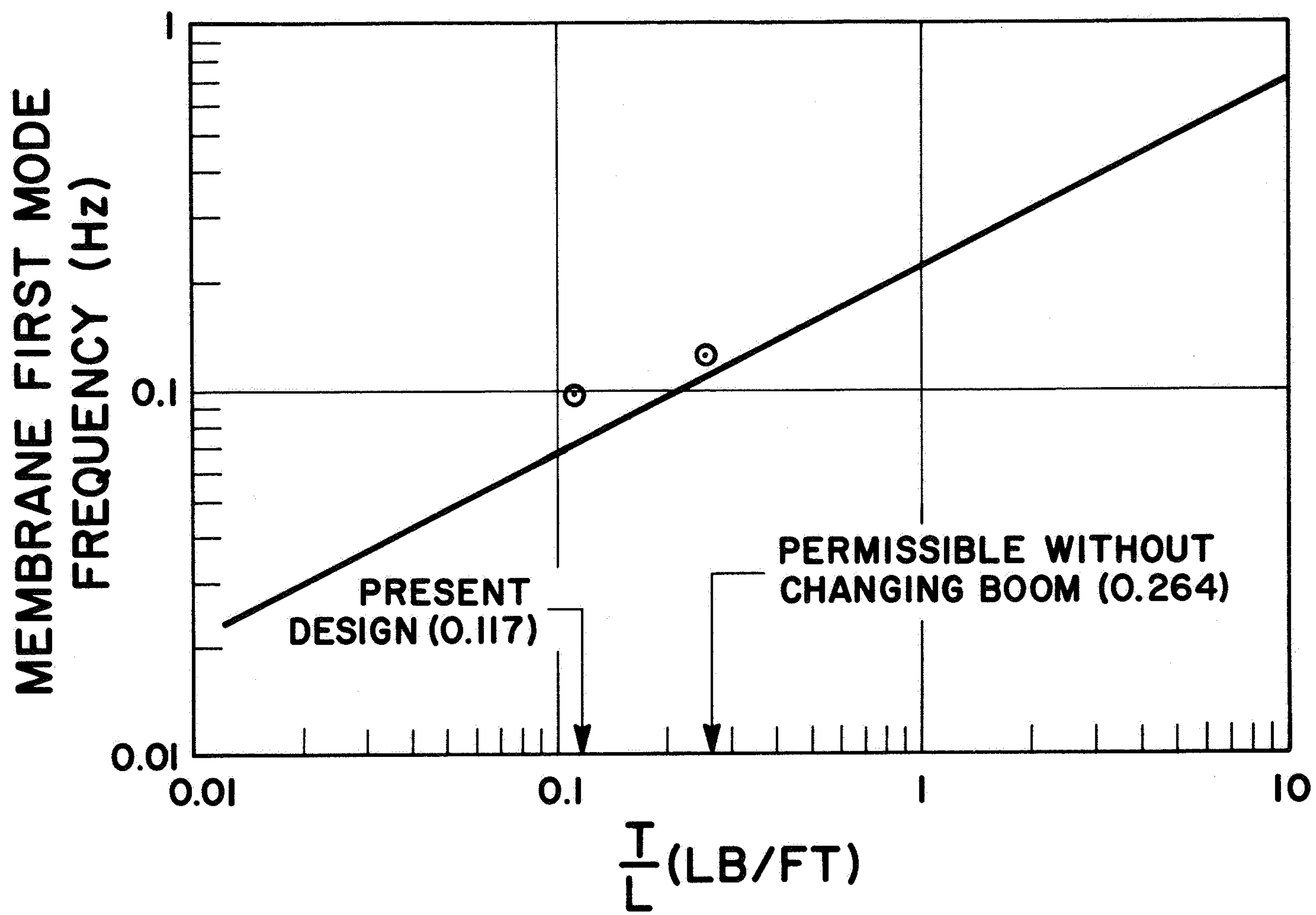

DEPLOYED ARRAY MODE SHAPES

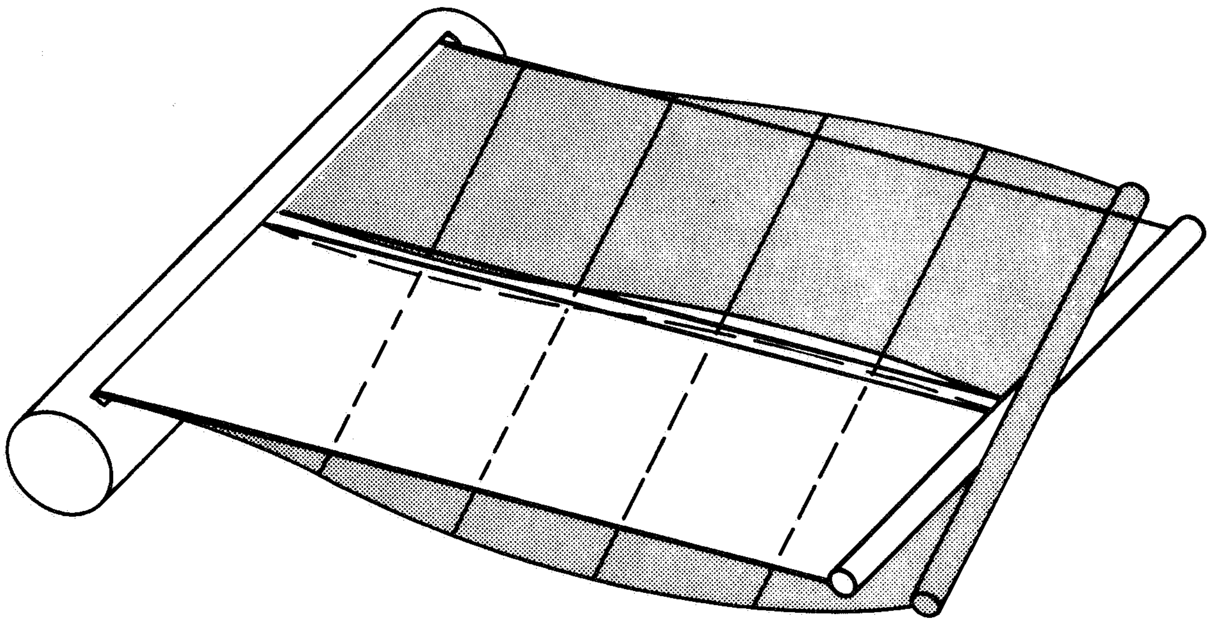

TORSION 0.075 Hz

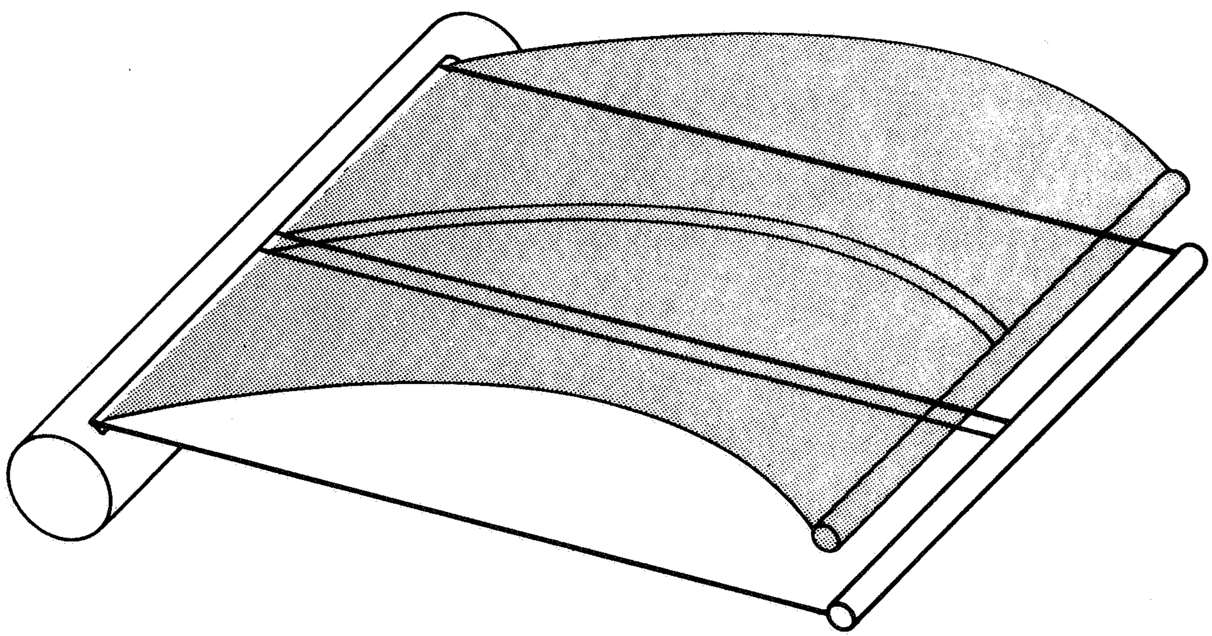

BENDING 0.099 Hz

END ROD RESTORING MOMENT AS A FUNCTION OF ANGLE

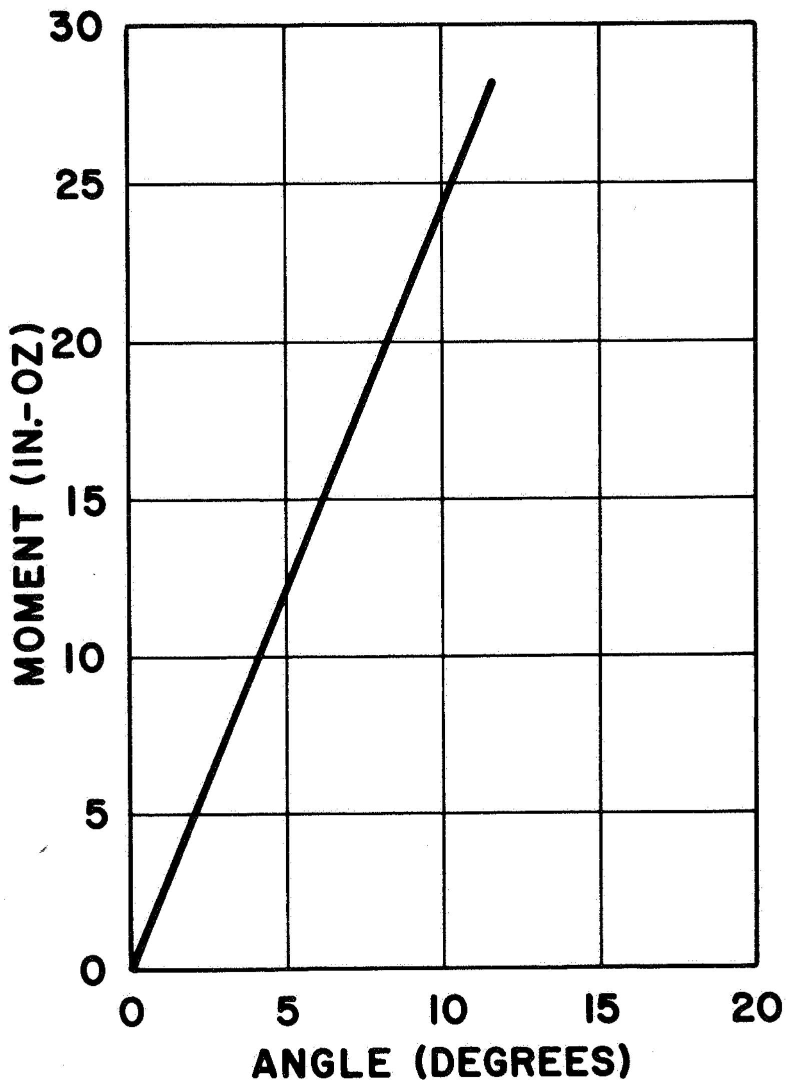

DEPLOYMENT ROD THERMOSTRUCTURAL LOADING

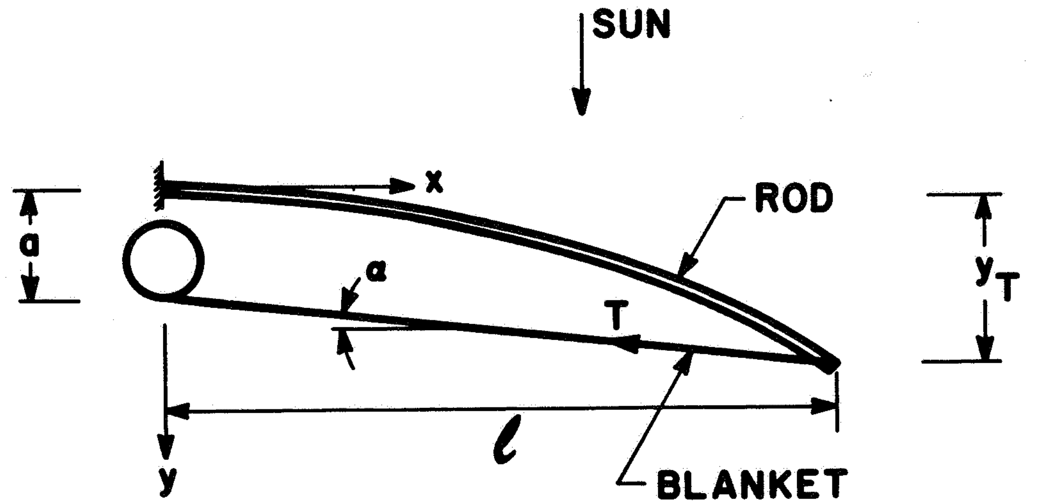

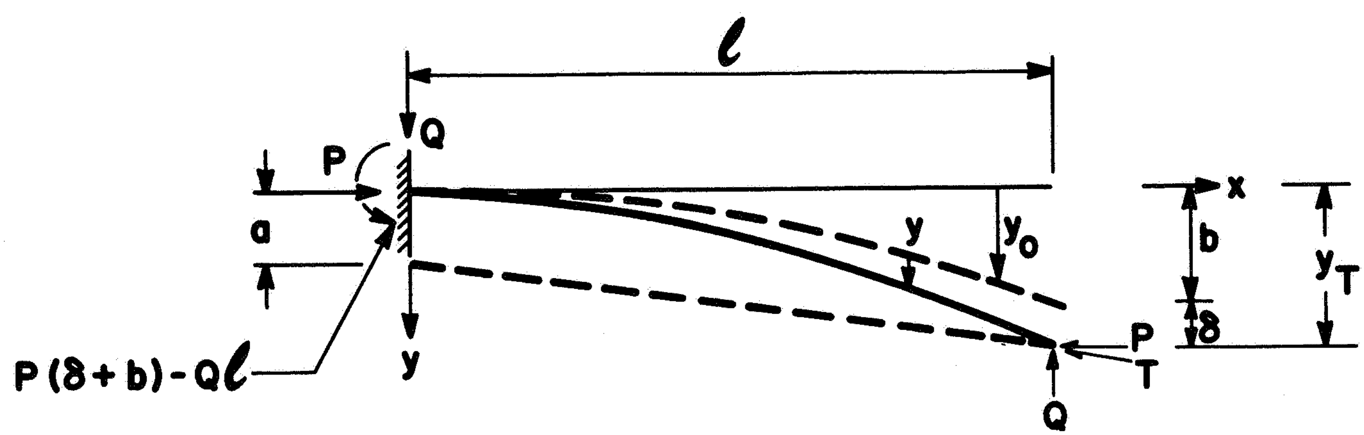

REQUIREMENTS

1. POSITIVE MARGIN OF SAFETY
2. $\alpha < 10°$

ANALYSIS

$$y_0 = \frac{b}{\ell^2} x^2$$

(APPROXIMATES DEFLECTION CURVE DUE TO LINEAR TEMPERATURE GRADIENT WITH PARABOLIC)

$$b = \frac{\alpha \Delta T \ell^2}{4r}$$

$$EI \frac{d^2y}{dx^2} = -M = -\left\{P(y + y_0) + Q\ell - P(\delta + b) - Qx\right\}$$

$$y = -\frac{Q}{kP} \sin kx + \left\{\frac{Q\ell}{P} - \delta - b - \frac{2b}{k^2\ell^2}\right\} \cos kx - \frac{b}{\ell^2} x^2$$

$$+ \frac{Q}{P} x + \delta + b + \frac{2b}{k^2\ell^2} - \frac{Q\ell}{P}$$

WHERE $k = \sqrt{\frac{P}{EI}}$

AT $x = \ell$
$y = \delta$

$$\delta = \frac{b\{2(1 - \cos k\ell) - k\ell \sin k\ell\} + a\{k\ell \cos k\ell (\tan k\ell - k\ell)\}}{k\ell \sin k\ell}$$

MEMBER BUCKLES AT THE SAME CRITICAL LOAD AS A PIN-ENDED COLUMN. $P_{CR} = \frac{\pi^2 EI}{\ell^2}$

- **FOR THE PROPOSED SYSTEM**

  $E = 29 \times 10^6$ PSI

  $I = 0.01185$ IN.^{4}

  $\ell = 402$ IN.

  $\Delta T = 53.9°F$ (SILVER PLATED BI-STEM AT 260 MW/CM^2)

  $T = 4.0$ LB

- **RESULTS**

ROD TIP DEFLECTION	35.68 IN.
PERMISSIBLE DEFLECTION	69.81 IN.
MAXIMUM BENDING MOMENT (AT ROD MID-LENGTH)	46.44 IN.-LB
$P_{CR} = \frac{\pi^2 E I}{\ell^2} = 20.97$ LB	
ULTIMATE BENDING STRENGTH	984 IN.-LB
MS = HIGH	

WEIGHT SUMMARY

COMPONENT		WEIGHT (LB)
ARRAY		42.5
STORAGE DRUM		14.9
SHELL	5.6	
OUTBOARD END CAP	1.5	
INBOARD END CAP	2.0	
BEARINGS	1.0	
NEGATOR + MOUNTING HDWE	1.3	
SLIP RINGS	0.8	
SUPPORT SHAFT	2.5	
POWER FEED THROUGHS	0.2	
OUTBOARD END SUPPORT		3.5
SUPPORT	2.6	
SEPARATION SYSTEM	0.9	
CENTER SUPPORT		2.1
LEADING EDGE MEMBER		1.0
TUBE	0.8	
CENTER BEARING	0.2	
SOLAR PANEL ACTUATOR		11.0
THERMAL CONTROL COATINGS		0.1
WIRING AND CONNECTORS		0.5
	SUBTOTAL	75.6
BALANCE REMAINING FOR GROWTH		7.7
SPECIFIED WEIGHT (2500 WATTS AT 30 WATT/LB)		83.3
PRESENT SPECIFIC POWER = 33.1 WATT/LB		

SUMMARY OF POWER LOSSES

ARRAY BUS STRIP AT 55° C	50 WATTS
SLIP RINGS	4
	54 WATTS

COMPONENT DESIGNS

- ARRAY BLANKET
- SOLAR PANEL ACTUATOR
- STORAGE DRUM
- LEADING EDGE MEMBER
- OUTBOARD END SUPPORT
- CENTER SUPPORT

ARRAY DESIGN CHARACTERISTICS

NUMBER OF CELLS	55,176.
NUMBER OF PARALLEL CELLS SUBMODULE	19.
NUMBER OF SERIES CELLS/STRING	242.
NUMBER OF PARALLEL STRINGS/ARRAY	12.
MAXIMUM POWER VOLTAGE AT +55°C	91. VDC
MAXIMUM POWER AT +55° C, 10.55 % EFF. AMO (INCLUDES 6% COVER GLASS LOSS)	2500. WATTS
ACTIVE CELL AREA	226.03 FT^2
GROSS MODULE AREA	250.09 FT^2
GROSS ARRAY AREA	261.67 FT^2

ARRAY V-I CURVE

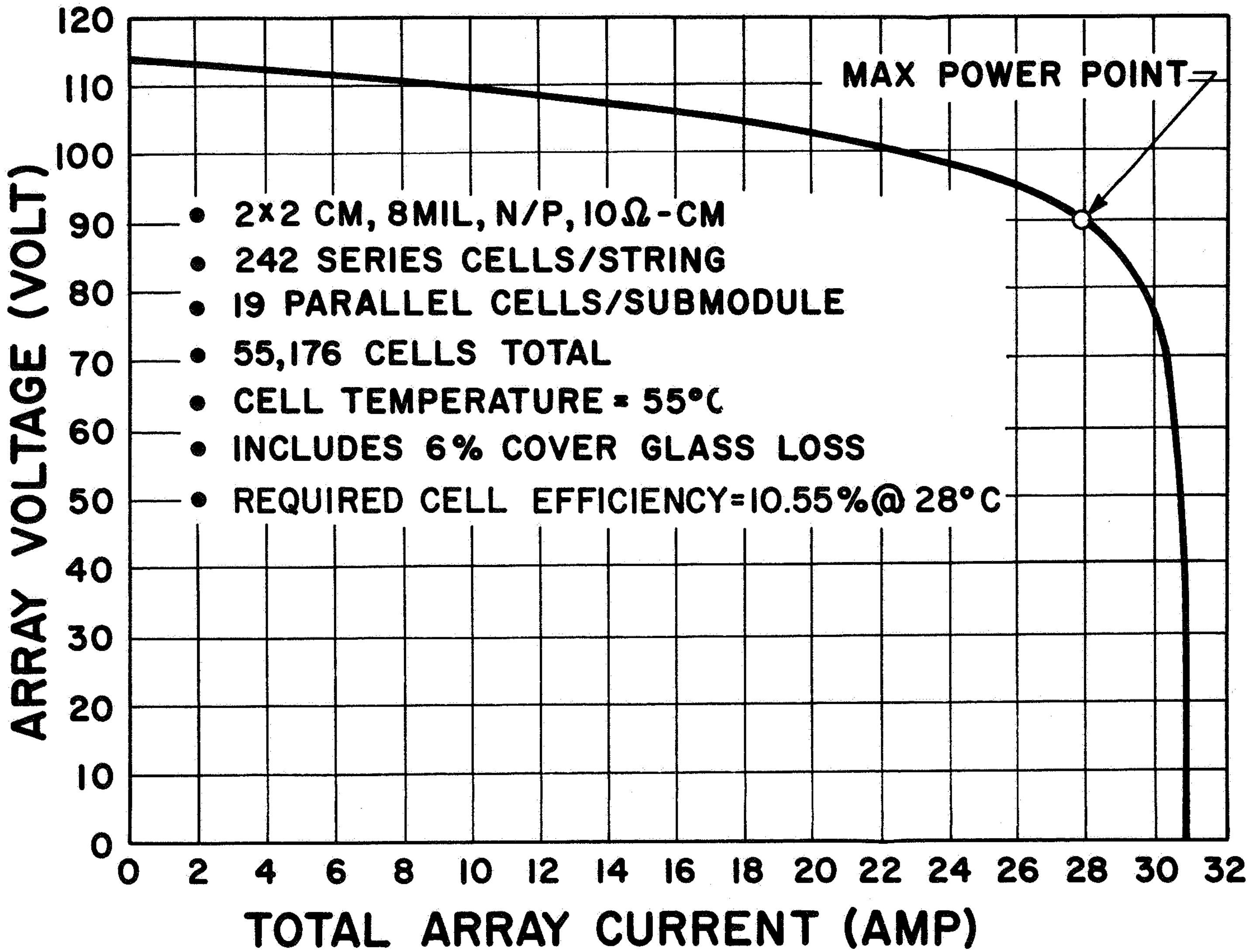

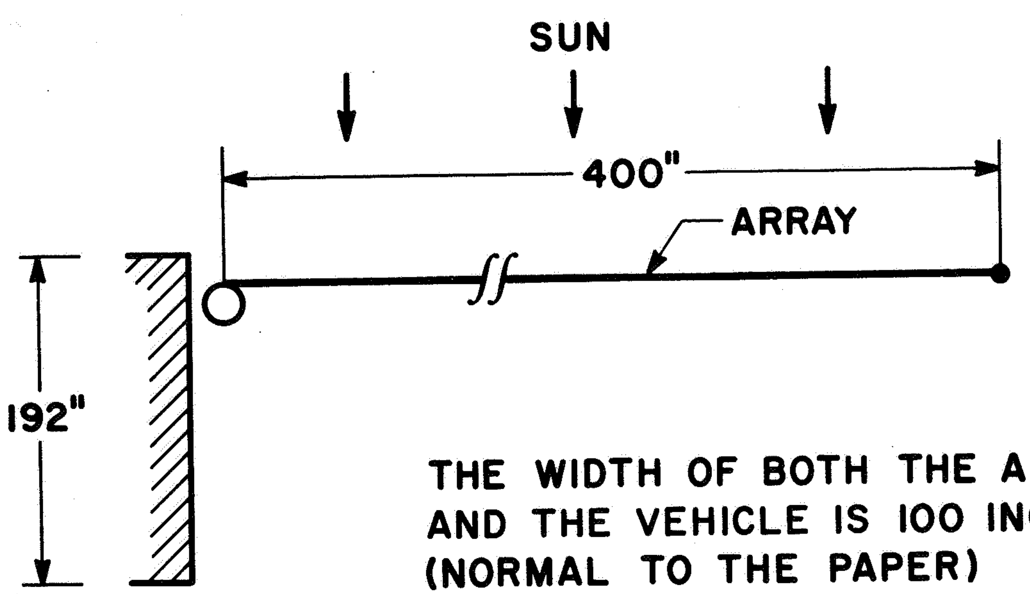

THE WIDTH OF BOTH THE ARRAY AND THE VEHICLE IS 100 INCHES (NORMAL TO THE PAPER)

OPTICAL PROPERTIES OF ARRAY COMPONENTS

	α_S	ϵ
SOLAR CELL/FILTER/GLASS COMPOSITE	0.71	0.8
2 MIL KAPTON BACKED BY SOLAR CELLS	---	0.67
INACTIVE ARRAY SURFACE	0.70	0.65

$$S\alpha_S - P = (F_{F-S}\bar{\epsilon}_F + F_{B-S}\bar{\epsilon}_B)B_A + (F_e F)_{B-V_1}(B_A - B_{V_1}) + (F_e F)_{B-V_2}(B_A - B_{V_2})$$

WHERE: S = INCIDENT SOLAR FLUX AT 1 AU, (.733 AU)

α_S = SOLAR ABSORPTANCE OF THE ARRAY FRONT SURFACE

P = SOLAR ENERGY CONVERTED

F = GEOMETRIC VIEW FACTOR

F_e = EMITTANCE FACTOR

B = BLACK BODY EMISSION

$\bar{\epsilon}$ = AVERAGE SURFACE INFRARED EMITTANCE

SUBSCRIPTS

F, FRONT ARRAY SURFACE

B, ARRAY BACK SURFACE

V_1, VEHICLE SECTION NEAREST ARRAY

V_2, VEHICLE SECTION FURTHEST FROM ARRAY

	1 AU		0.733 AU	
	°F	°C	°F	°C
ARRAY SECTION FURTHEST FROM VEHICLE:	121	(49.4)	224	(106.6)
ARRAY SECTION NEAREST THE VEHICLE:	125	(51.7)	226	(107.8)
ARRAY SECTION LOCATED BETWEEN THE ABOVE:	122	(50.0)	225	(107.2)
VEHICLE SECTION NEAREST THE ARRAY:	-82	(-63.3)	-16	(-26.7)
VEHICLE SECTION FURTHEST FROM ARRAY:	-168	(-111.1)	-116	(-82.2)

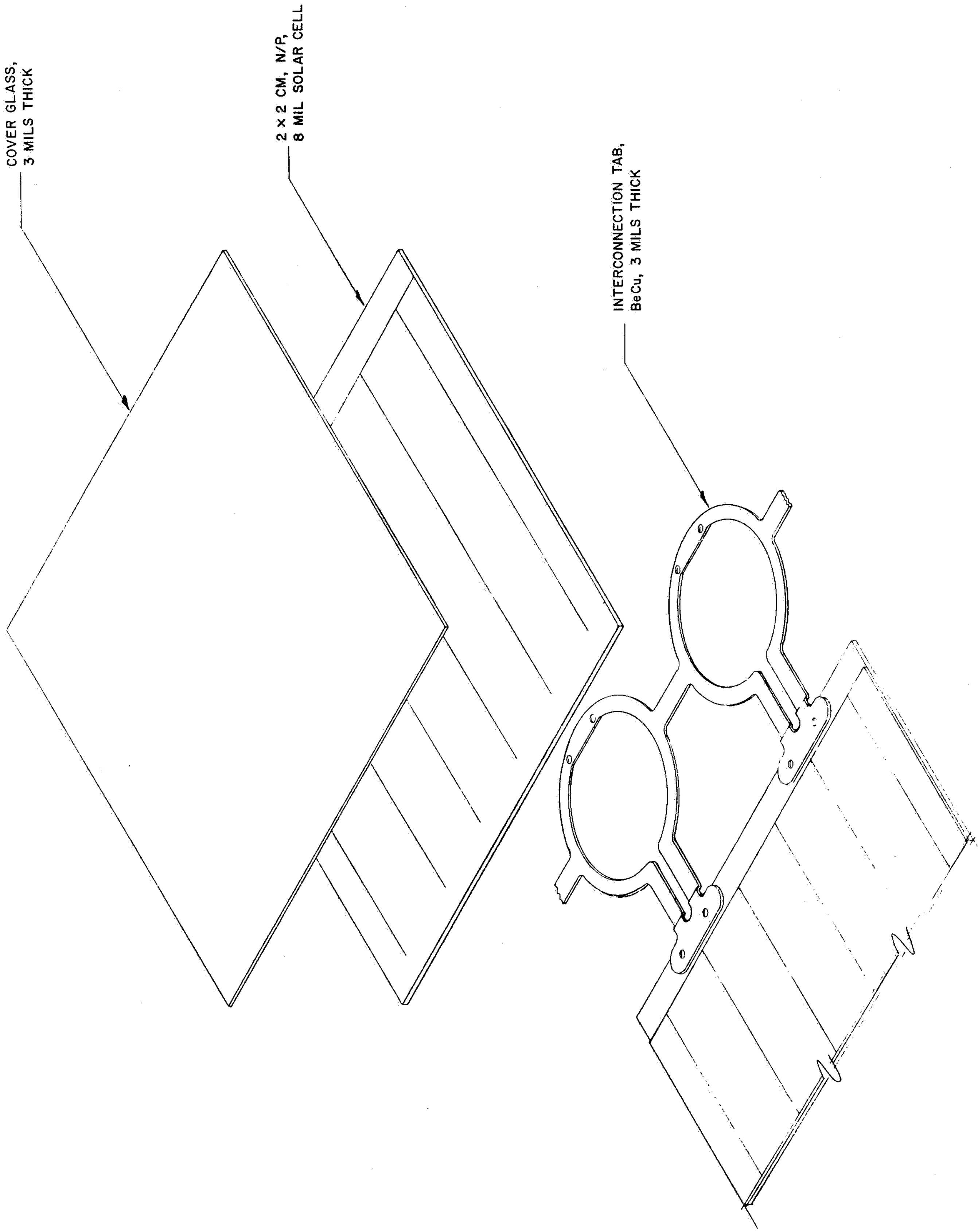
COVER GLASS,
3 MILS THICK
2 x 2 CM, N/P,
8 MIL SOLAR CELL
INTERCONNECTION TAB,
BeCu, 3 MILS THICK

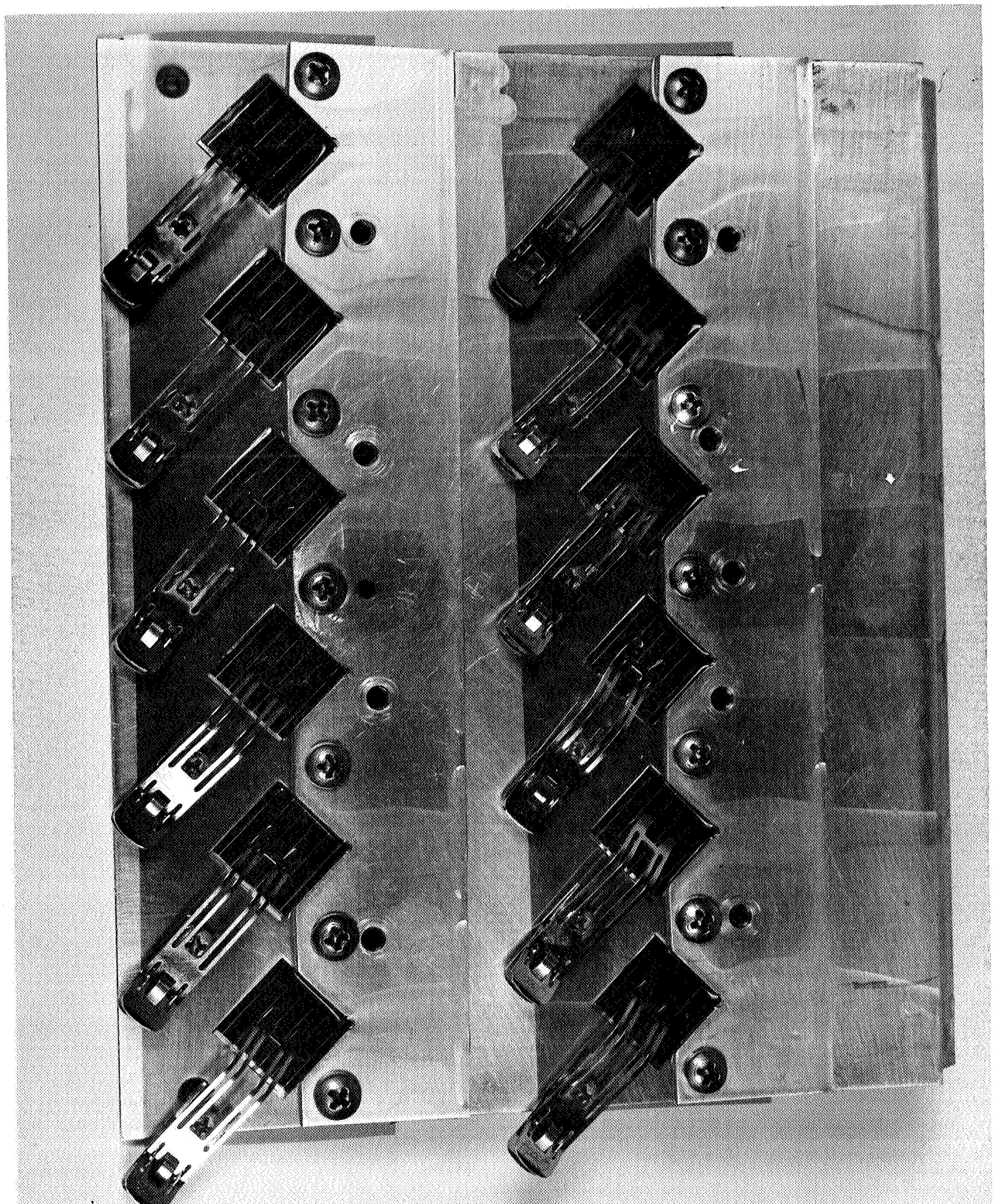

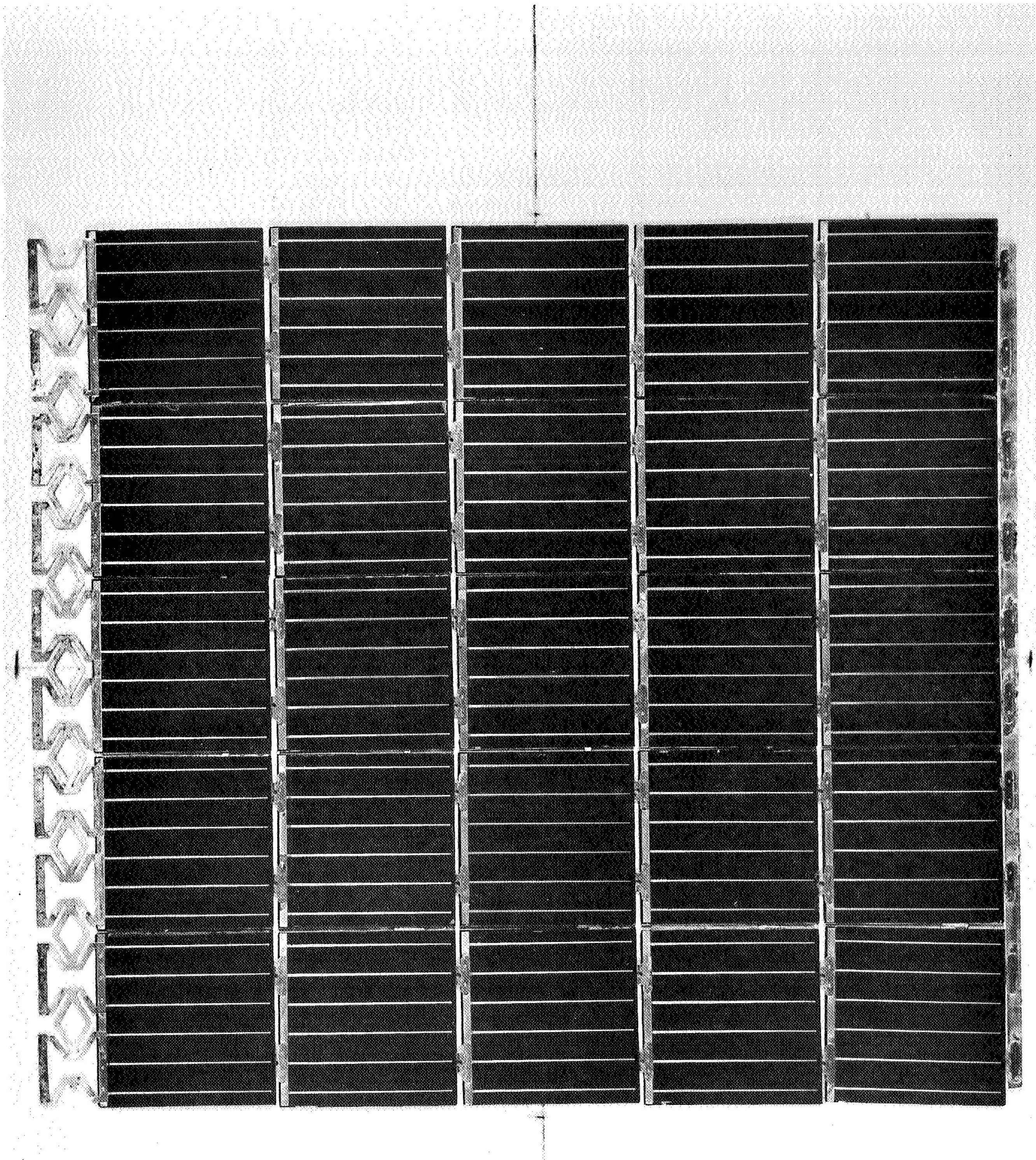

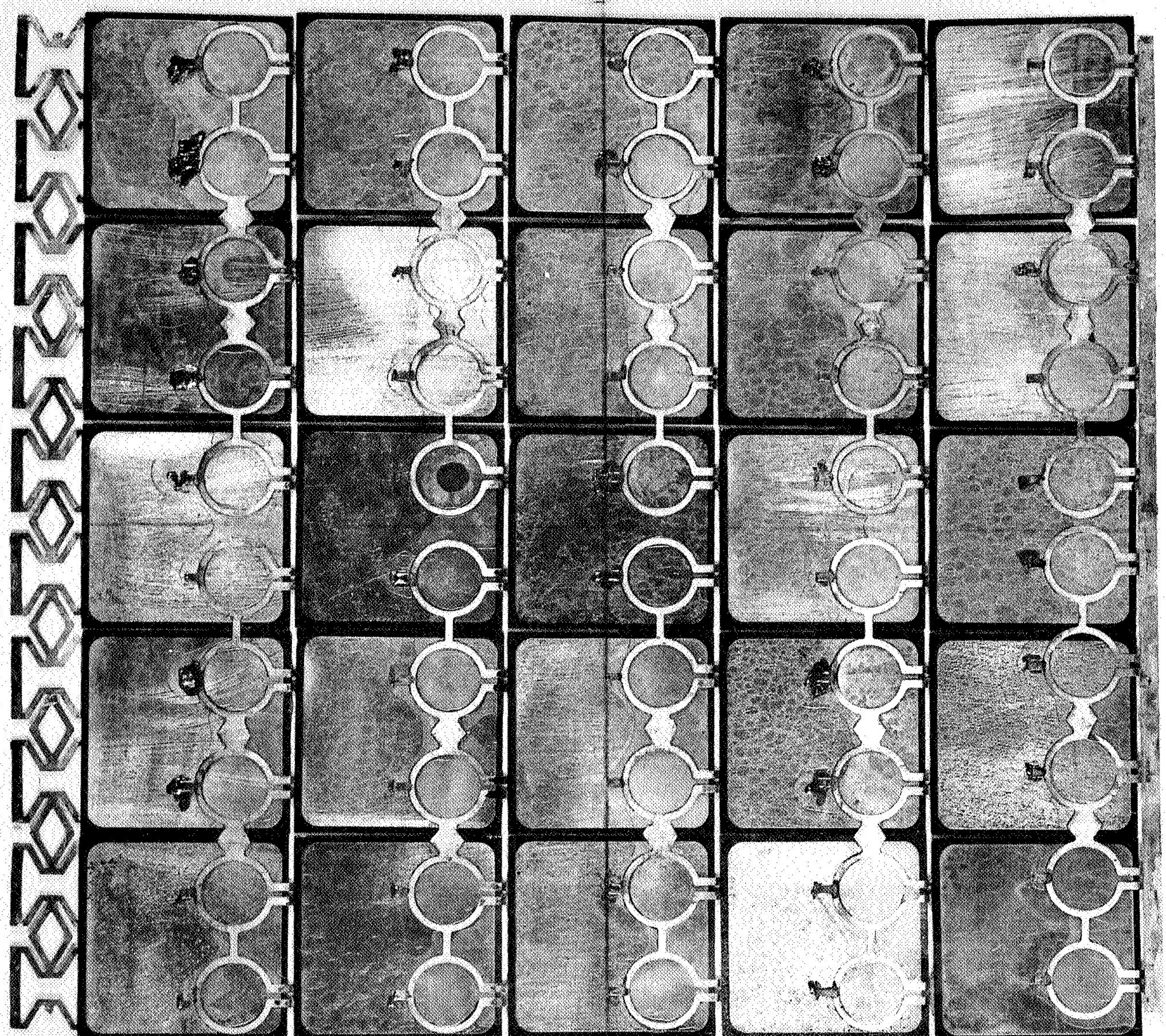

5X5 CELL MODULE WEIGHT

(USES CELLS WITH AVERAGE WEIGHT = 0.1737GM)

	TOTAL WEIGHT	=	13.4911 GM
LESS	KAPTON SUBSTRATE	=	-5.8285
LESS	(POSITIVE) END TAB	=	-0.0769
LESS	(NEGATIVE) END TAB	=	-0.1512
LESS	CELLS (25)	=	-4.3425

WEIGHT OF:

(a) INTERCONNECTION TABS

(b) SOLDER

(c) COVER GLASS

(d) COVER GLASS ADHESIVE

(e) CELL-TO-SUBSTRATE BOND

3.0920 GM

$$\frac{(3.0920)\,(55{,}176)}{(25)\,(453.59)} = 15.04 \text{ LB FOR TOTAL ARRAY}$$

THIS COMPARES WITH 15.97 LB USED FOR DESIGN

ARRAY WEIGHT BREAKDOWN

ITEM	WEIGHT	
	LB	LB/FT^2 MODULE AREA
COVER GLASS	8.73	0.0349
COVER GLASS ADHESIVE	0.98	0.0039
CELLS	19.46	0.0778
INTERCONNECTIONS	4.07	0.0163
SOLDER	0.19	0.0008
SUBSTRATE ADHESIVE	2.00	0.0080
SUBSTRATE	4.14	0.0166
BUTTONS	1.20	0.0048
BUS STRIP	1.20	0.0048
BUS STRIP ADHESIVE	0.53	0.0021
TOTAL	42.50	0.1700

BI-STEM ACTUATOR
SUMMARY OF DESIGN CHARACTERISTICS

ROD DIAMETER	1.34 IN.
ROD MATERIAL	SILVER PLATED STAINLESS STEEL
ROD MATERIAL THICKNESS	0.007 IN.
ROD LENGTH	33.5 FT
ROD WEIGHT	6.37 LB
MINIMUM MOMENT OF INERTIA	0.01185 $IN.^4$
COEFFICIENT OF THERMAL EXPANSION	9.3×10^{-6} IN./IN./°F
YOUNG'S MODULUS	29×10^6 PSI
SOLAR ABSORBTANCE	0.12
INFRARED EMITTANCE	0.04
ULTIMATE BENDING STRENGTH	984 IN.-LB
MOTOR VOLTAGE	27 VDC
EXTENSION/RETRACTION RATE	1.5 ± 0.5 IN./SEC
TOTAL WEIGHT	11.0 LB

DYNAMIC MODEL STOWED DRUM

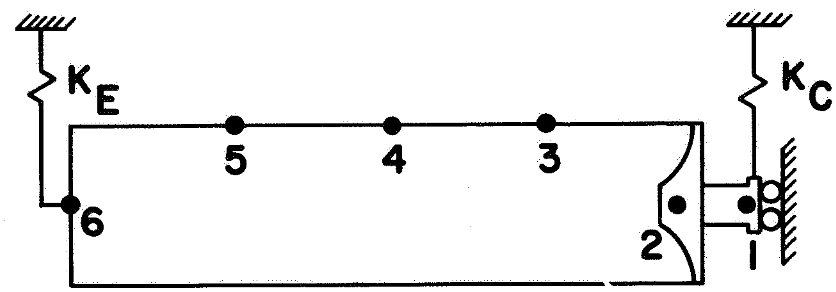

- MODEL FOR SYMMETRIC VIBRATION
- 6 TRANSLATIONAL DEGREES-OF-FREEDOM
- 5 ROTATIONAL DEGREES-OF-FREEDOM

1ST MODE NATURAL FREQUENCY = 205 H_Z

DRUM LOADS

- MAXIMUM SHEAR – 744 LB
- MAXIMUM MOMENT – 12340 IN.–LB

SECTION THROUGH STORAGE DRUM

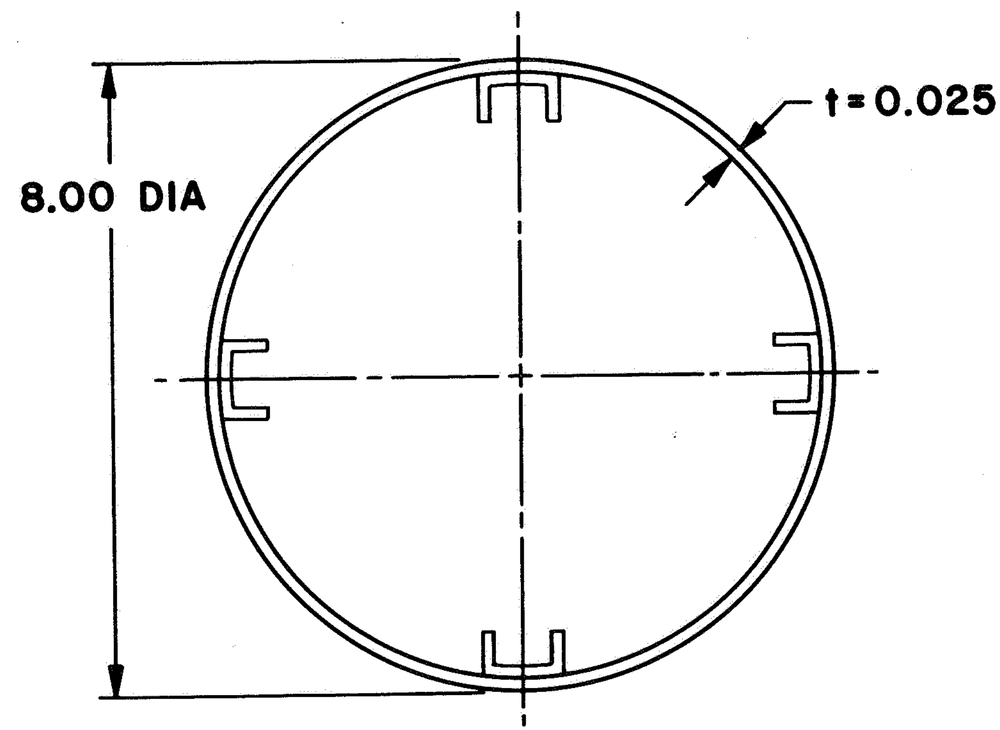

- HOT FORMED Be CROSS ROLLED SHEET
- SKIN MADE IN QUADRANTS
- CHANNEL DOUBLERS AT JOINTS
- FURNACE BRAZE (ALUMINUM OR SILVER) OR ADHESIVE BOND (EPOXY)

OUTBOARD, END CAP

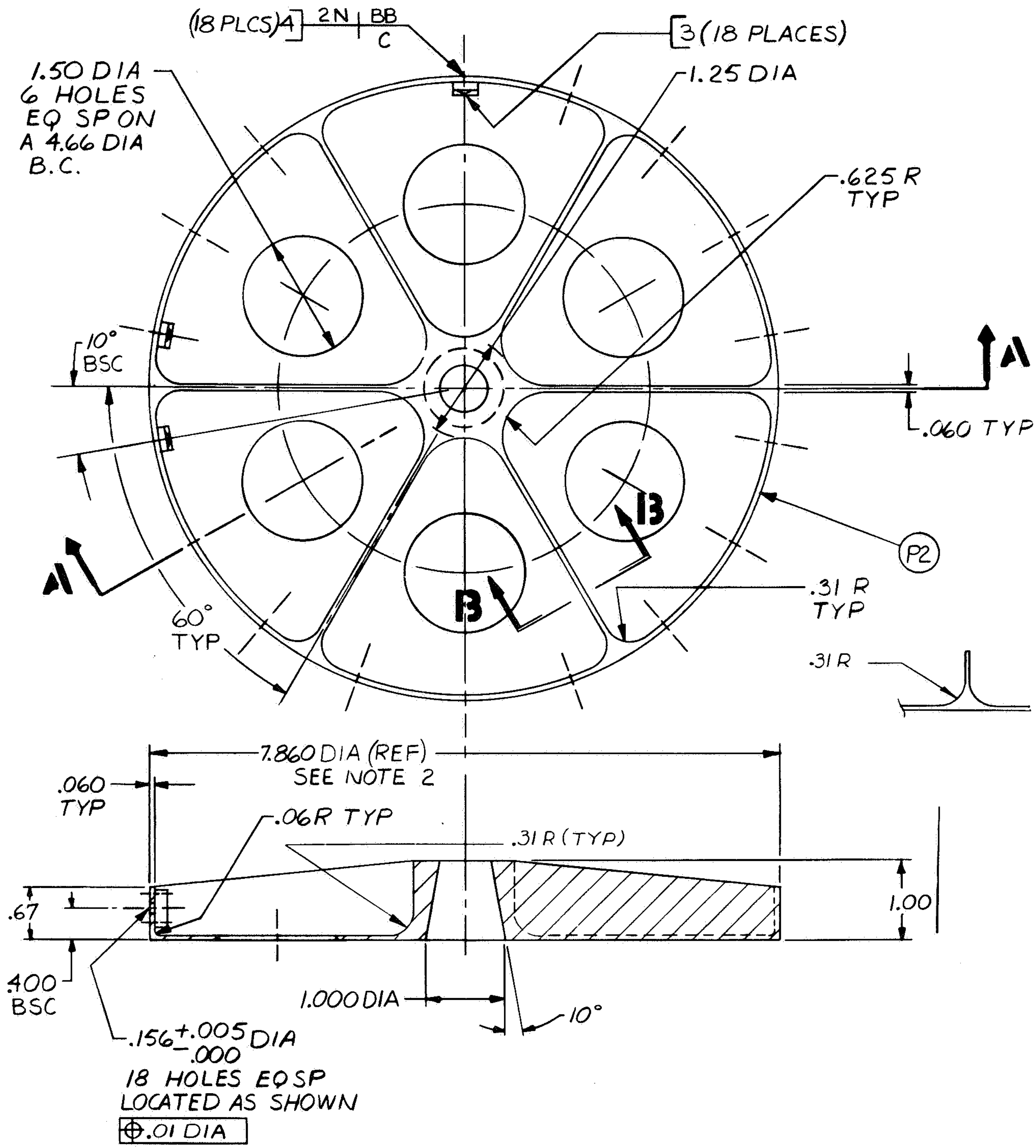

INBOARD ASSEMBLY OF END CAP

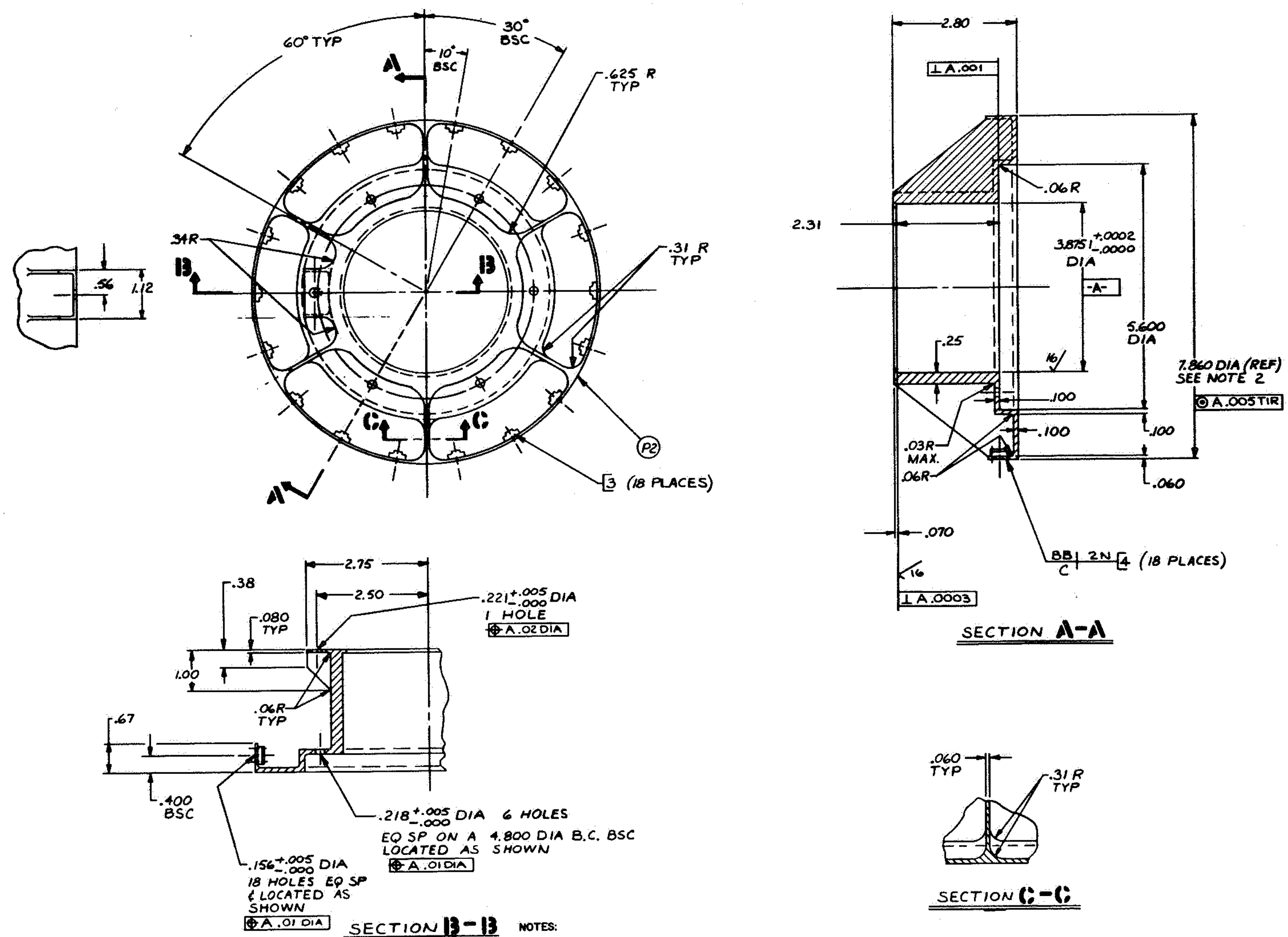

NOTES:

1. INTERPRETATION OF DRAWING TERMS AND TOLERANCES PER 118A 1664
2. THIS DIA TO MATE WITH END "E" OF 47D214514 G1 WITH A CLEARANCE OF .005 MAXIMUM
3. MARK PART GE 47E214516 G1 OR P1 AS APPLICABLE PER 118A 1526 CL 17
4. RIVET PER 171A 4287

- **BEARING SELECTION**
  - THIN SECTION, ANGULAR CONTACT, INSTRUMENT BEARING (SPLIT BALLBEARING-TAR SERIES)
  - 3.0625 IN. BORE
  - SIMILAR BEARINGS USED ON NIMBUS II SOLAR ARRAY DRIVE (IN ORBIT 20 MONTHS)

- **LUBRICATION SYSTEM SELECTION**

  TWO CHOICES
  - LUBECO 905 (DRY FILM)
  - REINFORCED TEFLON (TRANSFER FILM)
    "BAR TEMP" OR "DUROID" WITH MoS_2
    "RULON A" 'OR "RULON C" WITHOUT MoS_2

  SELECTED LUBECO 905 (USED ON SURVEYOR AND LUNAR ORBITER)

SLIP RING DESIGN PARAMETERS

RINGS PER ASSEMBLY	2
RING DIAMETER	1.00 IN.
RING MATERIAL	SILVER
BRUSHES PER RING	2
BRUSH MATERIAL	SILVER/NIOBIUM DISELENIDE
RATED CURRENT PER RING	13.8 AMP
CONTACT AREA/BRUSH	0.092 $IN.^2$
DESIGN CURRENT DENSITY	75 $AMP/IN.^2$
BRUSH CONTACT FORCE	340 GRAMS
STARTING TORQUE	
AIR	0.6 IN.-LB
VACUUM	0.3 IN.-LB
CONTACT RESISTANCE	0.003 OHMS
POWER DISSIPATION/ASSEMBLY	1.75 WATTS
WEIGHT/ASSEMBLY	0.4 LB
EFFECTIVE WEIGHT	2.2 LB

SECTION THROUGH LEADING EDGE MEMBER

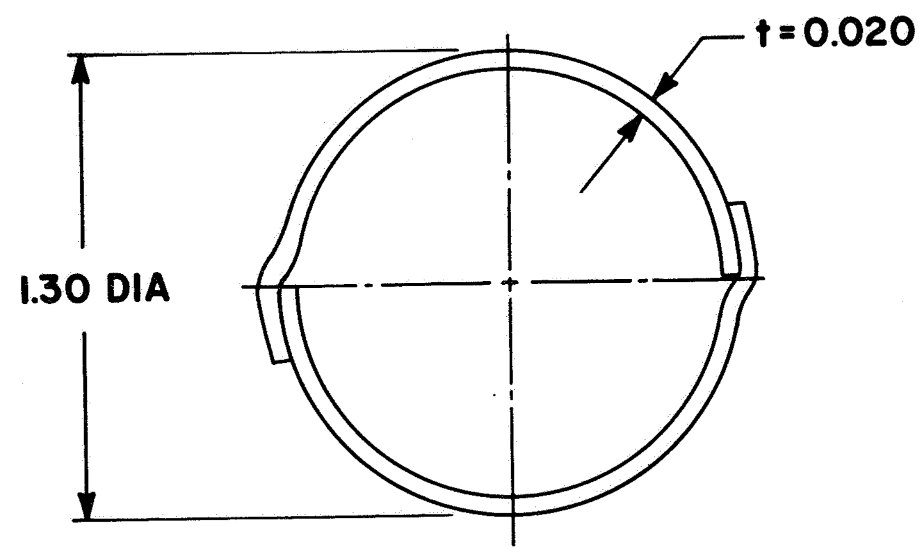

- HOT FORMED Be CROSS ROLLED SHEET
- FURNACE BRAZE (Al OR Ag) OR ADHESIVE BOND (EPOXY)

ROLL-UP SOLAR ARRAY ASSEMBLY

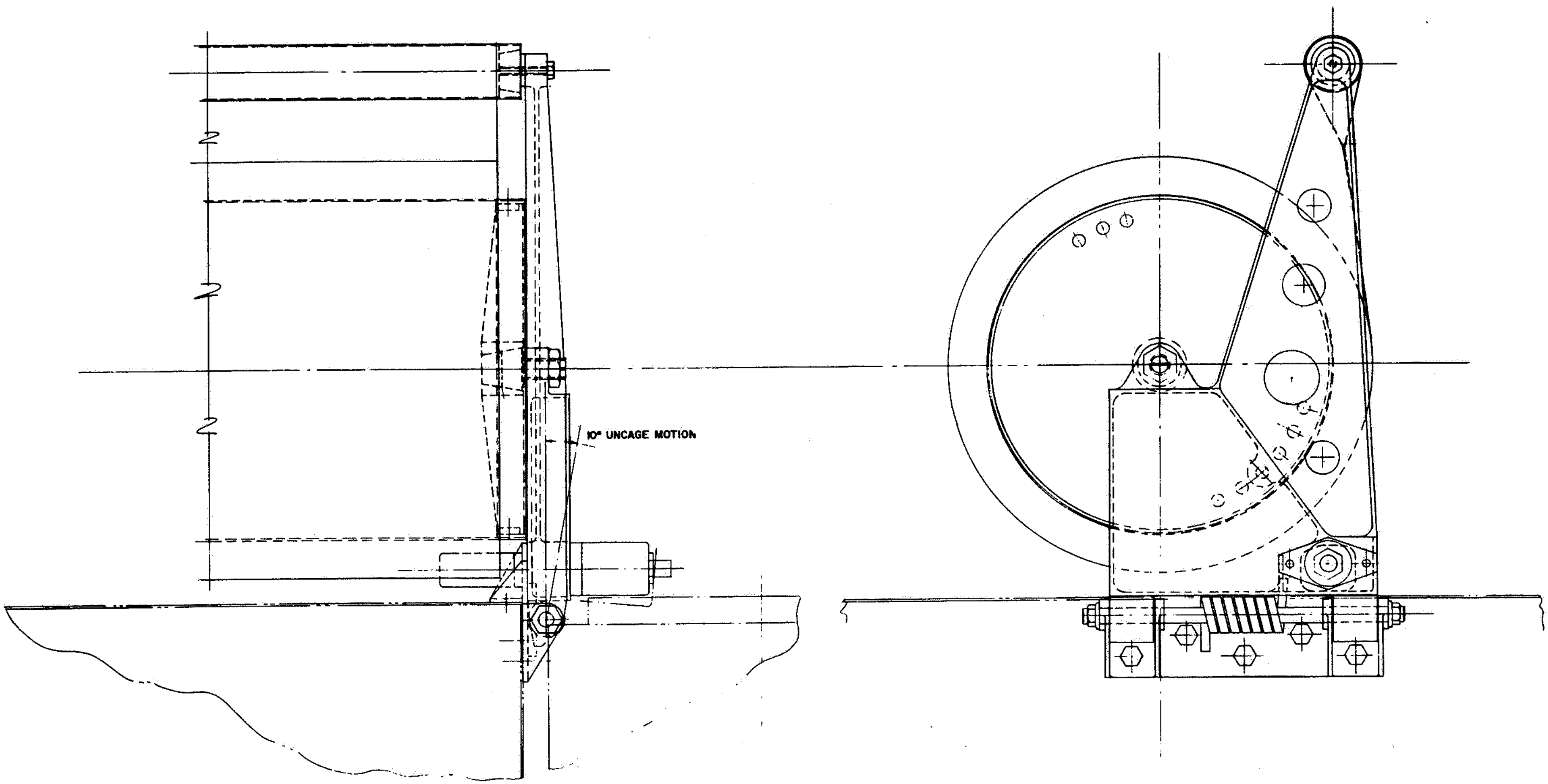

CENTER SUPPORT

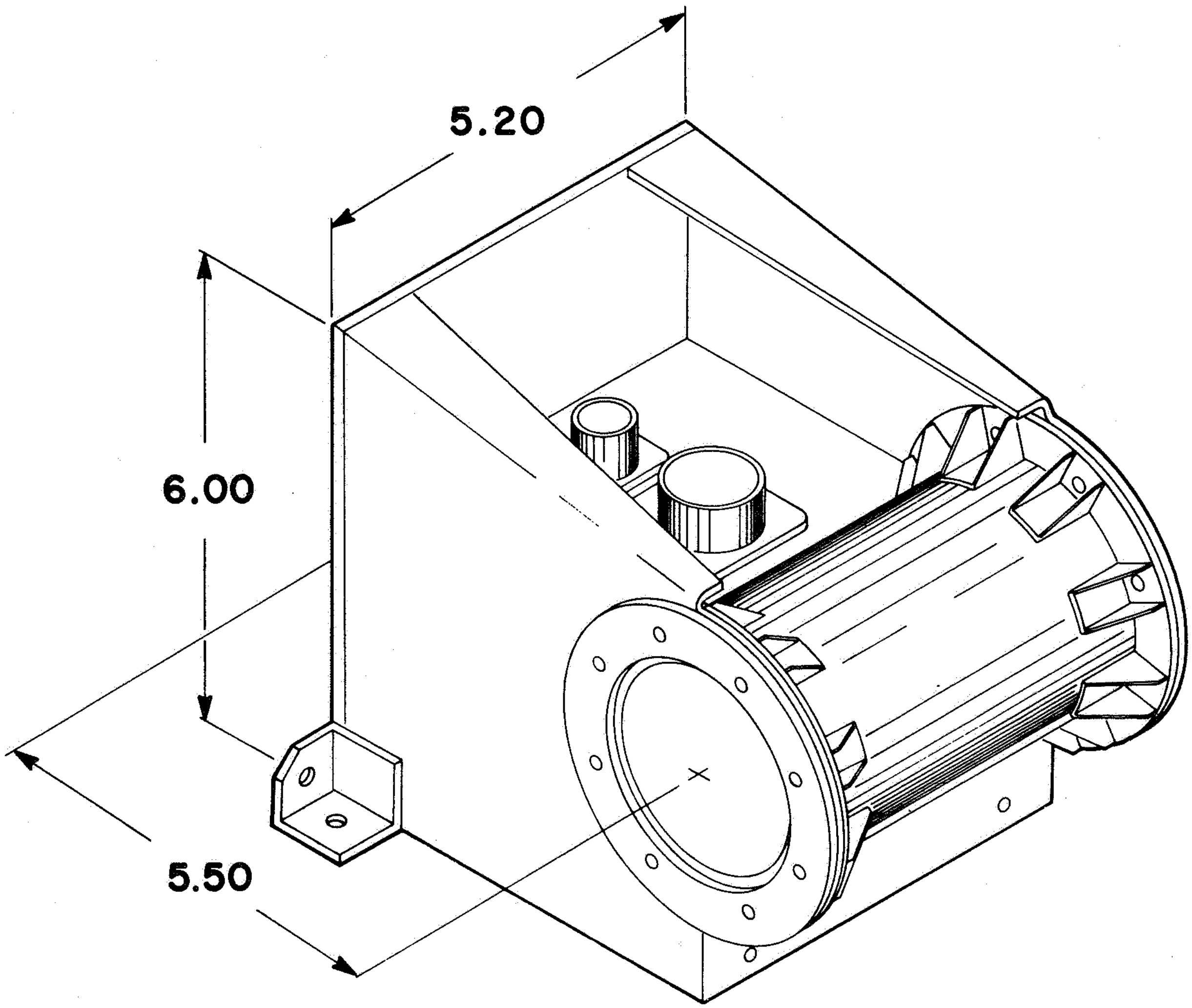

METHODS OF JOINING BERYLLIUM

*ADHESIVE BONDING

METALLURGICAL JOINING

- *SOLDERING
- *FURNACE BRAZING
- SOLID STATE BONDING
- *BRAZE WELDING
- ELECTRON BEAM WELDING
- *DIP BRAZING
- FRICTION WELDING
- ULTRASONIC WELDING
- RESISTANCE WELDING

*MECHANICAL FASTENING

*USED SUCCESSFULLY ON AEROSPACE-TYPE COMPONENTS

DIP BRAZING AL ALLOY (CAMERA HOUSING)

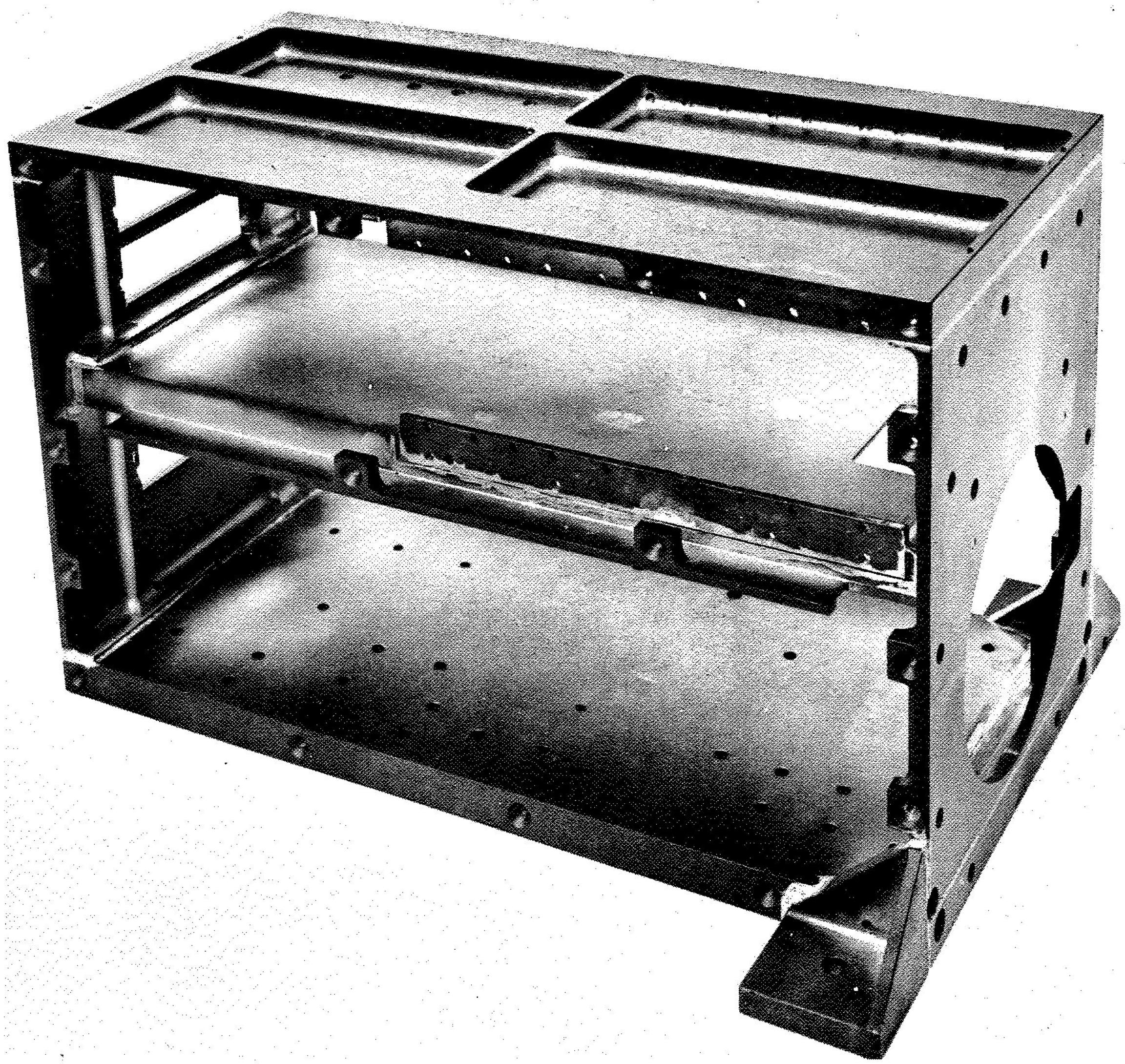

FURNACE BRAZING AG ALLOY
(X-RAY DIFFRACTION EQUIPMENT)

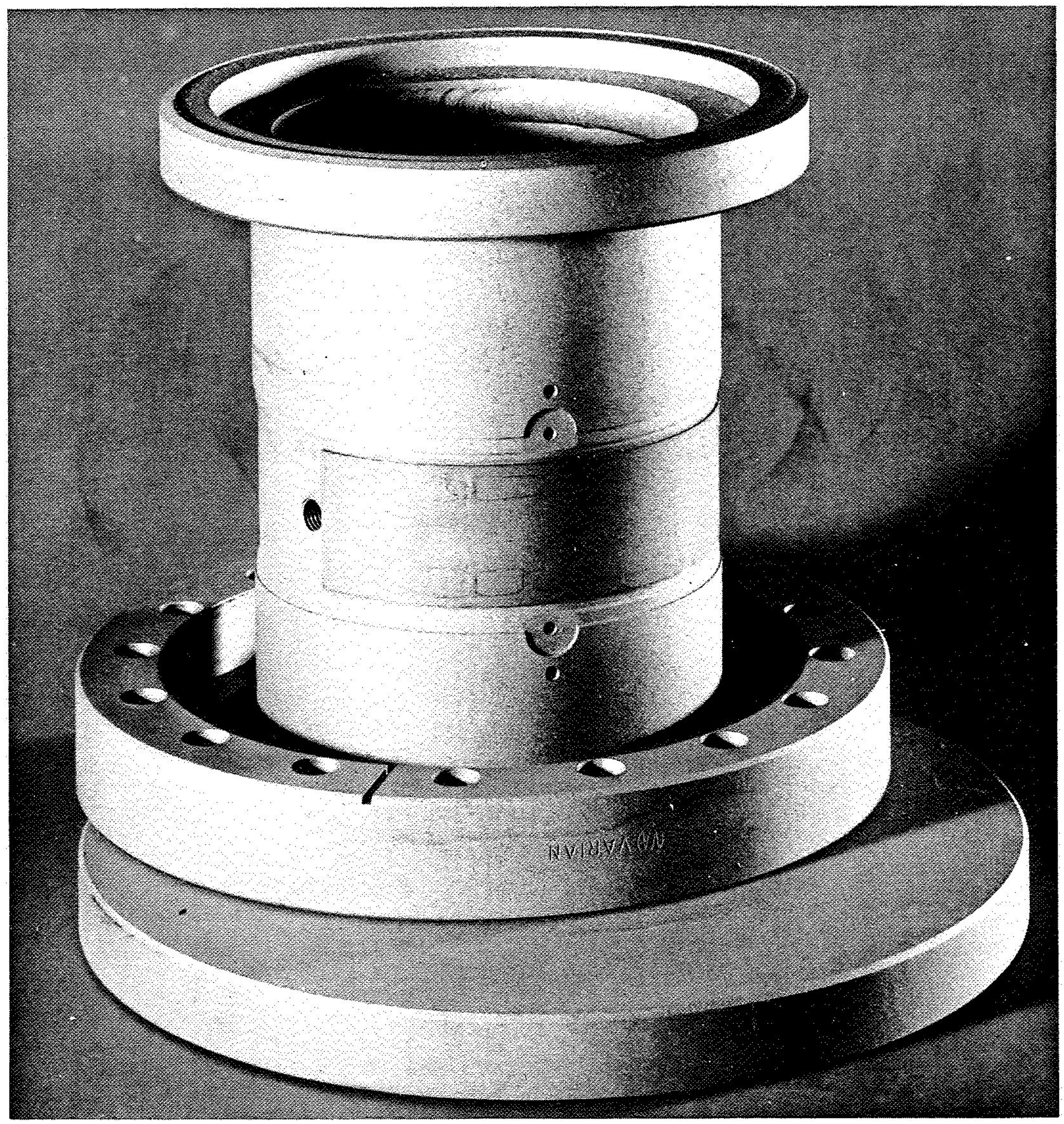

BRAZE WELDING AG ALLOY
(SNAP-27 R&D)

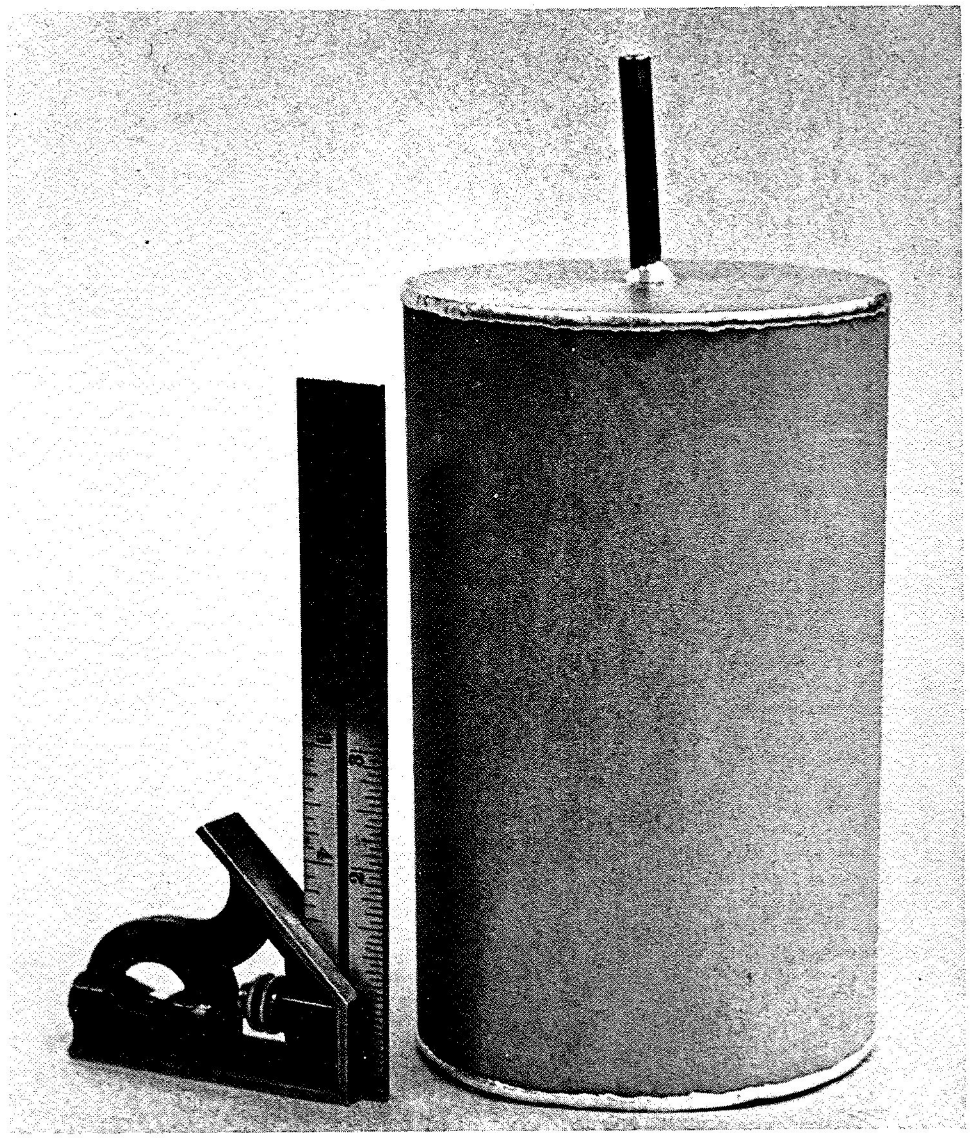

ENGINEERING DEMONSTRATION MODEL

ENGINEERING DEMONSTRATION MODEL

- PURPOSE

  PRESENT A CREDIBLE DEMONSTRATION OF ARRAY DEPLOYMENT

- GE APPROACH FEATURES

  FULL SCALE MODEL, EXCEPT FOR DRUM WIDTH

  VERTICAL DEPLOYMENT TO FULLY EXTENDED LENGTH (33.5 FT)

  FLIGHT-TYPE COMPONENTS WHERE FEASIBLE

  DEPLOYED NATURAL FREQUENCY CAN BE MEASURED

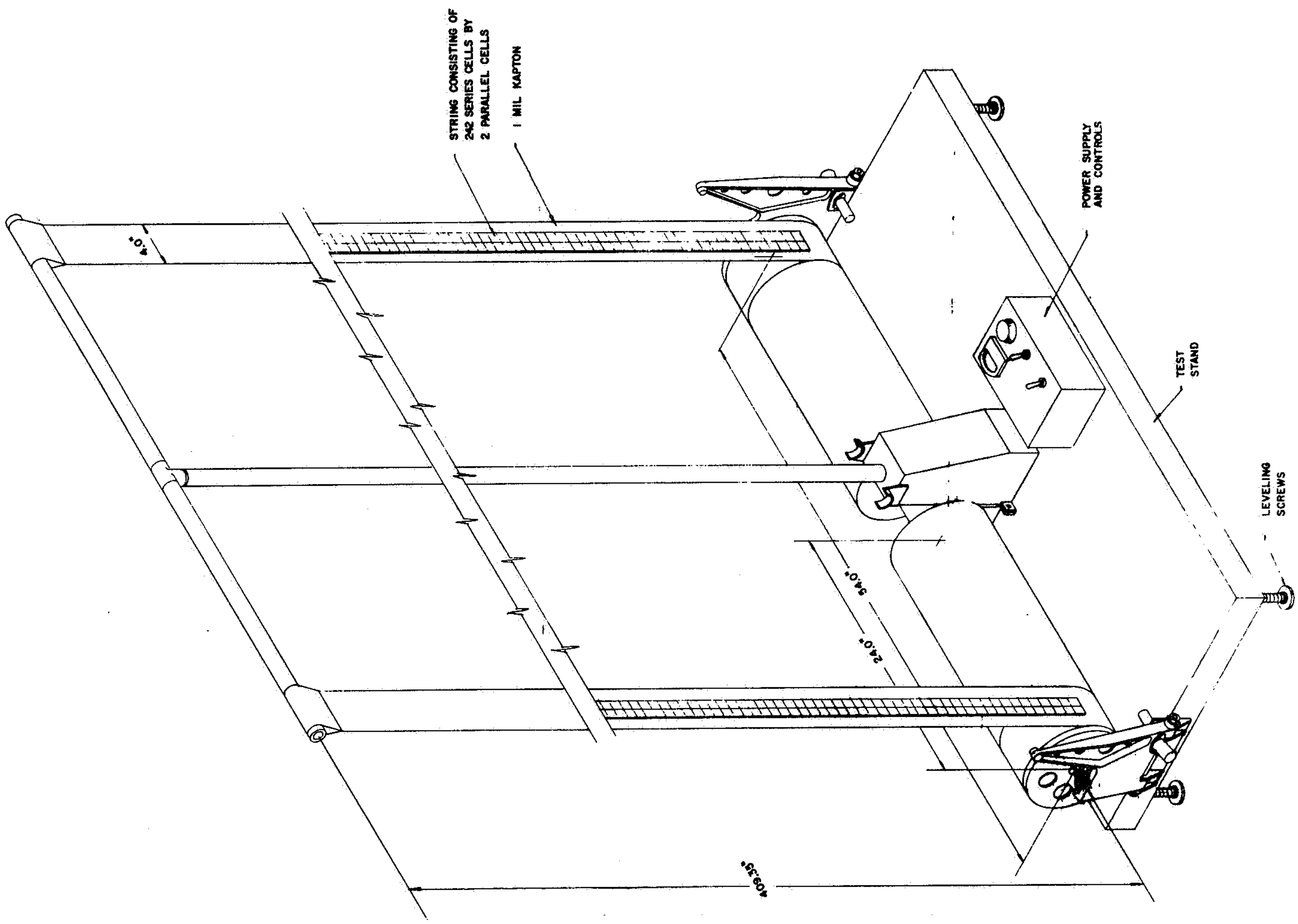

STRING CONSISTING OF 242 SERIES CELLS BY 2 PARALLEL CELLS
1 MIL KAPTON
4.0"
POWER SUPPLY AND CONTROLS
TEST STAND
LEVELING SCREWS
54.0"
24.0"
409.3"

EFFECT OF 1 g VERTICAL DEPLOYMENT

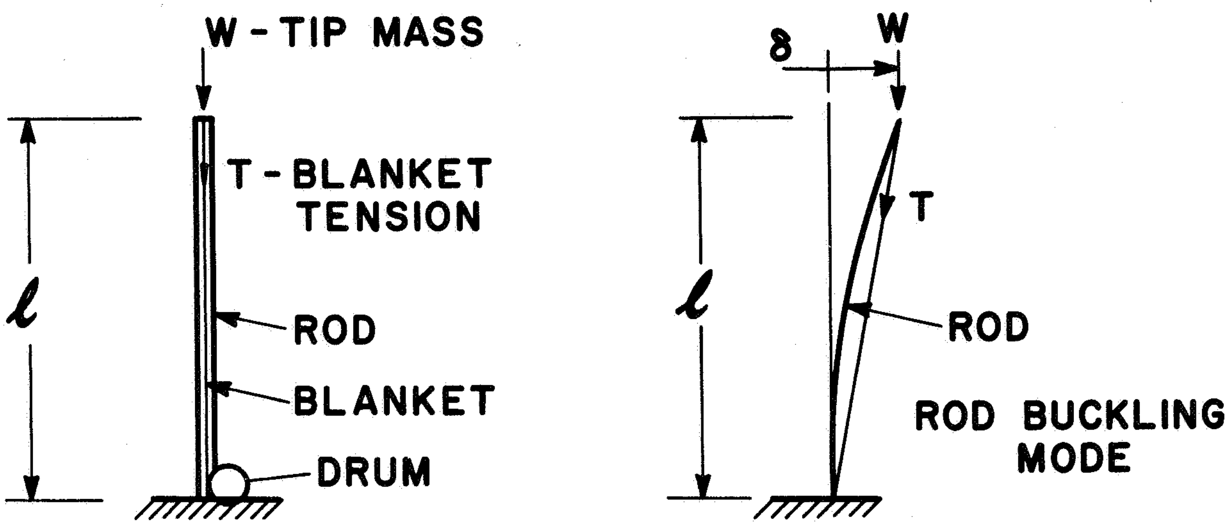

$$\delta = \frac{-Q}{Pk}(\mathrm{TAN}\ k\ell - k\ell)$$

FOR THIS CASE: $Q = T\left(\frac{\delta}{\ell}\right)$, $P = T + W$

$$\delta\left[1 + \frac{T}{Pk}(\mathrm{TAN}\ k\ell - k\ell)\right] = 0$$

$$\mathrm{TAN}\ k\ell = -\frac{W}{T}k\ell$$

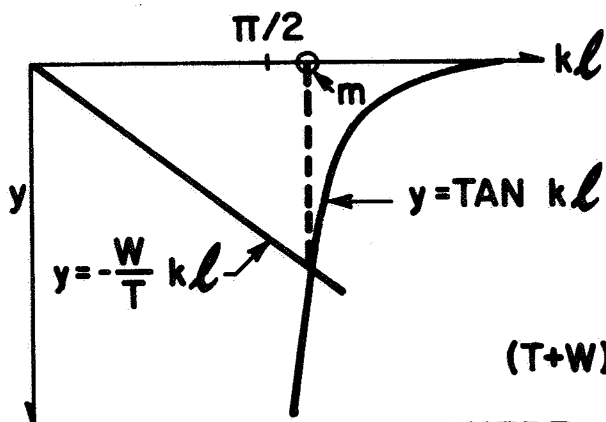

$$(T+W)_{CR} = \frac{M^2 EI}{\ell^2}$$

WHERE:

$k = \sqrt{\frac{P}{EI}}$

ℓ = COLUMN LENGTH

EI = MEMBER STIFFNESS

EFFECT OF 1g VERTICAL DEPLOYMENT

$T = 4.0$ LB

$W = 1.2 + 0.3(6.37) = 3.11$ LB

AT $\frac{W}{T} = 0.778 \qquad m = 1.71$

$$(T+W)_{CR} = \frac{m^2 EI}{\ell^2} = \frac{(1.71)^2 (29 \times 10^6)(0.01185)}{(402)^2}$$

$(T+W)_{CR} = 6.25$ LB

$T + W = 4.0 + 3.11 = 7.11$ LB

$$M.S. = \frac{6.25}{1.25(7.11)} - 1 = -0.30$$

EFFECT OF 1g VERTICAL DEPLOYMENT

BI-STEM STATIC LOAD TEST

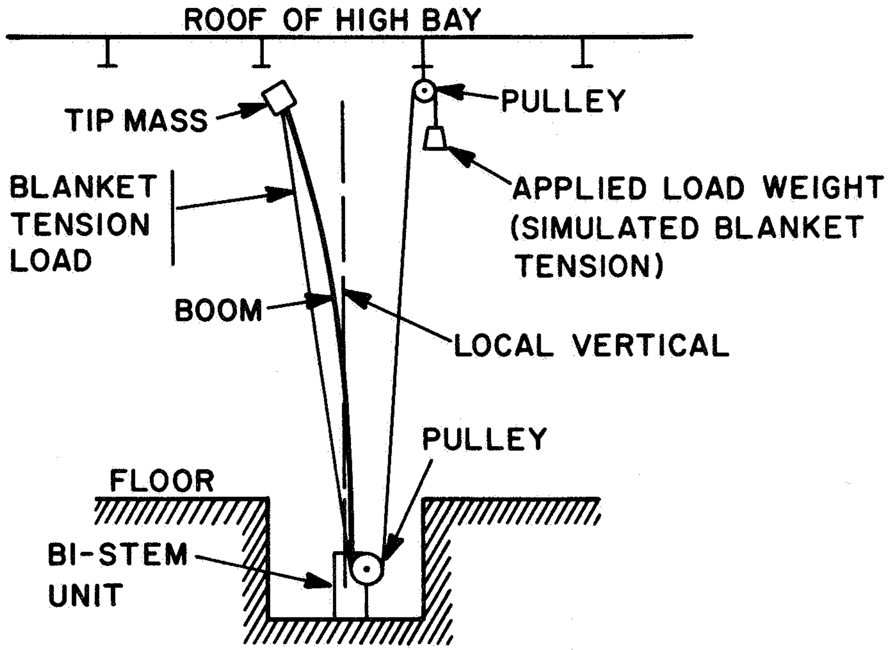

	BLANKET TENSION (LB)	TIP MASS (LB)	LENGTH ALONG BOOM (FT)	DEFLECTION (IN.)
DESIGN LOADS ON ENGINEERING DEMONSTRATION MODEL	4.0 ↓	1.2 ↓	31 (TIP)	13
			20	6 1/4
			14	3 3/8
			7.8	1 1/8
			0	0
LOADS INCREASED BY $\left(\frac{33.5}{31}\right)^2$	4.6 ↓	1.4 ↓	31 (TIP)	17
			26	13 1/4
			20	9
			14	5
			7.8	1 5/8
			0	0

NOTE

IN ALL CASES, THE BOOM WAS LOADED BY ITS OWN WEIGHT OF APPROXIMATELY 0.2 LB/FT

DESIGN REVIEW

POTENTIAL PROBLEM

WILL BLANKET TRACK DURING ARRAY RETRACTION?

APPROACH

- GUIDING LIP ON DRUM AND STIFFEN EDGE WITH BUS STRIP
- STIFFNESS OF ROD GUIDES BLANKET
- TEST ON ENGINEERING DEMONSTRATION MODEL WITH DUMMY BLANKET

POTENTIAL PROBLEM

WILL THERMAL CYCLING ENVIRONMENT DEGRADE ARRAY OUTPUT ?

APPROACH

- KEY TO DESIGN SOLUTION IS A FLEXIBLE INTERCONNECTION TAB (0.002 INCH CAN BE ACCOMMODATED WITH 0.001 LB)
- INTERCONNECTION TABS HAVE BEEN DESIGNED TO PROVIDE FLEXIBILITY OF GGTS WHILE ADAPTING TO FLAT LAY DOWN
- EARLY TEST WILL BE PERFORMED ON THE 5 x 5 CELL MODULE TO EVALUATE THE ADEQUATENESS WITH REGARD TO THINNER CELLS

POTENTIAL PROBLEM

WILL CELL/GLASS COMBINATION BE ADEQUATELY PROTECTED DURING LAUNCH?

- LAUNCH ENVIRONMENT

  4g (O-P) SINE

  0.1 g^2/Hz RANDOM

  ACOUSTIC 146 db OVERALL S.P.L.

- ARRAY MODEL PASSED

  5g (O-P) SINE 14 - 400 Hz

  7.5g(O-P) SINE 400-2000 Hz

  0.07g^2/Hz 25 - 400 Hz

  0.13g^2/Hz 400 - 2000 Hz

  ACOUSTIC 154 db OVERALL S.P.L.

- MODEL HAD RTV 580 FOAM BUTTONS ON UNDERSIDE OF BLANKET TO PROVIDE RADIAL (SPONGY) AND AXIAL (FRICTION) DAMPING

UNRESOLVED: WILL THINNER CELL/GLASS COMBINATION BE PROTECTED?

DOES GE HAVE THE OPTIMUM ASPECT RATIO?

CONCLUSION:
THERE IS NO CLEARLY DEFINED OPTIMUM

- 1.34 IN. BI-STEM (STAINLESS STEEL)
- 4 LB TOTAL PRELOAD
- 12 STRINGS/ARRAY
- VARIABLE WEIGHTS
  - BOOM
  - DRUM SHELL
  - LEADING EDGE MEMBER
  - NEG'ATOR CONSTANT TORQUE MOTOR
  - ARRAY BUS STRIP

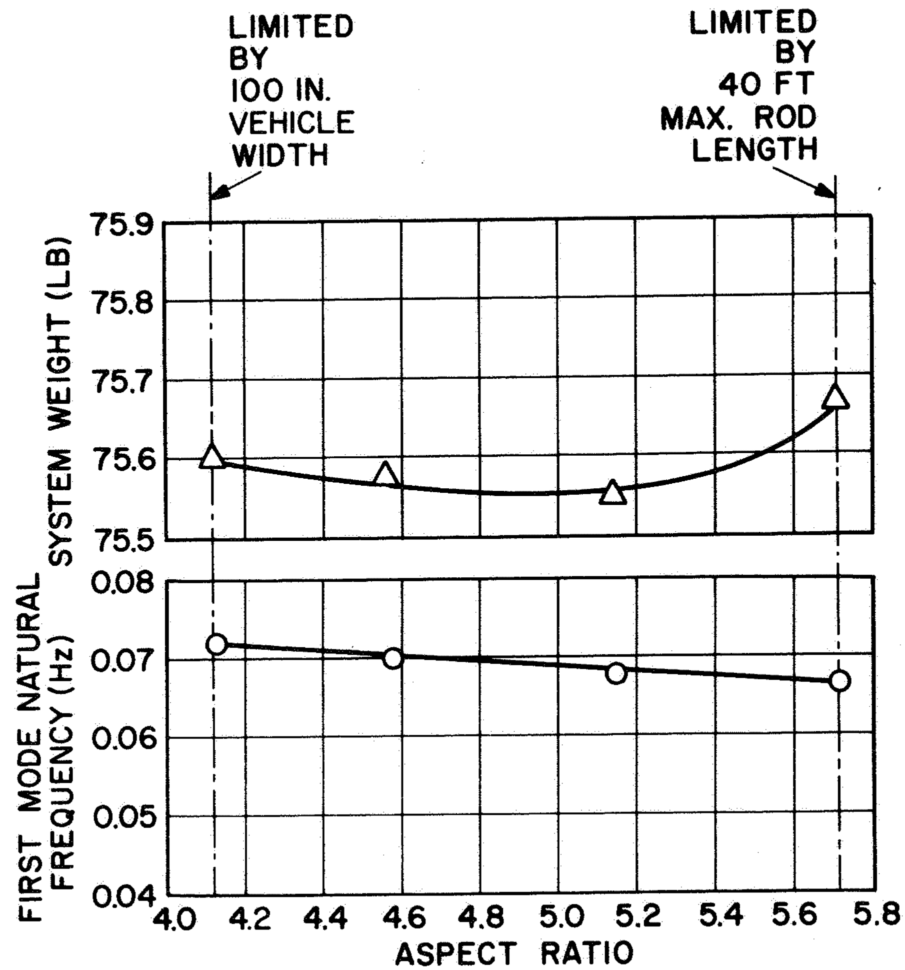

WHAT HAPPENS TO THE SYSTEM WEIGHT IF THE FIRST MODE NATURAL FREQUENCY REQUIREMENT IS INCREASED?

- WITH THE PRESENT BI-STEM UNIT (1.34 DIA), THE FIRST MODE NATURAL FREQUENCY COULD BE INCREASED TO 0.11 Hz WITH ONLY A 1.2 LB INCREASE IN SYSTEM WEIGHT

SLIP RING ASSEMBLY COMPARISON WITH NIMBUS DESIGN

PARAMETER	ROLL-UP ARRAY CONCEPTUAL DESIGN	NIMBUS POWER RINGS	NIMBUS SIGNAL RINGS
CURRENT RATING/RING (AMP)	13.8	10	1
CONTACT AREA/BRUSH ($IN.^2$)	0.092	0.019	0.009
BRUSHES/RING	2	2	2
CURRENT DENSITY ($AMP/IN.^2$)	75	263	55
BRUSH CONTACT FORCE (LB)			
MIN		0.176	0.088
MAX		0.220	0.132
NOMINAL	0.75		
BRUSH CONTACT PRESSURE (PSI)			
MIN		9.3	9.8
MAX		11.6	14.7
NOMINAL	8.2		
CONTACT RESISTANCE (OHMS)	0.003	0.005	0.005
COEFFICIENT OF FRICTION (STARTING)	0.4	0.212 TO 0.304	
WEIGHT WITHOUT WIRING	0.278	3.1	
WEIGHT PER RING	0.139	0.129	

WEIGHT SUMMARY

WEIGHT SUMMARY

COMPONENT		WEIGHT (LB)
ARRAY		42.5
STORAGE DRUM		14.9
SHELL	5.6	
OUTBOARD END CAP	1.5	
INBOARD END CAP	2.0	
BEARINGS	1.0	
NEGATOR + MOUNTING HDWE	1.3	
SLIP RINGS	0.8	
SUPPORT SHAFT	2.5	
POWER FEED THROUGHS	0.2	
OUTBOARD END SUPPORT		3.5
SUPPORT	2.6	
SEPARATION SYSTEM	0.9	
CENTER SUPPORT		2.1
LEADING EDGE MEMBER		1.0
TUBE	0.8	
CENTER BEARING	0.2	
SOLAR PANEL ACTUATOR		11.0
THERMAL CONTROL COATINGS		0.1
WIRING AND CONNECTORS		0.5
	SUBTOTAL	75.6
BALANCE REMAINING FOR GROWTH		7.7
SPECIFIED WEIGHT (2500 WATTS AT 30 WATT/LB)		83.3

PRESENT SPECIFIC POWER = 33.1 WATT/LB

WEIGHT DISTRIBUTION

COMPONENT	FRACTION OF SYSTEM WEIGHT	DOMINANT DESIGN CONSTRAINT
ARRAY BLANKET	0.56	ELECTRICAL OUTPUT WITH SELECTED CELLS
DRUM	0.20	LAUNCH VIBRATION
ACTUATION BOOM	0.15	FIRST MODE FREQUENCY (THERMAL BENDING)
END SUPPORT STRUCTURE	0.05	LAUNCH VIBRATION
CENTER SUPPORT	0.03	LAUNCH VIBRATION
LEADING EDGE	0.01	LAUNCH VIBRATION

SUMMARY

SUMMARY

- EXCEED PERFORMANCE REQUIREMENTS
  - 33 WATTS PER POUND
  - MINIMUM NO. OF ACTIVE ELEMENTS
- ADAPTABLE DESIGN
  - SINGLE POINT ATTACHMENT
  - VARIABLE ASPECT RATIOS & SIZE
  - INCREASED NATURAL FREQUENCY
  - MODULAR ELEMENTS

SUMMARY

- NO TECHNOLOGICAL BREAKTHROUGHS REQUIRED

  ADHESIVES
  ROD MATERIALS
  LUBRICANTS
  MECHANISMS

  } DEVELOPED, TESTED

- USE OFF-THE-SHELF HARDWARE

  BOOMS
  BEARINGS
  PYROTECHNICS

SUMMARY

- TEST DESIGN AGAINST SUCCESSFUL FLIGHT SYSTEMS

  SLIP RINGS - NIMBUS

  BEARINGS - NIMBUS

  LUBRICANTS - SURVEYOR
LUNAR ORBITER

- ROLL-UP ARRAYS FOR NEXT SPACECRAFT

  DBS

  ATS

  CLASSIFIED I

  CLASSIFIED 2

GENERAL
ELECTRIC

MISSILE AND SPACE DIVISION

Valley Forge Space Technology Center

P.O. Box 8555 • Phila. Penna., 19101